

# Journal of Materials Chemistry B

Accepted Manuscript



This is an *Accepted Manuscript*, which has been through the Royal Society of Chemistry peer review process and has been accepted for publication.

*Accepted Manuscripts* are published online shortly after acceptance, before technical editing, formatting and proof reading. Using this free service, authors can make their results available to the community, in citable form, before we publish the edited article. We will replace this *Accepted Manuscript* with the edited and formatted *Advance Article* as soon as it is available.

You can find more information about *Accepted Manuscripts* in the [Information for Authors](#).

Please note that technical editing may introduce minor changes to the text and/or graphics, which may alter content. The journal's standard [Terms & Conditions](#) and the [Ethical guidelines](#) still apply. In no event shall the Royal Society of Chemistry be held responsible for any errors or omissions in this *Accepted Manuscript* or any consequences arising from the use of any information it contains.

## Scaffold-based regeneration of skeletal tissues to meet clinical challenges

*Jiao Jiao Li<sup>1</sup>, David L. Kaplan<sup>2</sup>, Hala Zreiqat<sup>1\*</sup>*

<sup>1</sup>Biomaterials and Tissue Engineering Research Unit, School of AMME, University of Sydney, Sydney, NSW 2006, Australia

<sup>2</sup>Department of Biomedical Engineering, Tufts University, Medford, MA 02155, USA

\*Correspondence to: A/Prof Hala Zreiqat Email: hala.zreiqat@sydney.edu.au

**Keywords:** Scaffold; Bone regeneration; Cartilage regeneration; Osteochondral; Bioactive Ceramic; Silk; Coating

### Abstract

The management and reconstruction of damaged or diseased skeletal tissues have remained a significant global healthcare challenge. The limited efficacy of conventional treatment strategies for large bone, cartilage and osteochondral defects has inspired the development of scaffold-based tissue engineering solutions, with the aim of achieving complete biological and functional restoration of the affected tissue in the presence of a supporting matrix. Nevertheless, significant regulatory hurdles have rendered the clinical translation of novel scaffold designs to be an inefficient process, mainly due to the difficulties of arriving at a simple, reproducible and effective solution that does not rely on the incorporation of cells and/or bioactive molecules. In the context of the current clinical situation and recent research advances, this review will discuss scaffold-based strategies for the regeneration of skeletal tissues, with focus on the contribution of bioactive ceramic scaffolds and silk fibroin, and combinations thereof, towards the development of clinically viable solutions.

### 1. Introduction

Trauma and disease of skeletal tissues often involve structural damage to bone and cartilage, resulting in severe pain and disability for millions of people worldwide and represent major clinical challenges. Over the past two decades, significant advances have been made in the development of biomaterial scaffolds for the repair and regeneration of skeletal tissues via

tissue engineering strategies (**Fig. 1**). Many promising results have been obtained in the laboratory and in preclinical models, but clinical translation has remained a lengthy process. A highlight of this review is the development of silk-coated ceramic scaffolds for more effective reconstruction of skeletal tissues, which holds potential for rapid clinical translation. Building towards this, the role of ceramic scaffolds as competitive choices for clinical bone reconstruction will be discussed, as well as research into silk fibroin as a promising polymeric biomaterial for the regeneration of skeletal tissues. The review will also address current progress and challenges in the regeneration of osteochondral tissues at joint surfaces, which involve both articular cartilage and subchondral bone. An overview of existing scaffold strategies for osteochondral regeneration will be presented, and potential contributions of silk and silk-coated ceramic scaffolds will be highlighted.

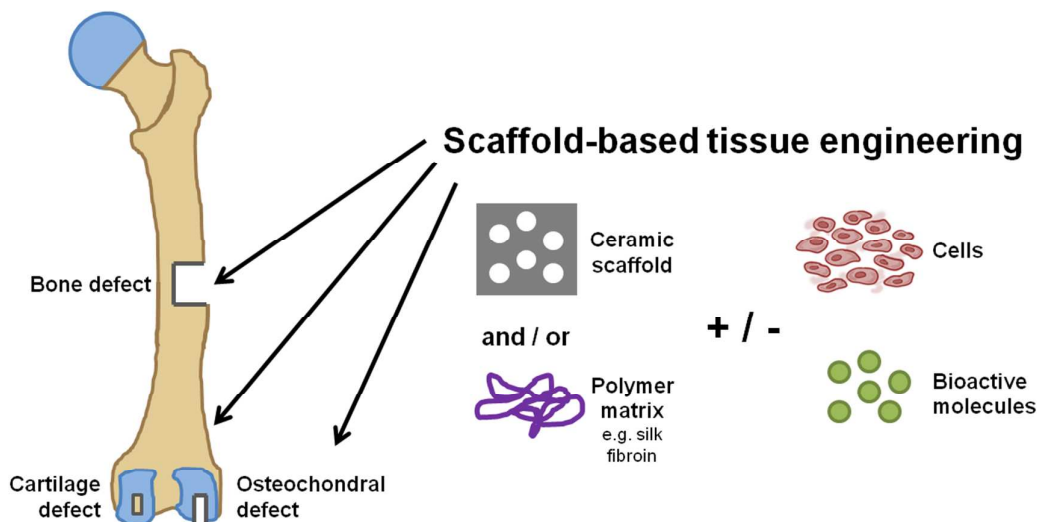


**Fig. 1** The concept of skeletal tissue regeneration via scaffold-based tissue engineering strategies.

## 2. The need to develop biomaterial scaffolds for the regeneration of skeletal tissues

Many clinical treatment options exist for the healing of bone and cartilage defects. However, none has proven to be fully satisfactory in terms of achieving optimal regenerative outcomes or the complete and permanent restoration of function. Large defects have remained particularly problematic due to the lack of adequate clinical options for their treatment to date. Such clinical challenges have necessitated the development of biomaterial scaffolds to augment the repair and regeneration of skeletal tissues.

## 2.1 Clinical status for the treatment of bone defects and scaffold requirements

Bone is a highly dynamic and vascularised tissue that provides vital structural support to the body, and undergoes constant remodelling via the processes of bone deposition by osteoblasts and bone resorption by osteoclasts.<sup>1</sup> For this reason, bone has innate regenerative potential and most bone lesions can heal well with conventional conservative therapy or surgery provided that skeletal continuity is not disrupted. However, complete repair is unlikely if the defect reaches a critical size and natural bone tissue cannot regenerate across the gap.<sup>2</sup> Such defects, if left untreated, will not heal spontaneously during the lifetime of the animal.<sup>3</sup> **Table 1** shows the critical sizes of bone defects in humans and various *in vivo* models. The treatment of large traumatic and post-surgical bone defects is challenging, and often requires reconstructive orthopaedic surgery for skeletal continuity to be restored and bone function to be regained.<sup>4</sup> The current clinical dilemma is that the two main categories of surgical treatment for large bone defects, namely bone transport methods (Ilizarov technique) and bone graft transplantation, still experience significant limitations that impair their success. Bone transport methods take advantage of the regenerative potential of bone.<sup>5</sup> However, these procedures require long recovery times, bring substantial inconvenience to the patient, and often result in high complication rates.<sup>5,6</sup> Bone grafts are widely used for the clinical reconstruction of critical-sized bone defects and represent the second most common transplantation tissue.<sup>7</sup> Autograft transplantation remains the gold standard for bone grafting and has high success rates of 80–90% with no risk of immune rejection.<sup>8</sup> However, complications and non-unions are also common, and application of the procedure is restricted by donor site morbidity and limited availability for large reconstructions.<sup>9,10</sup> Allograft transplantation is frequently performed as an alternative. Although more abundant, allografts yield more variable clinical results and pose potential risks of immune rejection and disease transmission.<sup>11,12</sup> Freeze-drying the allograft minimises immunogenicity but reduces its mechanical integrity and ability to integrate with host bone.<sup>7</sup>

Due to the challenges experienced with clinical reconstruction of critical-sized bone defects using conventional approaches, there has been increasing research focus towards the development of biomaterial scaffolds to serve as synthetic bone graft substitutes. The healing of critical-sized bone defects often requires regeneration of large amounts of cancellous bone, which is an interconnected network of small bone trabeculae containing vasculature and bone marrow.<sup>1</sup> The extracellular matrix (ECM) of bone consists of an organic phase comprising collagen fibres (mainly collagen type I) and noncollagenous proteins (including osteopontin,

bone sialoprotein, osteonectin and osteocalcin), and a mineral phase comprising plate-like hydroxyapatite crystals which occupy discrete spaces within the organic matrix.<sup>13</sup> An optimal bone scaffold replicates the structure and functions of the ECM to provide guidance and support during bone tissue development, and should have the following characteristics:<sup>14,15</sup>

- Biocompatible and facilitates integration with native bone, by allowing the formation of bone tissue, and not fibrous tissue, at the bone-scaffold interface to provide anchorage.<sup>16</sup>
- Osteoconductive and osteoinductive. An osteoconductive scaffold allows the attachment, growth, and ECM formation of bone-related cells on its surface and pores, while an osteoinductive scaffold can actively induce new bone formation via biomolecular signalling and recruitment of osteoprogenitor cells.<sup>16</sup>
- Mechanically compatible with native bone and promote proper load transfer, by matching the mechanical properties of cancellous bone which have midrange values of 2–12 MPa for compressive strength and 50–500 MPa for modulus.<sup>17,18</sup>
- Highly porous and interconnected to promote vascularisation and facilitate nutrient and oxygen exchange. The scaffold should match the porosity of cancellous bone at 50–90%,<sup>19</sup> and pore sizes of 100–500 $\mu$ m are considered as optimal for encouraging cell attachment, migration and ingrowth throughout the scaffold.<sup>20</sup>
- Have suitable surface characteristics, including surface chemistry and topography, to direct the attachment, proliferation and differentiation of osteoprogenitor cells.
- Biodegradable at a controlled rate that is coupled to the rate of new bone formation with no release of toxic or inhibitory products.

## 2.2 Clinical status for the treatment of cartilage defects and scaffold requirements

Articular cartilage is composed of hyaline cartilage and allows smooth and frictionless joint motion with substantial durability.<sup>21</sup> However, once damaged, articular cartilage has limited capacity for self-repair and regeneration due to its avascular and aneural nature.<sup>22</sup> A further limiting factor is its low density of chondrocytes, which have low mitotic potential and are embedded in rich hydrated ECM composed primarily of collagen type II and proteoglycans (mainly aggrecan).<sup>22,23</sup> There are two types of focal cartilage defects: partial-thickness and full-thickness.<sup>24</sup> A partial-thickness defect is limited to the cartilage and has poor capacity for spontaneous repair. A full-thickness defect penetrates through the cartilage to the level of the subchondral bone, and is classified as an osteochondral defect in the event that the

damage extends into the subchondral bone (**Fig. 2**).<sup>25</sup> Such defects can access stem cell populations to undergo some spontaneous healing through the formation of fibrocartilage, which contains a high percentage of collagen type I. However, fibrocartilage is mechanically and biologically inferior to hyaline cartilage and undergoes gradual degradation.<sup>24</sup> Both partial- and full-thickness cartilage defects, as well as osteochondral defects, can expand over time and escalate degenerative processes resulting in osteoarthritis.<sup>26</sup> **Table 1** shows the critical sizes of cartilage defects in humans and various *in vivo* models. The adequate treatment of cartilage defects has been a longstanding clinical dilemma. Current cartilage repair techniques mainly benefit by relieving symptoms and functional limitations rather than the restoration of fully functional hyaline cartilage, and long-term outcomes are often unsatisfactory. Surgical treatment for cartilage defects can be reparative or restorative. Reparative or marrow stimulation techniques, including microfracture, can reduce pain and swelling by inducing the formation of fibrocartilage to cover exposed bone, but lack clinical durability and show functional decline over time.<sup>27,28</sup> Restorative techniques include joint replacements, osteochondral grafts and autologous chondrocyte implantation (ACI). Joint replacements are performed in cases of cartilage layer separation from subchondral bone or large osteochondral defects, which provides functional restoration but is limited by the lifetime of the prosthesis (approximately 20 years).<sup>24</sup> Osteochondral grafts include autografts (mosaicplasty) and allografts. Although effective with good long-term outcomes, this technique can only be applied to small lesions less than 4cm<sup>2</sup> and is limited by the availability of donor tissue.<sup>21</sup> ACI is used for full-thickness cartilage defects or osteochondral defects, and involves harvesting and *in vitro* expansion of autologous chondrocytes which are subsequently implanted into the defect. The first generation of this technique produced 80–90% satisfaction with good medium- to long-term outcomes,<sup>29,30</sup> but experienced limitations relating to graft fixation<sup>31</sup> and chondrocyte senescence and dedifferentiation in culture.<sup>22</sup> To address these limitations, second generation matrix-induced ACI (MACI) has been developed and utilises a biomaterial scaffold such as a collagen membrane to act as a chondrocyte carrier. This technique has generally shown good short- to medium-term clinical results,<sup>32,33</sup> but long-term results are still lacking. Recent third generation techniques aim to reduce surgical intervention, as well as improve mechanical and biological properties of the implant and initial fixation, but very limited clinical information is available on their use.<sup>34</sup>

The lack of a consistent, superior and reliable clinical method for the treatment of cartilage defects has directed research towards tissue engineering strategies. Unlike for bone, the

essential properties of a scaffold for cartilage regeneration are less clearly defined. In general, the scaffold should be biocompatible and provide initial mechanical stability. For effective cartilage regeneration, the scaffold should promote uniform cell distribution and occupy the entire defect site to achieve optimal integration with surrounding native cartilage.<sup>24</sup> The scaffold should also have sufficient mechanical properties to withstand *in vivo* articulation forces, while allowing remodelling and gradual replacement by naturally synthesised cartilage ECM.<sup>35</sup> Optimal regenerative outcomes may rely on the ability of the scaffold to drive cell proliferation and differentiation by mimicking the ECM environment of native cartilage.<sup>36</sup> To this end, several natural polymers have been employed as cartilage scaffold materials including collagen, hyaluronic acid, gelatin, fibrin glue, chitosan, agarose and alginate. These materials can facilitate enhanced biological interaction, but may experience problems with suboptimal mechanical strength, antigenicity, and rapid or variable host-related degradation.<sup>37</sup>

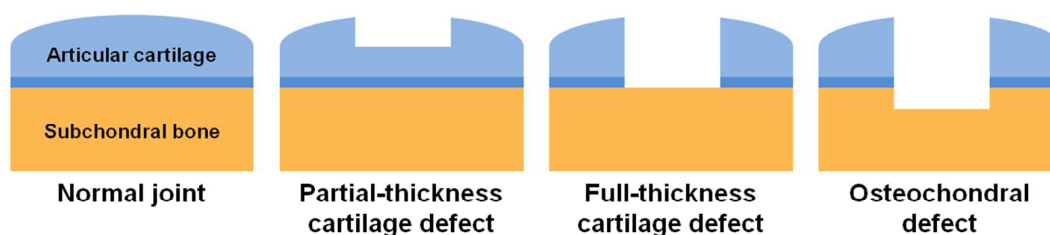


**Fig. 2** Types of focal defects in articular joint injury.

### 2.3 Scaffold fabrication techniques

The engineering of functional tissues relies on the realisation of scaffold designs which facilitate cell distribution, guide tissue regeneration in three dimensions, and mimic the macroscopic and microscopic features of native tissues. A variety of fabrication techniques have been utilised to manufacture 3D scaffolds from ceramic and polymeric biomaterials for the regeneration of bone, cartilage and osteochondral tissues (**Fig. 3**). These techniques are summarised in **Table 2** together with a list of example studies.

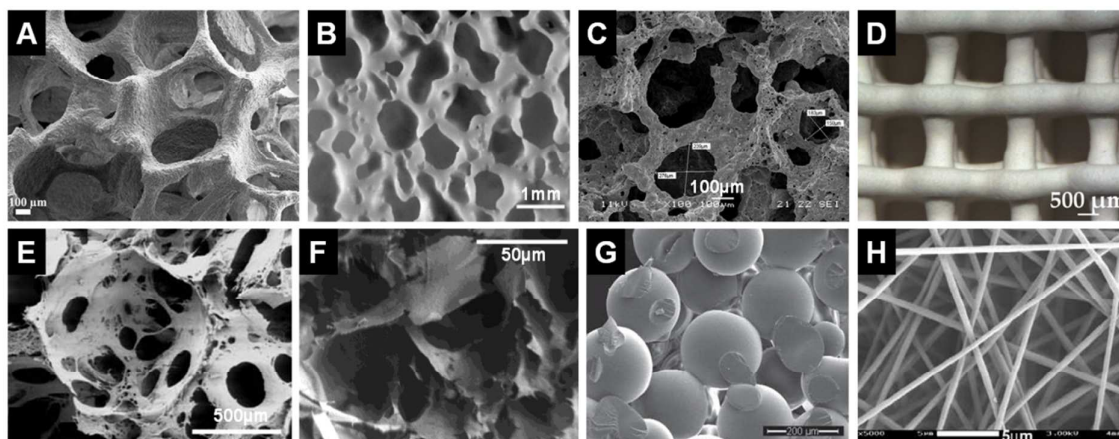


**Fig. 3** Representative internal structures of porous scaffolds produced via (A) polymer sponge replication,<sup>38</sup> (B) impregnate sintering,<sup>39</sup> (C) gel-cast foaming,<sup>40</sup> (D) solid free-form fabrication,<sup>41</sup> (E) solvent casting and particulate leaching,<sup>42</sup> (F) phase separation,<sup>43</sup> (G) microsphere sintering,<sup>44</sup> and (H) electrospinning.<sup>45</sup> (A) Adapted with permission from Elsevier, Copyright © 2013; (B) adapted with permission from John Wiley and Sons, Copyright © 2006 Orthopaedic Research Society; (C, D) adapted with permission from Elsevier, Copyright © 2011; (E) adapted with permission from Elsevier, Copyright © 2005; (F) adapted with permission from American Chemical Society, Copyright © 2004; (G) adapted with permission from John Wiley and Sons, Copyright © 2013 WILEY-VCH Verlag GmbH & Co. KGaA, Weinheim; (H) adapted with permission from Elsevier, Copyright © 2006.

### 3. Bioactive ceramic scaffolds for bone regeneration in a clinical setting

Bioactive and biodegradable ceramic scaffolds are competitive choices for bone graft substitutes in the clinical reconstruction of critical-sized bone defects. The most widely studied ceramic scaffolds for clinical bone regeneration include hydroxyapatite, beta-tricalcium phosphate ( $\beta$ -TCP), biphasic calcium phosphate (BCP), and bioactive glass. These materials are inherently bioactive as they share similarities in chemical composition and surface structure with the mineral phase of bone, which consists of plate-like hydroxyapatite crystals.<sup>13</sup> The bioceramic can form a direct bond with bone through ion release and substitution mechanisms at the scaffold surface,<sup>46</sup> as well as mediate the adsorption of bone ECM proteins.<sup>47</sup> These processes create a favourable environment for the attachment, proliferation and differentiation of osteoprogenitor cells resulting in enhanced bone formation.<sup>47</sup> An additional advantage offered by ceramic scaffolds in bone regeneration is

their relative ease of fabrication into a porous and interconnected structure resembling cancellous bone, through methods such as polymer foam replication<sup>48,49</sup> and, more recently, solid free-form fabrication (or rapid prototyping).<sup>50</sup> Ceramic scaffolds which are frequently employed for clinical bone reconstruction will be discussed, and some of the common and unaddressed challenges will be identified.

### 3.1 Calcium phosphates

Calcium phosphate ceramics have had a long history of application in bone regeneration due to their chemical similarity to the natural composition of bone mineral. The bioactive properties of calcium phosphate-based scaffolds originate from their ability to form a carbonate apatite (CHA) layer at the bone-scaffold interface.<sup>51</sup> This creates an intimate physicochemical and mechanical bond between the scaffold and host bone, which encourages bone formation and ingrowth.<sup>52</sup> The mineralised interface is thought to be formed by a cell-mediated dissolution and precipitation process, where the release of calcium and phosphate ions from the scaffold into the microenvironment encourages the precipitation of CHA microcrystals. The bone ECM surrounding the scaffold hence becomes richly mineralised, producing a favourable environment for bone formation.<sup>53</sup> Furthermore, there is evidence to suggest that the higher concentrations of extracellular calcium and phosphate adjacent to the scaffold may exert beneficial effects in osteogenesis. High calcium concentrations can stimulate chemotaxis<sup>54,55</sup> and osteogenic differentiation<sup>54,56</sup> of osteoprogenitor cells, while phosphate is believed to play a key role in bone matrix mineralisation, partly by inducing the production of mineralisation-related proteins such as osteopontin via the activity of alkaline phosphatase.<sup>57,58</sup> The most commonly used calcium phosphate-based ceramics for clinical bone reconstruction are hydroxyapatite,  $\beta$ -tricalcium phosphate ( $\beta$ -TCP) and biphasic calcium phosphate (BCP).

#### 3.1.1 Hydroxyapatite

Commercially available hydroxyapatite is either naturally derived from sea coral or synthetically prepared by precipitation under basic conditions and subsequent sintering. Stoichiometric hydroxyapatite ( $\text{Ca}_{10}(\text{PO}_4)_6(\text{OH})_2$ ) has a calcium to phosphate (Ca/P) ratio of 1.67 and is the closest in composition to bone mineral.<sup>59</sup> Early uses of porous hydroxyapatite as a bone graft substitute showed no adverse reactions and good functional recovery over 5 years of long-term follow-up.<sup>60</sup> Clinical reports on bone reconstruction using hydroxyapatite scaffolds combined with autologous osteoprogenitor cells have demonstrated good scaffold-

bone integration in large (4–7cm) bone defects within 2 months post-implantation<sup>61</sup> which was maintained over 6–7 years,<sup>62</sup> functional restoration of a stable and biomechanically sound thumb after 28 months in a distal phalanx replacement,<sup>63</sup> and immediate healing potential when implanted into bone defects created by tumour resection.<sup>64</sup> Experimental studies have confirmed the ability of hydroxyapatite to induce changes in osteoblast gene expression to influence osteogenic outcomes.<sup>65,66</sup> However, the application of hydroxyapatite in bone reconstruction at load-bearing sites is limited by its low solubility and mechanical properties. Hydroxyapatite scaffolds and particles showed little biodegradation after implantation in long bone segmental defects for 5 years<sup>61,67</sup> and in the mandible for 9 years.<sup>68</sup> Persisting hydroxyapatite at the implantation site interferes with bone formation and is prone to mechanical failure. This weakness is amplified by the brittleness of hydroxyapatite and its low resistance to crack growth and propagation.<sup>69</sup> Furthermore, due to its low surface reactivity, hydroxyapatite is osteoconductive but not osteoinductive,<sup>47</sup> and often needs to be combined with autologous stem cells to enhance its bioactivity in clinical applications. Recent research has attempted to address these drawbacks by making ionic substitutions in the structure of hydroxyapatite.<sup>70</sup> Cationic substitutions for calcium include zinc,<sup>71,72</sup> strontium<sup>73,74</sup> and magnesium,<sup>75</sup> while anionic substitutions for phosphate include silicate,<sup>76,77</sup> all of which are essential trace elements in the human body with the ability to stimulate bone formation and/or reduce bone resorption. These substitutions have been shown to improve the bioactivity and biodegradability of hydroxyapatite.

### 3.1.2 $\beta$ -TCP

$\beta$ -TCP is the stable phase of tricalcium phosphate ( $\text{Ca}_3(\text{PO}_4)_2$ ) at low sintering temperatures (below 1100°C) and has a Ca/P ratio of 1.5.<sup>59,78</sup> Its high biodegradability allows rapid precipitation of a surface CHA layer in physiological fluid,<sup>79</sup> which contributes to the reported osteoconductive and sometimes osteoinductive properties of  $\beta$ -TCP.  $\beta$ -TCP scaffolds implanted into *in vivo* models showed the presence of new bone after 7 days and consistent bone formation over 4 weeks in the rat femoral condyle,<sup>80</sup> complete repair of a goat tibial defect with restoration of normal biomechanical properties after 32 weeks when combined with autologous bone marrow stromal cells,<sup>81</sup> and ability to induce ectopic bone formation in dog dorsal muscle as evidence of their osteoinductive properties.<sup>82</sup> When employed as a bone graft substitute in clinical bone reconstruction,  $\beta$ -TCP scaffolds showed excellent incorporation and remodelling into new bone, coupled with good resorption, over follow-up periods of 2–3 years by clinical, radiographic and histological assessment in a wide

spectrum of indications.<sup>83,84</sup> Early histological assessment of implanted scaffolds showed bioresorption by osteoclasts, osteoblast attachment, and vascular invasion into the macropores after 14 days, as well as direct bonding with host bone and prominent bone formation after 28 days (**Fig. 4**).<sup>85</sup>  $\beta$ -TCP scaffolds used to treat bone cavity defects were reported to allow fast functional recovery with return to unrestricted daily activities within 3 months,<sup>86</sup> while those used to fill bone defects from tumour resection encouraged bone remodelling by undergoing complete or partial resorption and replacement by new bone.<sup>87,88</sup> The results of these clinical studies established the osteoconductive properties of  $\beta$ -TCP, while its osteoinductive properties were suggested by the ability of  $\beta$ -TCP particles to attract and localise osteoprogenitor cells in human maxillary sinus floor elevation.<sup>89</sup> A major drawback of  $\beta$ -TCP scaffolds in clinical application, however, is its rapid degradation *in vivo* accompanied by loss of scaffold integrity, which may impede bone formation. One study reported less than 5% of  $\beta$ -TCP scaffolds remaining after being implanted for 24 weeks in the cancellous bone of sheep, and faster scaffold resorption was correlated with lower bone content.<sup>90</sup> Another study reported that the rapid dissolution of  $\beta$ -TCP scaffolds in rabbit osteochondral defects resulted in loss of scaffold integrity and generated significant amounts of loose particulate debris, which provoked an inflammatory response leading to impaired and reversed bone apposition at the defect site.<sup>91</sup> The high solubility of  $\beta$ -TCP may exceed the rate of tissue regeneration and complicate clinical outcomes due to decoupling of scaffold degradation and bone formation,<sup>86</sup> and may lead to imbalances in bone remodelling resulting in net bone loss at the defect site.<sup>92</sup>

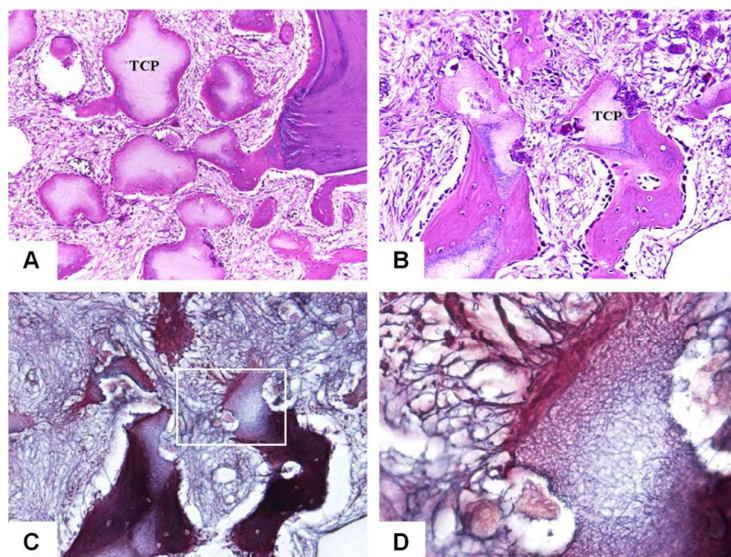


**Fig. 4** Histological assessment of a porous  $\beta$ -TCP implant harvested 4 weeks after implantation into the femur of a patient. Haematoxylin and eosin staining showed marked

new bone formation around the implant which was (A) directly connected to existing bone with lamellar structure, and (B) lined by osteoblasts. (C) Silver impregnation of a serial section of (A) showed (D) numerous collagen fibrils within the implant which was directly connected to the newly formed bone. Original magnification: (A–C) 50×; (D) 200×.<sup>85</sup> Adapted with permission from Elsevier, Copyright © 2006.

### 3.1.3 BCP

BCP is a two-phase ceramic composed of hydroxyapatite (HA) and  $\beta$ -TCP phases, which is obtained by either physically mixing the two powders or chemically sintering calcium-deficient apatite (Ca/P ratio < 1.67) at temperatures above 700°C.<sup>93</sup> The reactivity of BCP increases with decreasing HA/ $\beta$ -TCP ratio. The biodegradability of BCP can therefore be tailored to match the rate of bone formation, by controlling the phase composition to achieve an optimal balance between the more stable hydroxyapatite phase and the more soluble  $\beta$ -TCP phase.<sup>94</sup> BCP ceramics with HA/ $\beta$ -TCP ratios between 20/80 to 60/40 have typically displayed favourable degradation behaviour and ability to induce bone formation *in vivo*.<sup>95-97</sup> The osteoconductive and osteoinductive properties of BCP have been demonstrated in a wide range of *in vivo* models. BCP scaffolds implanted in the canine femoral cortex showed vascularised bone ingrowth after 6 weeks, the outer region of which was transformed into cortical bone after 18 weeks and was accompanied by bone remodelling.<sup>98</sup> In the rabbit femur or femoral condyle, extensive osteoconduction and major bone mass gain was observed in BCP scaffolds, with direct deposition of well-organised and mineralised lamellar bone around and inside the scaffold pores after 1–2 months.<sup>99-101</sup> BCP scaffolds loaded with mesenchymal stem cells (MSCs) were able to completely bridge critical-sized femoral defects in the rat and dog after 8 and 16 weeks, respectively.<sup>102</sup> Compared to hydroxyapatite or  $\beta$ -TCP scaffolds, BCP scaffolds showed advanced bridging of orthotopic bone defects in the dog<sup>103</sup> and goat<sup>104</sup> with significantly higher rate and amount of bone formation. The osteoinductive properties of BCP ceramics were demonstrated by ectopic bone formation in various *in vivo* models including the mouse,<sup>95</sup> rabbit,<sup>105,106</sup> dog,<sup>103,106</sup> goat,<sup>104,107,108</sup> sheep<sup>109</sup> and pig,<sup>110</sup> where BCP was found to be superior to hydroxyapatite,<sup>103,104,106,107</sup>  $\beta$ -TCP,<sup>105</sup> or both,<sup>95</sup> and was even comparable if not superior to autograft and allograft controls when combined with autologous MSCs.<sup>108</sup> Furthermore, the ectopic bone induced by BCP implants was shown to be mature<sup>109</sup> and sustainable *in vivo*.<sup>110</sup> More definitive evidence for the osteoinductivity of BCP ceramics was established by *in vitro* and *in vivo* studies

specifically investigating the interactions between BCP and MSCs. *In vitro* studies showed that BCP surfaces were able to stimulate osteogenic development in MSCs, as assessed by gene expression and alkaline phosphatase activity, in growth medium without the addition of osteogenic supplements.<sup>111,112</sup> An *in vivo* study in a canine model also proved the ability of BCP to induce the homing of MSCs from circulation to participate in ectopic bone formation at the implant site without growth factor delivery.<sup>113</sup> Other than differences in chemical composition, the better osteoinductive properties of BCP compared to hydroxyapatite or  $\beta$ -TCP may be partly attributed to differences in microstructure. Surface microporosity is characteristic of BCP ceramics, which may improve *in vivo* osteogenic outcomes by providing higher specific surface area for cellular interaction,<sup>39</sup> or facilitating multi-scale osteointegration where micropores are filled by osteogenic cells which proceed to form osteoid and mineralised matrix (**Fig. 5**).<sup>114</sup>

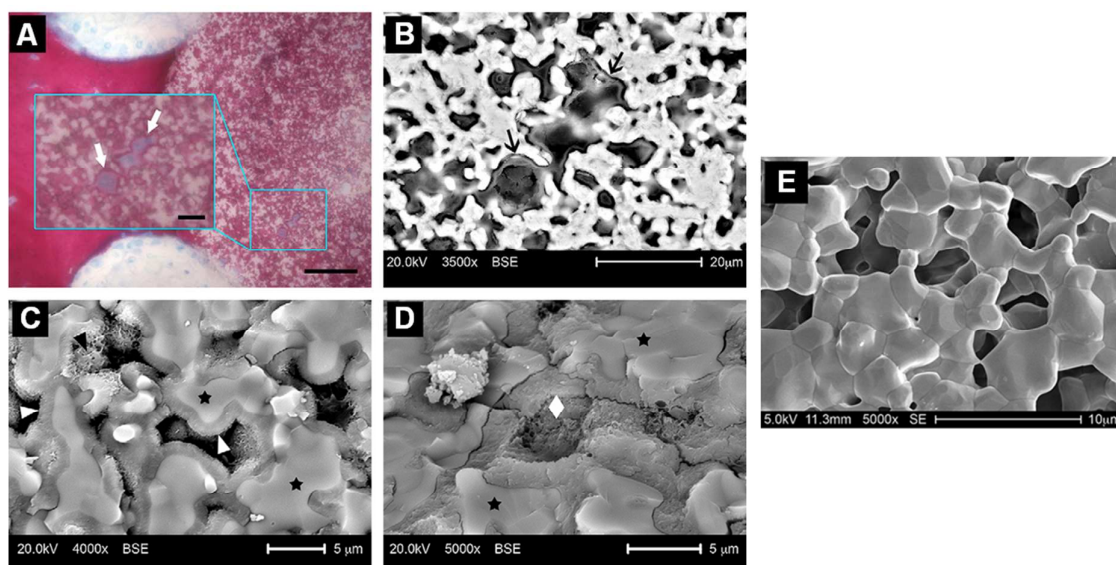


**Fig. 5** Bone formation in BCP scaffolds following *in vivo* implantation commenced with coating of the micropores. **(A)** Histological staining showed scaffold micropores coated with red/pink staining indicative of mineralised bone (white arrows), while the interiors stained blue/purple similar to osteoid or other soft tissue. **(B)** Bone coating in the same area as **(A)** was also shown via backscatter electron mode (BSE) scanning electron microscopy (SEM) (black arrows). BSE SEM images of fracture surfaces from implanted scaffolds showed **(C)** uniform bone coating approximately 1 $\mu$ m thick (white arrowheads) deposited within the micropores of BCP (black stars), the interiors of which appeared to be filled with unmineralised tissue (black arrowheads), and **(D)** a micropore of the BCP scaffold that was almost completely filled with bone (white diamond). **(E)** Surface microstructure of BCP

scaffold prior to implantation contained micropores measuring approximately  $5\mu\text{m}$ . Scale bars: (A)  $50\mu\text{m}$ ; (A, inset)  $12.5\mu\text{m}$ . Survival times: (A–C) 12 weeks; (D) 6 weeks.<sup>114</sup> Adapted with permission from Elsevier, Copyright © 2010.

Clinically, various forms of BCP have found application in maxillary sinus augmentation, filling of tibial osteotomies, and a wide range of orthopaedic reconstructions. Solid or macroporous particles of BCP used in maxillary sinus augmentation showed close contact with new bone which frequently bridged the particles,<sup>115,116</sup> as well as excellent implant survival and maintenance of function over 1–2 years.<sup>117</sup> When used as fillers in high tibial osteotomy, BCP in the form of macroporous granules achieved bone union by clinical and radiographic evaluation with no sign of osteotomy after 2 years,<sup>118</sup> while macroporous wedges showed considerable ingrowth of well-organised and mineralised lamellar and trabecular bone at 1 year with coupled implant degradation (**Fig. 6**).<sup>119</sup> Porous forms of BCP employed in a range of orthopaedic procedures showed fast integration and bone reconstruction both close to and within the implants,<sup>98,120</sup> with good to excellent final results.<sup>121</sup> Nevertheless, the application of BCP ceramics in clinical bone reconstruction is limited by their lack of mechanical strength, particularly in the porous forms required to encourage bone formation and ingrowth. For this reason, BCP is more frequently utilised in particulate form and as fillers, and its current uses are typically restricted to the treatment of bone defects at non-load bearing sites.<sup>122</sup> Alternatively, BCP implants need to be combined with internal or external fixation to achieve favourable reconstructive outcomes in large or load-bearing bone defects.<sup>119,121</sup>

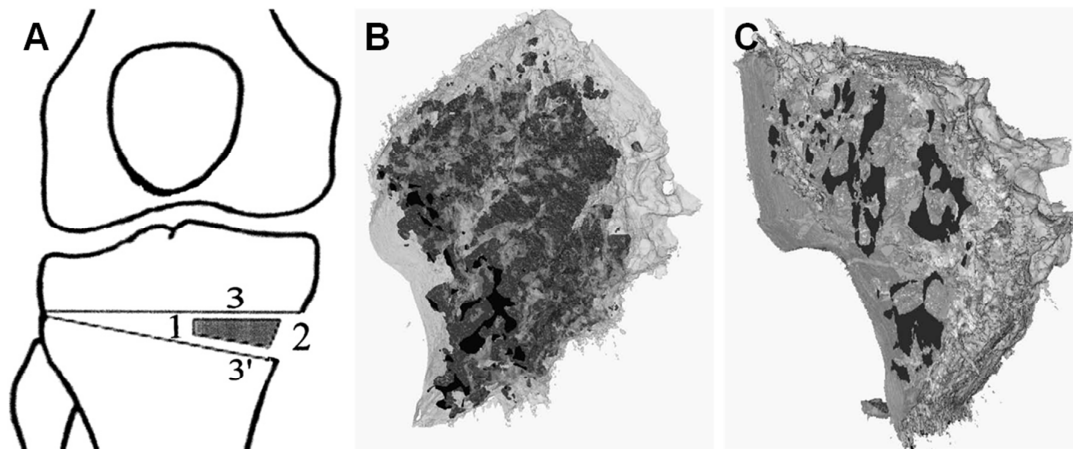


**Fig. 6** (A) Schematic showing the use of a macroporous BCP wedge as filler in high tibial osteotomy. (B) 3D reconstruction of a biopsy using microtomography after 1 year of implantation into a patient, and (C) cross-section of the biopsy. Newly formed bone was

shown in transparent grey and residual BCP was shown in black. The interconnected trabecular structure of the BCP implant was transformed into bone and only residual BCP particles remained, which were fully integrated and in close contact with the newly formed bone.<sup>119</sup> Adapted with permission from Elsevier, Copyright © 2009.

### 3.2 Bioactive glasses

Bioactive glasses consist of a silica network containing network modifiers bonded to the network via non-bridging oxygen bonds, such as calcium, sodium and phosphorus. The original and most widely investigated bioactive glass composition is Bioglass<sup>®</sup> 45S5 (45 wt% SiO<sub>2</sub>, 24.5 wt% Na<sub>2</sub>O, 24.5 wt% CaO and 6 wt% P<sub>2</sub>O<sub>5</sub>).<sup>123</sup> Hench, who pioneered the concept of bioactive glass, systematically studied a series of glasses in the SiO<sub>2</sub>–Na<sub>2</sub>O–CaO–P<sub>2</sub>O<sub>5</sub> four-component system with constant 6 wt% P<sub>2</sub>O<sub>5</sub> and divided their compositions into different regions based on bioactivity.<sup>124</sup> Bioactive glasses in region A with <60 mol% SiO<sub>2</sub>, high Na<sub>2</sub>O and CaO content, and high CaO:P<sub>2</sub>O<sub>5</sub> ratio are highly bioactive and can bond chemically to bone. 45S5 is representative of glasses with the highest level of bioactivity at the centre of region A, which bond rapidly with bone and even with soft tissues.<sup>125</sup> Different compositions of bioactive glass have been produced via the incorporation of various metallic oxides including MgO, SrO, ZnO, Fe<sub>2</sub>O<sub>3</sub>, B<sub>2</sub>O<sub>3</sub>, K<sub>2</sub>O, CaF<sub>2</sub> and TiO<sub>2</sub>, although the best biological properties remain to be held by the original 45S5 composition.<sup>126</sup> The bioactivity and bone bonding ability of bioactive glass are the result of rapid surface reactions which occur within 24 hours of implantation, thereby accelerating the formation of a CHA layer on the glass surface.<sup>124</sup> This CHA layer, which has similar composition to bone mineral, is believed to initiate the biochemical adsorption of growth factors and a synchronised sequence of cellular events that result in rapid formation of new bone.

The osteogenic properties of bioactive glass have been confirmed via a range of *in vitro* studies. Osteoprogenitor cells cultured on bioactive glass were able to proliferate, express markers of the osteoblast phenotype and form mineralised nodules as evidence of commitment to osteogenesis in the absence of osteogenic medium supplements.<sup>127-130</sup> Similar observations were made in human foetal osteoblasts exposed to dissolution products of Bioglass 45S5, suggesting that bioactive glass implants have the ability to recruit osteoprogenitor cells *in vivo* and induce differentiation along the osteogenic lineage.<sup>131,132</sup> The ionic dissolution products of bioactive glass, such as calcium and silicon, have been shown to affect the osteoblast cell cycle and induce both intracellular and extracellular

responses.<sup>133</sup> The activation or upregulation of several families of genes have been reported, including cell cycle regulators, growth factors, cell surface receptors and extracellular matrix regulators (**Fig. 7**).<sup>134-136</sup> Importantly, there is evidence that bioactive glass upregulates a range of bone-related genes including Cbfa1/Runx2, collagen type I, alkaline phosphatase, bone sialoprotein, osteopontin, osteocalcin, osteonectin, and bone morphogenetic protein (BMP)-2.<sup>137</sup> Bioactive glass has also been shown to stimulate the secretion of angiogenic growth factors such as vascular endothelial growth factor (VEGF) *in vitro* and enhance vascularisation *in vivo*, which becomes relevant for the production of large tissue engineered constructs.<sup>138,139</sup>

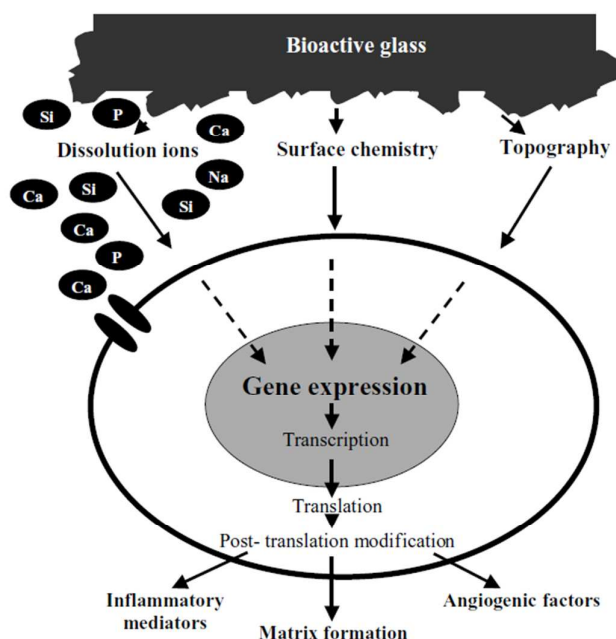


**Fig. 7** Mechanisms of gene expression regulation by bioactive glasses.<sup>137</sup> Reprinted with permission from Springer, Copyright © 2006.

Two compositions of bioactive glass are in clinical use for orthopaedic reconstructions in particulate form: 45S5 and S53P4 (53 wt% SiO<sub>2</sub>, 23 wt% Na<sub>2</sub>O, 20 wt% CaO and 4 wt% P<sub>2</sub>O<sub>5</sub>).<sup>123</sup> The feasibility of using bioactive glass particles to repair cancellous bone defects has been demonstrated in several *in vivo* models. Early and significant bone ingrowth was observed in the rabbit femur, with compressive properties of grafted defects matching normal bone by 12 weeks.<sup>140-142</sup> Other studies in the rabbit,<sup>143-145</sup> dog<sup>146</sup> and monkey<sup>147</sup> showed that both the quantity and rate of bone formation at the defect site were superior for bioactive glass particles compared to hydroxyapatite and other calcium phosphates. The osteoinductive properties of bioactive glass were also demonstrated by ectopic bone formation in a canine

model.<sup>148</sup> Clinically, bioactive glass particles elicited excellent tissue response in the treatment of periodontal defects, with stable outcomes over 1–2 years which were comparable to or exceeded conventional surgical or grafting procedures.<sup>149-154</sup> Bioactive glass particles used as a bone graft substitute in the treatment of tibial plateau fractures showed comparable performance to bone autografts both functionally and clinically while avoiding donor site complications.<sup>155,156</sup> Similar results were observed in the treatment of benign bone tumours with good long-term outcomes.<sup>157,158</sup> Other clinical uses of bioactive glass particles as a bone graft substitute also showed optimistic results with few complications, including in maxillary sinus augmentation,<sup>159</sup> spinal fusion<sup>160</sup> and treatment of osteomyelitis.<sup>161</sup> The benefits of using bioactive glass as a bone graft substitute lie in its bone bonding ability and osteogenic properties, as well as ease in controlling its chemical composition to produce tailored degradation rates matching the rate of bone ingrowth and remodelling.<sup>162</sup> However, the particulate systems in clinical use lack dimensional stability and, in the absence of additional fixation, are only useful in the treatment of bone cavity defects. Bioactive glass scaffolds are likely to be much more effective as synthetic bone grafts, since they can act as porous templates that imitate the structure of cancellous bone, but these scaffolds have not yet reached clinical translation for two main reasons. Firstly, the low mechanical strength and fracture toughness of bioactive glass are exacerbated in porous form, which limits its application at load-bearing sites.<sup>17</sup> Secondly, when glass particles of commercial composition 45S5 or S53P4 are fused via sintering to form porous scaffolds, they crystallise or partially crystallise to form a glass-ceramic. However, full crystallisation reduces bioactivity while partial crystallisation can lead to instability, which weakens the osteogenic ability of the scaffold.<sup>163</sup> Recent research has attempted to overcome this problem by modifying the glass composition to prevent crystallisation during sintering,<sup>164-166</sup> avoiding the sintering required for conventional melt-derived glasses by synthesising sol-gel glasses,<sup>167-170</sup> and exploring different processing routes to produce porous bioactive glass scaffolds from both melt- and sol-gel derived glasses (Fig. 8).<sup>40,41,48,171-174</sup>

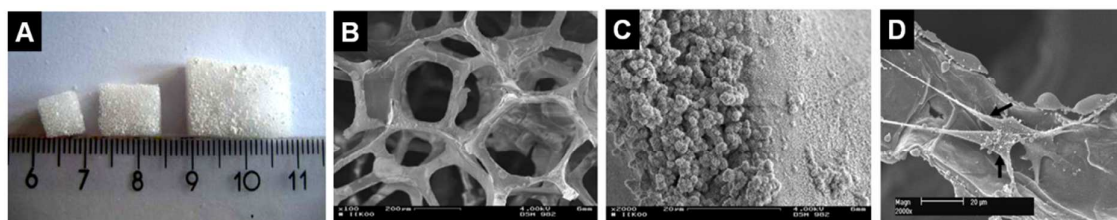


**Fig. 8** (A) Mesoporous bioactive glass scaffolds prepared for bone tissue engineering applications. SEM images showed that these scaffolds (B) had highly porous and

interconnected internal structure, (C) induced the formation of a CHA layer on the scaffold surface after soaking in simulated body fluid (SBF) for 24 hours, and (D) promoted the attachment and spreading of primary human bone-derived cells (arrows; image taken at 3 days).<sup>171</sup> Adapted with permission from Elsevier, Copyright © 2008.

### 3.3 Clinical challenges experienced with ceramic bone substitutes

Despite the ability of bioactive ceramic materials to integrate with bone tissue and promote bone formation and ingrowth, their clinical use has been restricted to scaffolds for the grafting of small areas of bone loss and particles for the filling of contained bone defects, and only at non-load bearing sites. Several challenges remain to be addressed before bioactive ceramics can find broad application in clinical bone repair and regeneration. Firstly, most bioactive ceramics have flexural strength, strain-to-failure, and fracture toughness that are significantly less than bone but an elastic modulus that is much higher than bone.<sup>175</sup> This gives rise to inherent brittleness and suboptimal mechanical performance in a dynamic and high load-bearing environment. For example, fracture toughness and modulus values for hydroxyapatite are 0.8–1.2 MPa.m<sup>1/2</sup> and 100 GPa, respectively, while those for Bioglass 45S5 are 0.5–1.0 MPa.m<sup>1/2</sup> and 35 GPa, compared to 2–12 MPa.m<sup>1/2</sup> and 12–18 GPa for human cortical bone (or 0.05–0.5 GPa modulus for cancellous bone).<sup>17,176</sup> Compressive strength of porous scaffolds with 30–90% porosity is generally in the range of 0.8–342 MPa for calcium phosphate scaffolds<sup>177</sup> and 0.2–150 MPa for bioactive glass scaffolds.<sup>162</sup> The large variations in these reported values are due to structural factors such as microporosity, grain size and presence of impurities.<sup>176</sup> Scaffolds with >70% porosity, which better resemble the structural characteristics of cancellous bone and facilitate improved bone ingrowth, typically display compressive strengths toward the lower end of the reported ranges (Fig. 9).<sup>162,177</sup> This trend highlights the dilemma in the design of ceramic scaffolds for bone regeneration, as their mechanical properties decrease significantly with increasing porosity,<sup>19</sup> and their susceptibility to crack growth and propagation makes brittle fracture more likely at higher porosities.<sup>124</sup> Secondly, increasing porosity and pore sizes can generate improved osteogenic outcomes by providing more surface area and space for cell adhesion and bone ingrowth, while complete pore interconnectivity facilitates better cell distribution and migration, as well as efficient vascularisation to sustain bone formation and remodelling.<sup>94</sup> However, due to mechanical constraints, clinically used ceramic materials are only available either in particulate form or as porous blocks with low interconnectivity, which hardly match the structural characteristics of cancellous bone.<sup>178</sup> Thirdly, low or unpredictable

biodegradation has been reported for ceramic bone substitutes, which may complicate long-term clinical outcomes.<sup>67,68,87,158</sup> These challenges have inspired research into developing novel biomaterials and scaffold designs to improve bone regeneration outcomes, many of which feature quite complex systems and incorporation of cells and/or bioactive molecules.<sup>14,179</sup> Despite promising results obtained in the laboratory, however, clinical translation has been inefficient due to stringent regulatory requirements. For this reason, established ceramic materials which have been in clinical use over the past few decades, such as calcium phosphates and bioactive glasses, have remained as the mainstream of bone graft substitute materials.

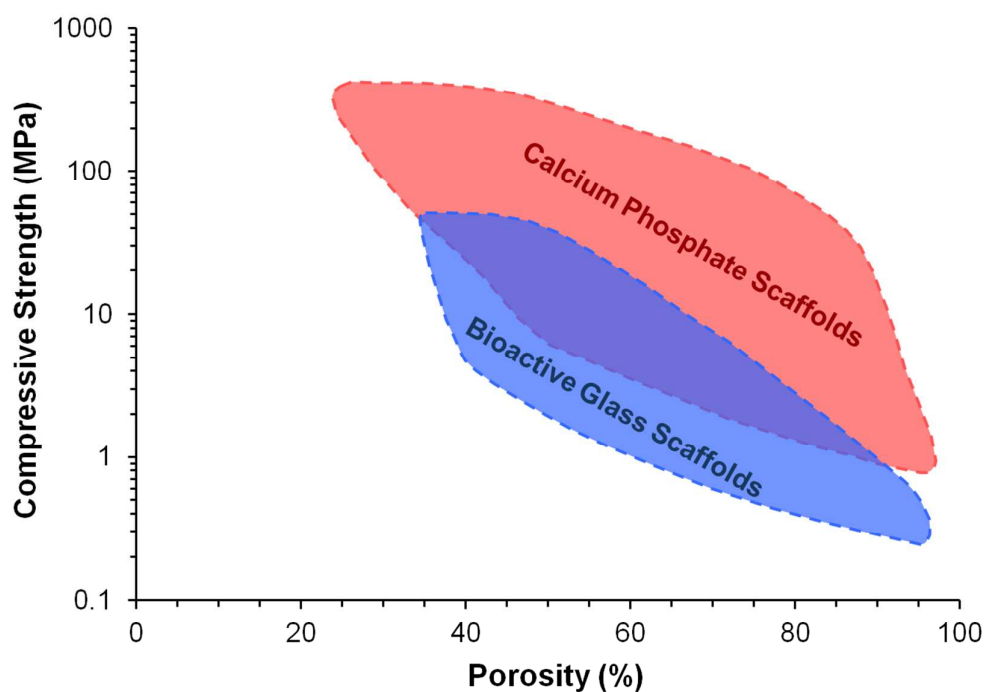


**Fig. 9** Dependence of compressive strength on porosity for bioactive ceramic scaffolds; plotted data ranges are representative of studies reviewed elsewhere.<sup>162,177</sup>

Calcium silicates represent a novel class of bioactive ceramics which, although not yet in clinical use, possess the same advantages as commercially available ceramic bone graft substitutes but with the potential to address some of the common aforementioned challenges. Similar to bioactive glasses, the high bioactivity of calcium silicates originates from the rapid formation of a surface CHA layer and ionic dissolution of calcium and silicate into the extracellular environment, which has been shown to promote osteogenesis *in vitro*<sup>180,181</sup> and *in vivo*.<sup>182</sup> However, the biological application of pure calcium silicate ( $\text{CaSiO}_3$ ) is limited by its high dissolution rate,<sup>183</sup> which may raise the pH of the surrounding environment to levels

unfavourable for cellular activity.<sup>184</sup> For this reason, a number of studies have focused on the chemical modification of calcium silicate to maximise its potential for clinical translation, via the incorporation of bioactive ions to produce novel ceramic compositions including zirconium (baghdadite<sup>185</sup>), zinc (hardystonite<sup>186</sup>), strontium (Sr-CaSiO<sub>3</sub>,<sup>187</sup> Sr-hardystonite<sup>188</sup>), and magnesium (akemanite,<sup>189</sup> bredigite,<sup>190</sup> diopside<sup>191</sup>). Recently, the unique composition of Sr-hardystonite-gahnite was developed by sintering Sr-hardystonite with aluminium oxide, giving a bioactive ceramic with greatly improved strength and toughness compared to conventional ceramic materials which are in current clinical use as bone graft substitutes.<sup>38</sup> Besides the capacity to undergo controlled degradation, all of these calcium silicate-based ceramic compositions were shown to stimulate osteogenesis *in vitro* via the release of bioactive ionic products. Notably, cell-free porous scaffolds of baghdadite<sup>192</sup> and Sr-hardystonite-gahnite<sup>38</sup> were able to achieve complete bridging and satisfactory regeneration of critical-sized bone defects in the rabbit over 12 weeks with improved outcomes compared to calcium phosphate controls (**Fig. 10**). Although verification in large *in vivo* models is pending, these results underline the prospect of introducing novel calcium silicate-based ceramic scaffolds for translational use, with the potential of alleviating the structural and mechanical constraints experienced by current ceramic bone graft substitutes.

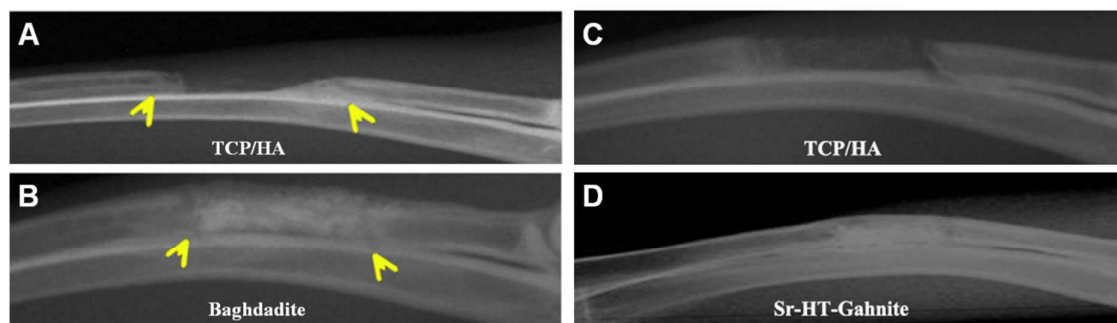


**Fig. 10** Cell-free porous scaffolds of **(B)** baghdadite<sup>192</sup> and **(D)** Sr-hardystonite-Gahnite<sup>38</sup> achieved complete bridging of critical-sized bone defects in the rabbit over 12 weeks, with improved radiographic outcomes compared to **(A, C)** BCP controls. (A, B) Adapted with permission from Elsevier, Copyright © 2012; (C, D) adapted with permission from Elsevier, Copyright © 2013.

### 3.4 The role of bioactive ceramics in the regeneration of cartilage and osteochondral tissues

Due to their inherent bioactivity and widespread clinical use in bone reconstruction, calcium phosphates and bioactive glasses have found additional application in research strategies

directed at the regeneration of cartilage and osteochondral tissues, under the rationale that the support provided by intact subchondral bone is a prerequisite to effective cartilage restoration at articular joints.<sup>193</sup> Particles of nano-hydroxyapatite,<sup>194</sup>  $\beta$ -TCP,<sup>195-197</sup> amorphous calcium phosphate,<sup>198</sup> and Bioglass 45S5<sup>199</sup> have been incorporated into synthetic polymer matrices in monophasic<sup>194,198</sup> or biphasic<sup>195-197,199</sup> scaffold systems for chondral and osteochondral repair. When implanted into a range of orthotopic *in vivo* models, these scaffold systems promoted bone formation and ingrowth in the subchondral region coupled with the regeneration of hyaline-like cartilage in the chondral region. The inclusion of bioactive ceramic particles was found to improve the quality of osteochondral repair in several studies, as implants with ceramic additives in the subchondral bone phase of a biphasic polymer construct resulted in the best cartilage repair,<sup>199</sup> while monophasic polymer implants without ceramic additives resulted in little bone formation and inferior cartilage repair with fibrocartilaginous tissue.<sup>194,198</sup> Furthermore, the degree of mineralisation within the subchondral region of a biphasic implant was shown to have a positive correlation with mechanical properties of the overlying neocartilage.<sup>195</sup> A more common use of bioactive ceramics for scaffold-based regeneration of chondral and osteochondral tissues is in the form of a porous scaffold composed of hydroxyapatite,<sup>200-203</sup>  $\beta$ -TCP,<sup>204-211</sup> BCP,<sup>212</sup> other calcium phosphates,<sup>213-215</sup> or bioactive glass.<sup>216</sup> The ceramic scaffold may constitute a monophasic scaffold,<sup>200,204-207</sup> subchondral support for a top layer of chondrogenic cells,<sup>201,202,213</sup> or the subchondral bone phase of a biphasic or multiphasic construct.<sup>203,208-212,214-216</sup> For the latter two types, ectopic implantations into immunodeficient mice demonstrated the formation of region-specific tissues in the cartilage and bone segments of the construct.<sup>201,203,214</sup> Experiments in orthotopic *in vivo* models showed that the concurrent restoration of hyaline-like cartilage and subchondral bone was possible using monophasic ceramic scaffolds or those with an additional cellular cartilaginous layer, although this relied on the inclusion of bioactive molecules<sup>200</sup> or cells within<sup>204-207</sup> or on top of the ceramic scaffold.<sup>202,213</sup> Some studies also noted substantial fibrocartilage formation<sup>204</sup> and focal separation of the cartilage layer from the ceramic scaffold.<sup>213</sup> Biphasic or multiphasic constructs incorporating a ceramic scaffold as the subchondral bone phase were generally effective at promoting osteochondral regeneration in a range of *in vivo* models, although the inclusion of cells particularly in the cartilage phase of the construct appeared to be necessary for the formation of hyaline-like cartilage.<sup>208-210,215,216</sup> In some studies, the implant produced comparable results to osteochondral autograft in overall histological score and biomechanical properties,<sup>209</sup> and biphasic constructs containing a bioactive ceramic scaffold as the subchondral bone phase

achieved superior integration to host bone and regeneration of hyaline-like cartilage compared to those containing a bone allograft.<sup>216</sup> Other studies showed evidence of zonal arrangement in the newly formed osteochondral tissue<sup>210,215</sup> and formation of a clear tidemark between cartilage and bone segments (**Fig. 11**).<sup>208,210</sup> These studies underline the feasibility of incorporating a bioactive ceramic component in improving the outcomes of scaffold-based osteochondral regeneration strategies. A more thorough discussion of this topic can be found in Section 6.

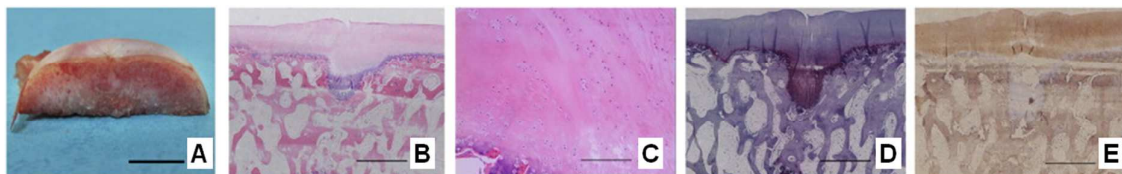


**Fig. 11** Osteochondral defect repair in a porcine model after 6 months using a biphasic construct containing a bioactive ceramic scaffold ( $\beta$ -TCP) as the subchondral bone phase and seeded with chondrocytes and osteoblasts respectively in the cartilage and bone phases. Defects implanted with the biphasic construct were repaired with hyaline-like cartilage and new bone tissue, which fused with a clear tidemark and integrated well with native tissues, as shown by (A) macroscopic appearance, haematoxylin and eosin staining at (B) low and (C) high magnifications, (D) Safranin O staining, and (E) immunohistochemical staining for collagen type II. Scale bars: (A) 8mm; (B, D, E) 2mm; (C) 200 $\mu$ m.<sup>208</sup> Adapted with permission from Elsevier, Copyright © 2011.

#### 4. Silk fibroin as a biomaterial for the regeneration of skeletal tissues

Silk fibroin has gained increasing popularity in recent years as a candidate material for a wide range of tissue engineering applications due to its unique combination of properties including biocompatibility, biodegradability, outstanding mechanical properties as a natural polymer, and ability to tailor its properties via versatile processing methods and chemical or surface modification.<sup>217</sup> Silks are natural fibres produced by a variety of insects, which consist of a filamentous core of fibroin protein coated by glue-like sericin proteins.<sup>218</sup> Fibroin from the silk of the domesticated silkworm, *Bombyx mori*, is a fibrous protein composed primarily of the amino acids glycine (43%), alanine (30%) and serine (12%).<sup>217</sup> *B. mori* silk fibroin has been used in over 85% of studies investigating silk fibroin as a scaffold material for tissue engineering<sup>219</sup> and will also be the focus of this review. Silkworm silk has been commercially used as biomedical sutures for decades. Early problems with biocompatibility

and hypersensitivity to virgin silk were found to be mainly caused by sericin proteins, which are now typically removed in hot alkaline solution (degumming) during silk processing for tissue engineering applications.<sup>220,221</sup> Degummed silk fibres can be used to fabricate fibre biomaterials or, more commonly after dissolving in hot salt solution and dialysing out the salt, they can be processed into aqueous silk fibroin solution for the preparation of various regenerated morphologies including films, hydrogels, non-woven mats and sponges for different applications (**Fig. 12**).<sup>217,221</sup> In addition, dissolving lyophilised silk fibroin solution in an organic solvent such as hexafluoroisopropanol (HFIP) provides solvent-derived processing options.<sup>221,222</sup> Upon exposure to increased salt concentrations, polar solvents such as methanol, changes in temperature or pH, or mechanical stresses such as shearing, drawing and spinning, silk fibroin irreversibly forms water insoluble crystalline  $\beta$ -sheets which contribute to its mechanical properties.<sup>223</sup> In fibre form, the mechanical properties of silk fibroin exceed most other polymeric materials, possessing high tensile strength (500–700 MPa) coupled with remarkable toughness and elasticity (elastic modulus of 10–15 GPa and up to 20% strain-to-failure).<sup>217</sup> Although the mechanical properties of silk products regenerated from silk fibroin solution are substantially weaker than native fibres due to the lack of structural and hierarchical features,<sup>224</sup> they generally still exceed other natural polymers and some synthetic polymers of equivalent morphologies,<sup>217</sup> while recent research is making continuous improvements. Predictable biodegradation of silk fibroin has been demonstrated both *in vitro* and *in vivo*, which proceeds as a function of proteolytic degradation and hydrophilic interactions within the protein structure.<sup>225-227</sup> For example, silk fibroin scaffolds can be made to retain over 50% of their mechanical properties after two months of *in vivo* implantation and completely degrade within one year, and such time frames can be controlled by processing route. The biocompatibility of silk fibroin is demonstrated by its minimal inflammatory potential.<sup>228-230</sup> When combined with stem cells in a range of skeletal tissue engineering applications, various forms of silk fibroin have been reported to support stem cell adhesion, proliferation and differentiation *in vitro* and promote tissue repair *in vivo*.<sup>231</sup> The versatility of sterilisation options is an additional advantage in tissue engineering, where several conventional sterilisation treatments were shown to have little effect on the structural and material properties of silk fibroin scaffolds, and their mechanical properties could be preserved by dry autoclaving.<sup>232</sup> This section will specifically discuss the use of silk fibroin as a biomaterial in scaffold-based tissue engineering of bone and cartilage.

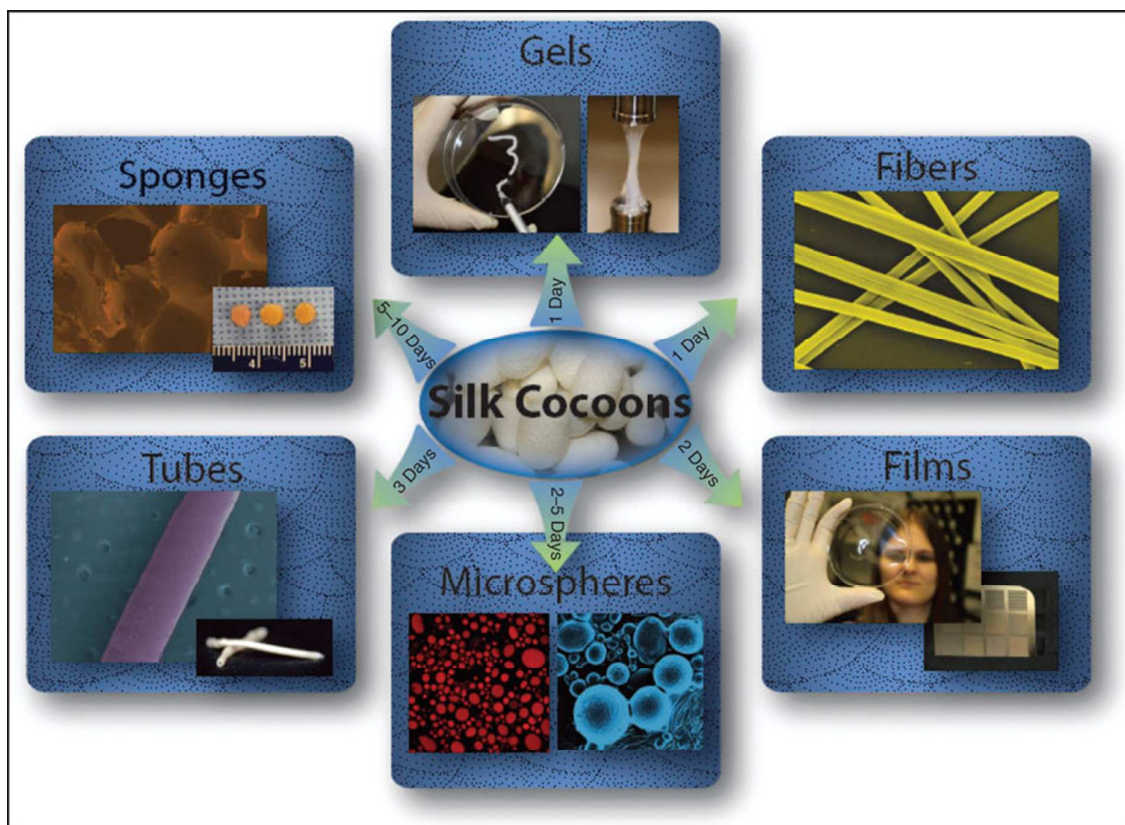


**Fig. 12** Regenerated morphologies fabricated from silk fibroin using both aqueous-derived and organic solvent-derived processing methods. The silk fibroin extraction process takes 4 days and further time required to process the silk fibroin solution into the morphology of choice is indicated within the arrows.<sup>221</sup> Reprinted with permission from Macmillan Publishers Ltd: Nature Protocols, Copyright © 2011.

#### 4.1 Silk fibroin in bone regeneration

The use of silk fibroin for bone regeneration has been extensively studied both *in vitro* and *in vivo* and features a variety of regenerated morphologies. Silk fibroin films, hydrogels, non-woven mats and porous sponges have been reported to promote *in vitro* osteogenesis in a range of bone-related cell types including mesenchymal stem cells, bone marrow stromal cells, osteoblasts and osteoblast-like cell lines derived from different sources. Silk fibroin films modified with BMP-2,<sup>233</sup> Arg-Gly-Asp (RGD) biomimetic peptide,<sup>234</sup> nano-hydroxyapatite particles,<sup>235</sup> silica particles,<sup>236</sup> or grooved patterns<sup>237</sup> mimicked native bone surfaces and enhanced the osteogenic activity of cultured cells. Silk fibroin hydrogels could be prepared via different processing methods<sup>238</sup> and supported the activity of human osteoblast-like cells.<sup>239,240</sup> Non-woven silk fibroin mats generated via electrospinning

resembled the nanofibrous structure of bone ECM,<sup>241</sup> while high porosities and large pore sizes could be introduced by the addition of salt particles as porogens,<sup>242,243</sup> which were shown to support the growth and differentiation of osteoprogenitor cells. Cell functionality was improved with the incorporation of nano-hydroxyapatite into this system,<sup>244</sup> and significantly enhanced with further addition of BMP-2 as assessed by calcium deposition and osteogenic gene expression.<sup>45</sup> Porous scaffolds of silk fibroin can be made with geometry and topography suitable for bone regeneration via control of different processing parameters such as choice of solvent (water or HFIP),<sup>42,245</sup> silk fibroin solution concentration,<sup>245</sup> and preparation methods including salt leaching, gas foaming and freeze-drying.<sup>43</sup> These parameters can be used to regulate the porosity and pore size, and to some extent the biodegradability and mechanical properties, of silk fibroin scaffolds, which in turn influence osteogenic outcomes (**Fig. 13**).<sup>246,247</sup> The ability of silk fibroin scaffolds to support the osteogenic differentiation of bone marrow-derived human mesenchymal stem cells (hMSCs) has been demonstrated via histological, biochemical and gene expression analyses in a number of studies. Advanced bone tissue development was observed in the scaffold within 8 weeks of dynamic culture in a spinner flask bioreactor.<sup>248</sup> Variations in scaffold geometry, such as pore size and distribution, porosity, and interconnectivity were shown to have significant effects in directing the morphology of regenerated bone.<sup>249,250</sup> Osteogenic outcomes were improved in silk scaffolds compared to control collagen scaffolds,<sup>251,252</sup> in aqueous-derived compared to HFIP-derived silk scaffolds,<sup>253</sup> and when BMP-2 or BMP-7 was included in the silk system as loaded proteins<sup>254</sup> or protein-encoding adenoviruses,<sup>255</sup> or produced by hMSCs transfected prior to seeding.<sup>256,257</sup> To better imitate the composition of natural bone and improve the bioactivity of silk fibroin scaffolds, calcium phosphate has been incorporated into the scaffold system via different approaches including alternate soaking to mineralise the scaffold,<sup>258-260</sup> co-precipitation to generate CaP/silk hybrid powders which can be integrated into the scaffold,<sup>261,262</sup> and mechanical mixing.<sup>263,264</sup> Enhanced bone-related outcomes were achieved with these composite scaffolds using hMSCs<sup>259,261,263</sup> and animal-derived osteoprogenitor cells.<sup>258,260</sup> Notably, one study reported that silk scaffolds impregnated with hydroxyapatite microparticles induced the formation of mineralised bone matrix by hMSCs in the absence of osteogenic growth factors, with significant increases in mechanical properties over the culture period.<sup>263</sup> Calcium phosphate in the silk system may exert its beneficial effects by enhancing osteoconductivity and providing nucleation sites to direct mineral deposition.

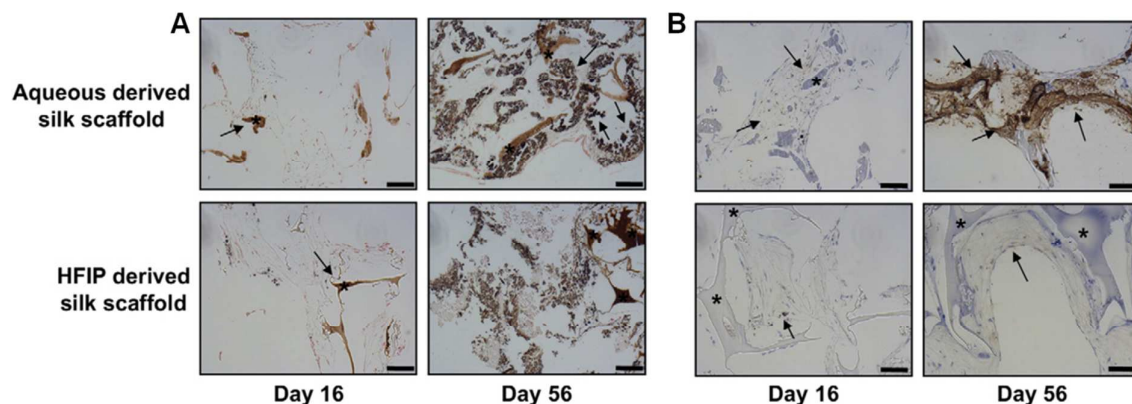


**Fig. 13** *In vitro* osteogenesis of hMSCs in aqueous-derived and HFIP-derived silk scaffolds after 16 and 56 days of dynamic culture in osteogenic medium was shown by **(A)** von Kossa staining for mineralised matrix deposition (arrows), and **(B)** immunohistochemical staining for collagen type I (arrows) within the scaffold structure (stars). The extent of osteogenesis as indicated by mineralised ECM deposition was greater in the aqueous-derived silk scaffolds, which had higher degradation rate compared to the HFIP-derived silk scaffolds. Scale bar: 100 $\mu$ m.<sup>247</sup> Reprinted with permission from Elsevier, Copyright © 2010.

Various bone defect models have been used to evaluate the *in vivo* osteogenic capacity of the above silk fibroin systems. An injectable silk fibroin hydrogel was found to promote better healing and accelerate remodelling of a critical-sized femoral defect in the rabbit compared to a commercial synthetic polymer.<sup>240</sup> Use of silk hydrogel as a delivery vehicle for BMP-2 also resulted in functional repair of a critical-sized rat femoral segmental defect, with biomechanical properties comparable to the intact femur.<sup>265</sup> When electrospun morphologies of silk fibroin were tested, a nanofibrous membrane with potential application in guided bone regeneration achieved complete healing of a rabbit calvarial defect over 12 weeks,<sup>266</sup> and repaired a rat calvarial defect with much higher bone volume than the control synthetic polymer.<sup>243</sup> Porous aqueous-derived silk fibroin scaffolds implanted into the rabbit femoral condyle without seeded cells were shown to support the ingrowth of cancellous bone.<sup>267</sup> Silk scaffolds seeded with hMSCs and pre-cultured under osteogenic conditions for 5 weeks demonstrated advanced bone formation and almost complete bridging of critical-sized defects when implanted into mouse calvaria for 5 weeks<sup>268</sup> and rat mid-femoral segmental defects for 8 weeks.<sup>269</sup> In both studies, bone formation was also observed in scaffolds seeded with undifferentiated hMSCs and unseeded scaffolds but to a lesser extent. Such differences in the extent of bone formation between groups were found to be minimised by the inclusion of

BMP-2 into the scaffold system.<sup>270</sup> Silk fibroin scaffolds containing hydroxyapatite in certain ratios were reported to achieve complete union<sup>271</sup> or substantial bone regeneration<sup>272</sup> in rabbit bone defects over 2–3 months, while similar outcomes were observed in rat femoral defects after 3 weeks.<sup>264</sup> Silk scaffolds incorporating CaP/silk hybrid powders promoted new bone formation in mouse calvarial<sup>261</sup> and rat osteoporotic femoral defects.<sup>262</sup> Premineralised silk scaffolds containing osteogenically induced autologous bone marrow stromal cells achieved complete repair of mandibular border defects in a canine model after 12 months, with bone mineral densities and quantities of new bone area comparable to autograft controls (**Fig. 14**).<sup>273</sup> The combination of premineralised silk scaffolds and gene therapy, where transfected bone marrow stromal cells over-expressing BMP-2 were seeded in the scaffolds and used to repair rat mandibular bone defects, was reported to maximise the osteogenic capacity of the system.<sup>274</sup>

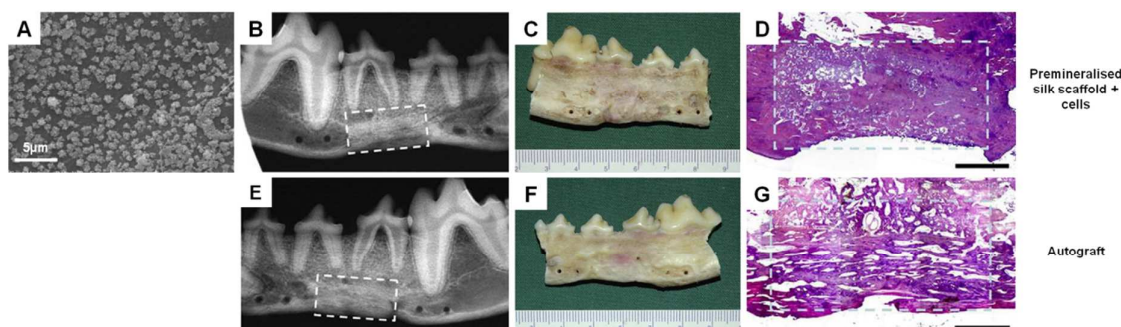


**Fig. 14** (A) Premineralised silk scaffolds were fabricated by depositing an apatite coating on the silk surface. When combined with osteogenically induced autologous bone marrow stromal cells, these scaffolds (top row) achieved comparable results to bone autograft (bottom row) in the repair of mandibular border defects in a canine model after 12 months, as shown by (B, E) radiographic, (C, F) macroscopic, and (D, G) histological examination. Scale bar: 5mm.<sup>273</sup> Adapted with permission from Elsevier, Copyright © 2009.

#### 4.1.1 Challenges encountered in the translation of silk matrices for bone regeneration

The translation of silk fibroin systems for use in clinical bone reconstruction faces certain common challenges, which current research is attempting to address. One of these is the requirement for rapid and stable vascularisation to be established following biomaterial implantation to ensure implant survival and tissue integration. To this end, the co-culture of human endothelial cells with primary osteoblasts on silk fibroin scaffolds was found to cause gradual tissue-like self-assembly with the formation of microcapillary-like structures,<sup>275</sup>

which resulted in rapid anastomosis with the host vasculature after implantation into a mouse model.<sup>276</sup> Other studies have established that the initiation of scaffold vascularisation by endothelial cells in such systems was driven by the activity of osteoblasts,<sup>277</sup> and that their osteogenic differentiation contributed to the progressive maturation of pre-vascular structures.<sup>278</sup> This co-culture-based method of scaffold pre-vascularisation holds potential for the clinical treatment of large bone defects. Another major challenge is the general inability of polymer-based systems to satisfy the mechanical requirements of bone regeneration at load-bearing sites. To overcome this, a composite silk scaffold containing an inorganic phase of calcium phosphate has been developed with average compressive strength and modulus of 14 MPa and 175 MPa, respectively.<sup>279</sup> However, this design involved cumbersome fabrication processes and generated small pore sizes of 50–100µm which might deter bone ingrowth and vascularisation. Recently, some reinforced silk-silk composite scaffolds have been developed to improve on the mechanical properties of silk fibroin systems while maintaining adequate architecture for bone regeneration. The incorporation of milled silk particles into the porous silk matrix led to significant improvements in mechanical properties with yield strength and compressive modulus up to 200 kPa and 2 MPa, respectively.<sup>280,281</sup> Loading the silk matrix with fine silk fibres could further increase the compressive modulus up to 13 MPa.<sup>282</sup> Although the mechanical properties of such reinforced silk systems may be sufficient for regenerating cancellous bone at certain sites, further improvements are necessary to meet the practical requirements for load-bearing bone reconstruction.

#### 4.2 Silk fibroin in cartilage regeneration

A wide range of studies have investigated the use of silk fibroin for cartilage regeneration in combination with stem cells or chondrocytes, and include several regenerated morphologies and polymer blends. Different morphologies of silk fibroin were shown to support the growth and ECM production of human articular chondrocytes.<sup>283</sup> Particular formulations of silk fibroin hydrogel supported the proliferation and maintenance of phenotype in encapsulated bovine chondrocytes and yielded cartilaginous constructs over 6 weeks of culture.<sup>284</sup> Nanofibrous silk fibroin meshes similar to the structure of natural ECM could be produced by electrospinning and significantly enhanced the activity of human articular chondrocytes when surface hydrophilicity was increased by microwave-induced argon plasma treatment.<sup>285,286</sup> Electrospun silk fibroin mats were also used to develop an *in vitro* model of mesenchymal condensation to understand the process of chondrogenesis during embryonic development.<sup>287</sup> hMSCs could sense subtle variations in the morphology and

stiffness of the nanofibrous silk matrix and were observed to undergo maximal migration in matrices with lower stiffness, which allowed them to assume rounded and aggregated morphologies leading to chondrogenesis. Porous silk fibroin scaffolds with varying porosity, pore interconnectivity and mechanical properties could be produced for cartilage tissue engineering by controlling the processing method and using different initial concentrations of silk fibroin solution.<sup>288</sup> The feasibility of using silk scaffolds to promote chondrogenesis has been established *in vitro* when combined with both hMSCs and chondrocytes. Silk scaffolds were able to promote chondrogenesis in hMSCs as evidenced by gene expression, histological and immunohistochemical analyses,<sup>289-291</sup> and produced constructs with spatial cell arrangement and collagen type II distribution resembling native articular cartilage after 3 weeks of culture (**Fig. 15**).<sup>289</sup> Compared to control collagen scaffolds, hMSCs cultured in silk scaffolds showed enhanced chondrogenic activity in terms of cell distribution and deposition of glycosaminoglycan (GAG) and collagen type II.<sup>290,291</sup> Chondrogenic outcomes could be further improved by controlled release of insulin-like growth factor (IGF)-I from the silk scaffold.<sup>292</sup> As an alternative cell source to mesenchymal stem cells, chondrocytes have been combined with silk fibroin scaffolds for *in vitro* cartilage tissue engineering in a range of studies. Silk scaffolds supported the attachment, proliferation and re-differentiation of culture-expanded human articular chondrocytes over 3 weeks, and initial seeding density was identified as an important factor contributing to chondrogenic outcomes in this system.<sup>293</sup> Rabbit chondrocytes have been more frequently used to investigate the chondrogenic capacity of silk scaffolds due to their better accessibility. The amount and distribution of cartilage tissue formation by cultured rabbit chondrocytes were shown to be influenced by the surface topography, biodegradability and mechanical properties of silk scaffolds produced via different processing methods.<sup>294</sup> One scaffold system produced by phase separation of frozen silk fibroin solution encouraged the formation of hyaline cartilage-like tissue over 4 weeks, and allowed the proliferation of rabbit chondrocytes without loss of differentiated phenotype as evidenced by the production of cartilage ECM components.<sup>295</sup> The distribution of cartilaginous tissue was shown to be more uniform in scaffolds with 100–140 $\mu$ m pores compared to those with smaller pore sizes.<sup>296</sup> The dynamic viscoelastic<sup>297,298</sup> and frictional<sup>299</sup> properties of the regenerated cartilage from this scaffold system were also evaluated. In another scaffold system, the effect of a silk scaffold with the Arg-Gly-Asp-Ser (RGDS) sequence genetically interfused in the fibroin protein on initial adhesion and cartilage synthesis by rabbit chondrocytes was investigated.<sup>300</sup> The adhesive force of these cells on silk fibroin substrate was previously shown to undergo time-dependent changes.<sup>301</sup> The

interfused RGDS sequence increased cell adhesive force to the silk scaffold and enhanced the early expression of integrins  $\alpha 5$  and  $\beta 1$ , as well as aggrecan, which contributed to the maintenance of chondrogenic phenotype.<sup>300</sup>

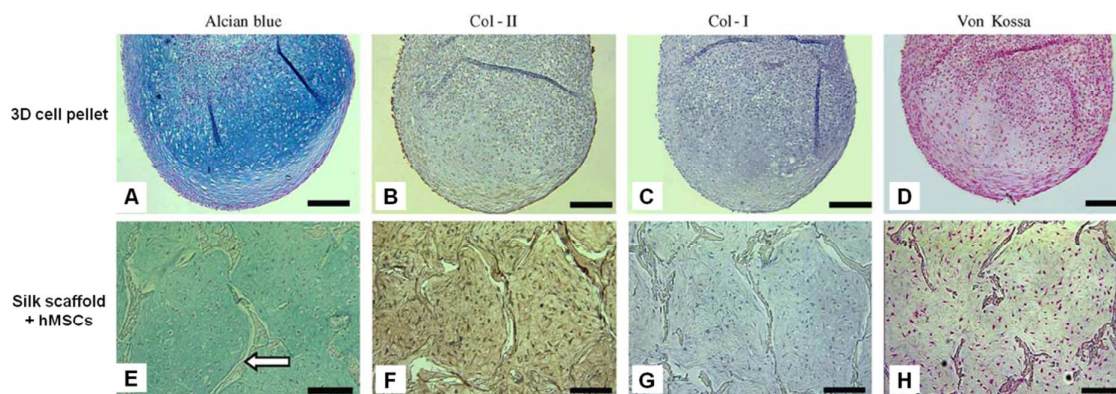


**Fig. 15** Silk scaffolds containing hMSCs (bottom row) achieved a similar extent of chondrogenesis as high-density pellet culture (top row) under the same chondrogenic conditions after 3 weeks of *in vitro* culture, as shown by histological and immunohistochemical evaluation of cartilage-specific ECM components via (A, E) alcian blue staining for sulfated proteoglycans and (B, F) immunohistochemical staining for collagen type II, and absence of (C, G) immunohistochemical staining for collagen type I and (D, H) von Kossa staining for mineral deposition. Scale bar: 200 $\mu\text{m}$ .<sup>289</sup> Adapted with permission from Elsevier, Copyright © 2005.

To approximate the dynamic loading environment which native articular cartilage is exposed to *in vivo*, mechanical stimulation has been introduced into various *in vitro* systems of chondrogenesis and reported to improve the matrix composition and mechanical properties of tissue-engineered cartilage generated using chondrocytes<sup>302,303</sup> and hMSCs.<sup>304,305</sup> Similar results were obtained in silk fibroin scaffold systems. Silk scaffolds seeded with ESC-derived hMSCs and cultured in a perfusion bioreactor for 4 weeks contained significantly higher amounts of DNA, GAG, total collagen and collagen type II compared to static culture, with distinct improvements in mechanical stiffness and expression of chondrogenic markers.<sup>306</sup> A hydrodynamic environment created by rocking culture was found to encourage the proliferation, integrin gene expression, chondrogenic differentiation with limited hypertrophic differentiation, and production of cartilaginous matrix by rat chondrocytes cultured in silk scaffolds for 2 weeks, which exerted a synergistic effect with higher scaffold porosities around 90%.<sup>307</sup> Rabbit chondrocytes seeded on silk scaffolds and cultured in a stirring chamber bioreactor for 3 weeks showed significant increases in DNA and GAG

content compared to static controls, and histological examination of proteoglycan and collagen type II deposition also confirmed maturation of the cartilaginous tissue regenerated under dynamic conditions.<sup>308</sup> The clinical feasibility of this system was assessed by implanting the cartilage construct into critical-sized defects in the rabbit knee joint, which resulted in histological repair of the defect with hyaline cartilage-like tissue after 12 weeks. Comparable results were obtained in a separate study utilising a similar *in vivo* model and silk constructs containing placenta-derived hMSCs cultured statically for 8 days prior to implantation.<sup>309</sup>

Several blends of silk fibroin with other natural polymers have been explored for use in cartilage regeneration. Silk fibroin/chitosan blended scaffolds were developed on the basis that chitosan bears structural resemblance to glycosaminoglycans, and such systems were reported to improve GAG and collagen deposition in the scaffold by bovine chondrocytes<sup>310</sup> and rat MSCs.<sup>311</sup> Silk fibroin/chitosan scaffolds combined with chondrogenically induced bone marrow-derived MSCs also achieved good repair of cartilage defects in the rabbit knee over 12 weeks by macroscopic, histological and immunohistochemical examination.<sup>312</sup> Silk fibroin/hyaluronic acid blended scaffolds exploit the biological characteristics of hyaluronic acid as one of the most ubiquitous glycosaminoglycans in the human body. These systems promoted cellular ingrowth and chondrogenic gene expression in cultured hMSCs,<sup>313</sup> and mechanical properties were also improved as hyaluronic acid could enhance the formation of  $\beta$ -sheet structures in silk fibroin.<sup>314</sup> To produce more stable and ordered polymer composite structures for cartilage tissue engineering, genipin cross-linked blends of silk fibroin/chitosan,<sup>315</sup> silk fibroin/hyaluronic acid,<sup>316</sup> and silk fibroin/gelatin<sup>317</sup> were developed as scaffolds or hydrogels and shown to support the activity of skeletal tissue-related cell lines. An electrospun blend of silk fibroin/wool keratose, which contained amino acid sequences to induce cell adhesion, was reported to promote chondrogenesis in neonatal human articular chondrocytes, particularly when treated with microwave-induced argon plasma.<sup>318</sup> Unlike for applications in bone regeneration, however, the efficacy of silk fibroin-based scaffolds for cartilage regeneration remains to be verified in large *in vivo* models before clinical translation can be envisaged.

##### **5. The effective reinforcement of ceramic scaffolds with polymer coatings and the unique combination of silk-coated ceramic scaffolds**

To broaden the applications of clinically established ceramic materials in bone repair and regeneration, increasing research has been directed at improving the structural integrity and mechanical properties of ceramic scaffolds, with the aim of producing reinforced scaffolds which are suitable for use at load-bearing sites even at high porosities. The coating of ceramic scaffolds with biocompatible and biodegradable polymers represents a particularly promising approach, which can lead to effective reinforcement while conserving the high porosity and interconnectivity of the scaffold. The approach has been extended to include scaffolds with interpenetrating network structures, where the polymer not only constitutes a surface coating but is also made to infiltrate the struts of the ceramic scaffold through processes such as coating in vacuum or centrifugation. The polymer-coated ceramic scaffolds mimic the composite structure of bone, and hold potential for rapid clinical translation due to simplicity of the fabrication process. In general, a ceramic scaffold has open micropores and surface defects such as microcracks in the struts after sintering. The polymer can fill existing voids in the ceramic microstructure, resulting in structural reinforcement and reduced brittleness by lowering the chance of crack propagation under load (**Fig. 16**).<sup>319</sup> During fracture, the polymer filaments function in crack-bridging and energy dissipation, thereby retarding advancement of the crack tip and increasing fracture toughness of the scaffold,<sup>320</sup> in a similar manner as collagen fibres enhance the fracture toughness of bone.<sup>321</sup>

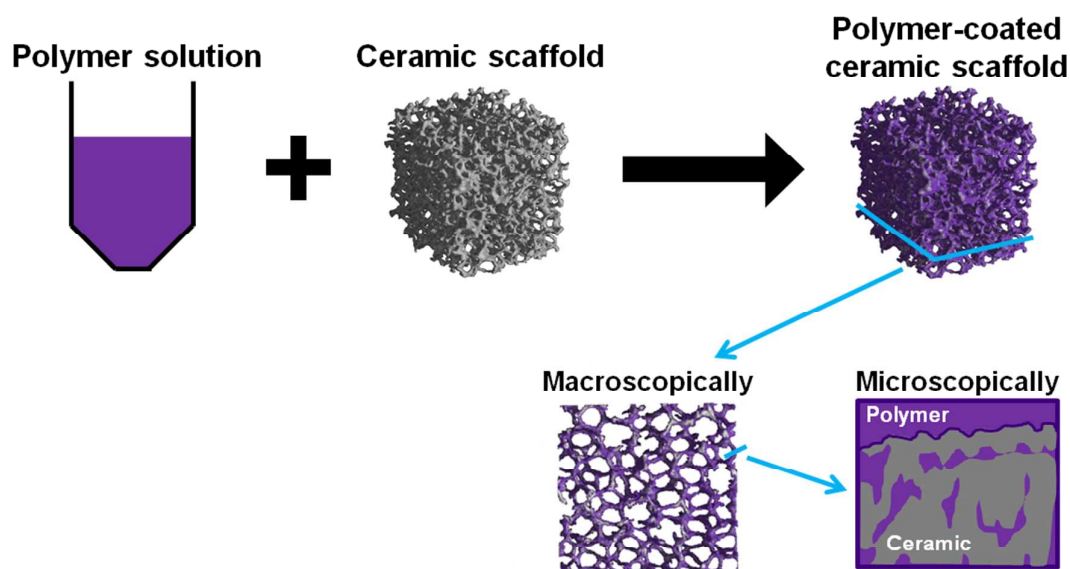


**Fig. 16** Mechanism of structural reinforcement in polymer-coated ceramic scaffolds.

A wide range of polymer-coated ceramic scaffolds have been developed using different combinations of clinically used bioactive ceramics, including hydroxyapatite,<sup>322-329</sup>  $\beta$ -TCP,<sup>330-333</sup> BCP,<sup>104,334-343</sup> and bioactive glasses,<sup>344-351</sup> and natural or synthetic polymers, including collagen,<sup>326,349</sup> alginate,<sup>343,348,349,351</sup> gelatin,<sup>322,334,344,347,349</sup> poly(3-hydroxybutyrate) (PHB),<sup>323,345</sup> polylactic acid (PLA),<sup>104,331,349</sup> poly(L-lactic acid) (PLLA),<sup>327,333,337,338</sup> poly(D,L-lactic acid) (PDLLA),<sup>329,346,350</sup> poly(lactic-co-glycolic acid) (PLGA),<sup>324,330,335,336</sup> and polycaprolactone (PCL).<sup>325,328,331-333,339-342,349</sup> The majority of studies reported significant improvements in mechanical properties of the polymer-coated scaffolds, particularly in terms of strength and toughness, without substantial reductions in scaffold porosity and interconnectivity. Notably, a number of coated scaffolds exhibited compressive strengths which were within the range of cancellous bone and at least several folds higher than those of uncoated controls.<sup>324,327,330,331,336,338,340</sup> Other important improvements in toughness,<sup>330,332,333,339,342</sup> bending strength<sup>330,346</sup> and work of fracture<sup>345,346</sup> were also observed. Some studies evaluated the influence of the polymer coating on biological properties of the scaffold, mainly via attachment and proliferation of bone-related cells,<sup>325,329,335,337,339,343</sup> as well as osteogenic activity *in vitro*<sup>330,340-342,345</sup> and *in vivo*.<sup>104,326,338</sup> Theoretically, as naturally derived polymers which bear resemblance to ECM, coatings of collagen, alginate and gelatin should enhance bioactivity and osteoconductivity of the scaffold, but these beneficial effects were either not evaluated or shown to be not significant in the case of collagen<sup>326</sup> and alginate.<sup>343</sup> The motivation for their use is therefore diluted considering that they also produced only moderate improvements in mechanical properties. Other polymeric coatings of PHB, PLA, PLLA, PDLLA, PLGA and PCL can significantly enhance mechanical properties of the ceramic scaffold, but require the use of organic solvents in the fabrication process which may be harmful to transplanted cells or host tissues if not completely removed. These coatings are also more inert and may mask bioactivity of the underlying ceramic substrate, as exemplified by a study which showed delayed orthotopic bone formation in a goat model due to the addition of a PLA coating to implanted BCP scaffolds.<sup>104</sup> This problem can be addressed by the incorporation of a bioactive ceramic component into the coating, including hydroxyapatite powder,<sup>329</sup> hydroxyapatite nanoparticles,<sup>337,338,340</sup> calcium phosphate deposition,<sup>328</sup> bioactive glass powder,<sup>324,336</sup> and bioactive glass nanoparticles.<sup>341</sup> Such strategies are effective at improving osteoconductivity of the coated surface, but rely on homogeneous dispersion of the ceramic component in the coating, introduce additional processing complexity, and do not circumvent the use of organic solvents during fabrication. The potential use of the polymer coating as a delivery vehicle for drugs or bioactive

molecules to enhance scaffold functionality and bioactivity has also been explored in several studies. Coatings of PCL<sup>352</sup> or PCL-based hybrids<sup>353-356</sup> and PHB<sup>357,358</sup> significantly increased the compressive strength and toughness of bioactive ceramic scaffolds, while facilitating the sustained release of model proteins (bovine serum albumin<sup>352</sup>) or antibiotic drugs (tetracycline<sup>353,354,358</sup> and vancomycin<sup>355-357</sup>).

### 5.1 Silk-coated ceramic scaffolds and their unique characteristics

Compared to other polymers, the use of silk fibroin as a coating material to enhance the properties of bioactive ceramic scaffolds for broader applications in clinical bone reconstruction offers unique advantages. The coating of silk fibroin on polyurethane foams resulted in increased biocompatibility, as demonstrated by improved human fibroblast adhesion, proliferation and metabolic activity.<sup>359</sup> A silk fibroin coating on PDLLA films also enhanced osteoblast interaction with the substrate and their differentiated function.<sup>360,361</sup> Backed by the rich body of literature supporting the use of silk fibroin in osteogenesis, as well as unique characteristics of the material including the capacity for aqueous processing and versatility of sterilisation options, the biological effects of silk fibroin coatings motivate the development of silk-coated ceramic scaffolds for bone regeneration. Limited studies have investigated the efficacy of this unique combination, comprising coatings of single silk layer on bioactive glass,<sup>362</sup> hybrid silk/PCL layer on BCP,<sup>363</sup> and multiple silk layers on BCP.<sup>364</sup> These studies provided evidence that the silk coating could simultaneously improve mechanical and biological properties of the scaffold while maintaining a highly porous and interconnected architecture. Mechanical reinforcement of the ceramic scaffold by the silk coating was significant in all studies, producing improvements of 4–6 folds in compressive strength,<sup>362-364</sup> over 6 folds in failure strain,<sup>363</sup> and up to 12 folds in toughness.<sup>364</sup> Also worth noting was the elastic behaviour of the silk-coated scaffolds in compression as evidence of reduced brittleness.<sup>363,364</sup> This was particularly pronounced in the scaffold with multiple silk coatings, which resembled an interpenetrating composite structure with silk-infiltrated ceramic struts (**Fig. 17**).<sup>364</sup> In terms of biological behaviour, prominent improvements in the osteogenic activity of primary human osteoblasts,<sup>363</sup> human bone marrow stromal cells,<sup>362</sup> and hMSCs<sup>364</sup> were observed in the silk-coated compared to bare ceramic scaffolds during both short-term (1–2 weeks)<sup>362,363</sup> and long-term (up to 6 weeks)<sup>364</sup> *in vitro* culture, as assessed by attachment, proliferation, bone-related gene expression and alkaline phosphatase activity. To augment the biological properties of the scaffold, drug delivery capabilities of the silk fibroin coating can be exploited and warrant further investigation,<sup>223,365</sup> and

preliminary tests have already been performed.<sup>362</sup> Strategies such as optimisation of the silk coating process and deposition of multiple silk layers may maximise the efficacy of the system, and potentially obviate the need to improve coating properties by incorporation of other polymers. Due to their unique combination of properties, silk-coated ceramic scaffolds possess distinct advantages over other polymer-coated systems for use in bone regeneration, and represent a simple and effective method of reinforcing porous ceramic bone substitutes from a translational perspective.

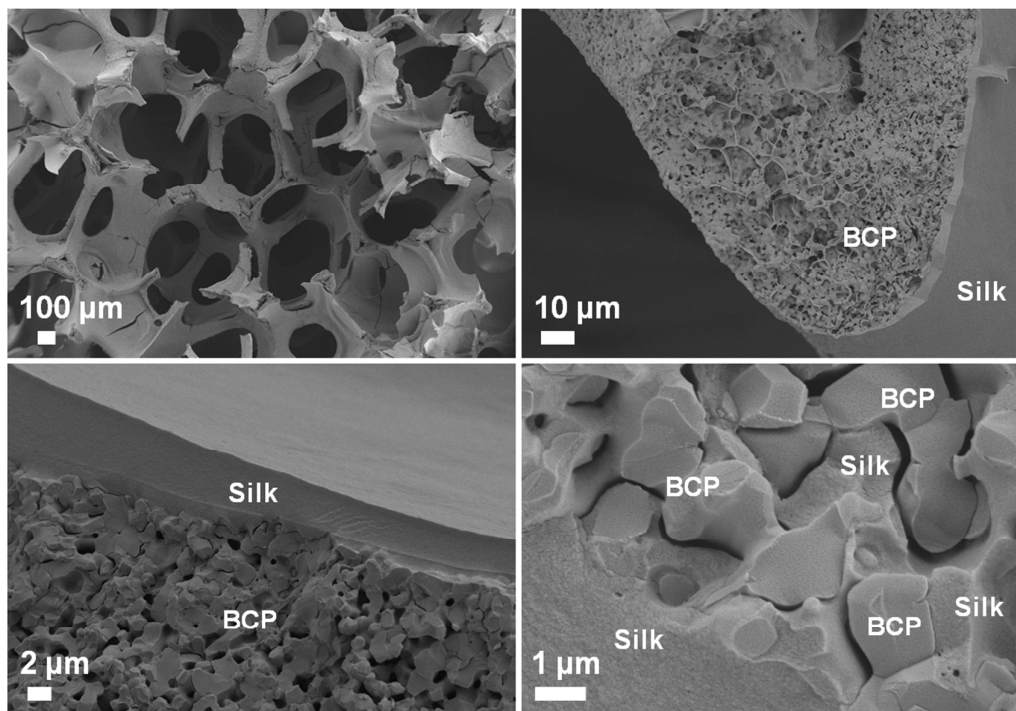


**Fig. 17** SEM images showing the unique structure of a silk-coated ceramic (BCP) scaffold with multiple silk coatings. Silk fibroin not only deposited on the ceramic scaffold surface but also infiltrated the scaffold struts, resulting in the formation of a structure that was highly porous and interconnected on the macroscopic level and an interpenetrating polymer-ceramic composite on the microscopic level.<sup>364</sup> In the context of bone regeneration, coating porous ceramic scaffolds with silk fibroin represents a simple and effective method of reinforcement. Reprinted with permission from American Chemical Society, Copyright © 2013.

## 6. An insight into the regeneration of osteochondral tissue: current progress and potential contribution of novel scaffold designs

Osteochondral defects encompass damage to the articular cartilage, subchondral bone and interfacial tissues, often resulting in mechanical instability of the joint and ultimately

contributing to the development of degenerative osteoarthritic changes.<sup>366</sup> Backed by such realisations and fuelled by the gradual maturation of tissue engineering techniques to tackle the regeneration of complex and hierarchical tissues, the challenging field of osteochondral tissue regeneration has received increasing research attention in recent years. The development of relevant scaffold strategies is complicated by the different compositional, structural, mechanical and biochemical requirements of each osteochondral tissue segment. On the most basic level, cartilage differentiation is induced by softer or natural polymeric matrices and low porosity to limit vascularisation, as well as in the presence of a different set of bioactive molecules compared to bone differentiation, which is induced by stiffer or inorganic matrices and high porosity to promote vascularisation.<sup>367</sup> To satisfy these requirements, osteochondral scaffold designs need to incorporate bioactive material compositions and biomimetic structures for both cartilage and bone, while still being able to maintain sufficient mechanical integrity to restore the load-bearing characteristics of the joint. Furthermore, adequate integration between phases is imperative for multiphasic designs, and the degradation rate should also be coupled between phases while being matched to the rate of tissue formation and/or remodelling. Many osteochondral scaffold designs have emerged and achieved variable levels of success *in vitro* and *in vivo*, which can be grouped according to different strategies,<sup>368-372</sup> although an optimal strategy or ‘ideal’ design has not yet been realised. **Table 3** gives an overview of current scaffold strategies for osteochondral regeneration together with a list of representative studies (representative images are shown in **Fig. 18**). Closer examination of these studies allows the identification of several prominent issues irrespective of scaffold strategy, which may explain the scarcity of commercialised products for the specific treatment of osteochondral lesions. Firstly, some scaffold designs have only been characterised *in vitro*<sup>44,373-386</sup> or ectopically in immunodeficient mice,<sup>203,383,387-389</sup> and their efficacy remains to be verified in orthotopic *in vivo* models. Secondly, perhaps influenced by the intrinsic regenerative ability of the *in vivo* model selected, orthotopic scaffold-based osteochondral regeneration has generally yielded promising results in small animals such as the rat<sup>194,390</sup> and rabbit,<sup>197,202,210,215,216,391-407</sup> but satisfactory results appear more difficult to achieve in larger animals such as the pig,<sup>195,196,208,408</sup> goat<sup>409,410</sup> and sheep.<sup>204-207,209,213,411</sup> Some of the persistent issues which remain to be addressed include the formation of repair tissue that resembles fibrocartilage rather than hyaline cartilage,<sup>195,204,210,398,407,408,410</sup> the lack of complete integration between neocartilage and native tissues,<sup>196,197,210,390,403,404,408</sup> and the rare formation of a continuous and integrated bone-cartilage interface.<sup>395</sup> Furthermore, mechanical properties of the

regenerated tissue as a measure of functional restoration were only evaluated in selected studies, of which the majority conducted tests on the cartilage layer only rather than the entire osteochondral unit.<sup>195-197,205,208,209,213,403,407</sup> Thirdly, in anticipation of stringent regulatory requirements, solutions featuring scaffold-only designs are more appealing for clinical translation. However, *in vivo* studies to date suggest that the majority of osteochondral scaffold designs require the inclusion of cells and/or bioactive molecules to achieve satisfactory regenerative outcomes.<sup>195,202,213,215,393,395,396,399,400,406,408,411,412</sup>

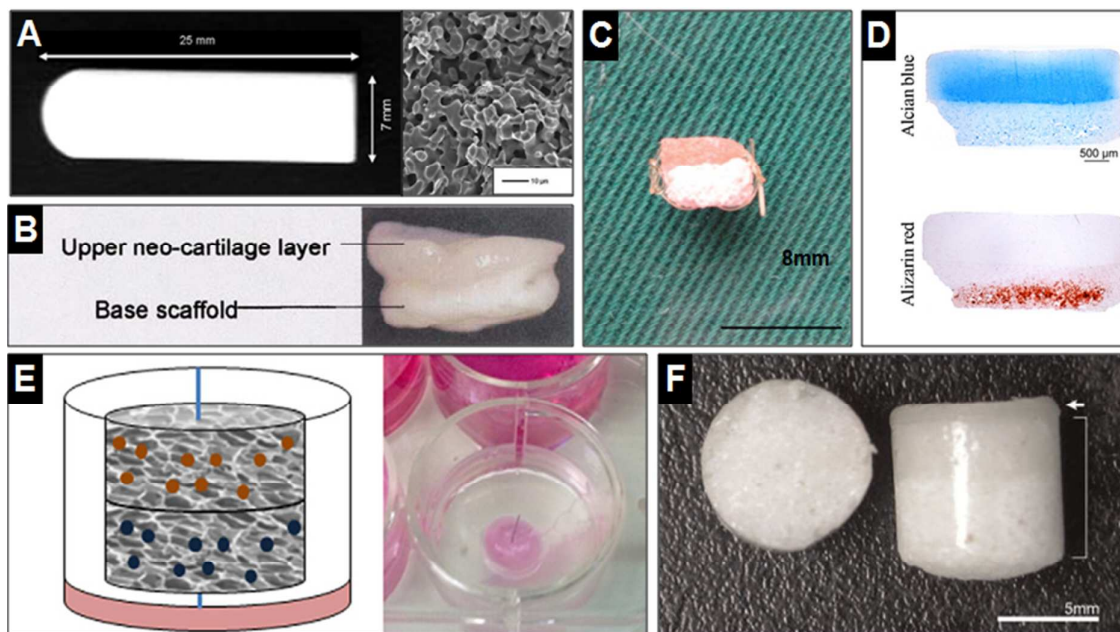


**Fig. 18** Representative images of current scaffold strategies for osteochondral regeneration. (A) Monophasic scaffold: microporous  $\beta$ -TCP scaffold which was implanted into a sheep model;<sup>205</sup> (B) cells for cartilage phase and scaffold for bone phase: porcine chondrocytes were grown on top of a base scaffold (PLLA, PDLA or collagen-hydroxyapatite) and formed an osteochondral construct ready for implantation after 3–4 weeks;<sup>386</sup> (C) assembled scaffold with individual scaffolds for cartilage and bone: PLGA cartilage phase and tricalcium phosphate bone phase were pre-cultured separately with chondrocytes and osteoblasts and sutured together before implantation into a mini-pig model;<sup>208</sup> (D) homogeneous scaffold with different cell populations for cartilage and bone: agarose hydrogel containing chondrocytes and MSCs in two layers generated region-specific tissue after implantation into immunodeficient mice;<sup>383</sup> (E) homogeneous scaffold with continuous gradient of bioactive molecules: growth factors for chondrogenesis and osteogenesis were affinity bound to an alginate scaffold to form a bioactive gradient for implantation into a rabbit model;<sup>402</sup> (F) single scaffold with integrated phases: PLGA cartilage phase (arrow)

and PLGA/ $\beta$ -TCP bone phase (bracket) were formed into a single scaffold via solvent casting and particulate leaching, which was implanted into a mini-pig model.<sup>196</sup> (A, D) Adapted with permission from Elsevier, Copyright © 2013; (B) Adapted with permission from Elsevier, Copyright © 2004; (C) Adapted with permission from Elsevier, Copyright © 2011; (E) Adapted with permission from Elsevier, Copyright © 2012; (F) adapted with permission from John Wiley and Sons, Copyright © 2007 Orthopaedic Research Society.

### 6.1 Commercially available scaffolds for the treatment of osteochondral defects

Despite the above challenges, a small number of scaffold designs which do not incorporate cells or bioactive molecules, or necessitate use in combination with other treatment techniques, have become commercially available for the clinical treatment of osteochondral defects.<sup>413</sup> Chondromimetic<sup>TM</sup> and TruFit<sup>TM</sup> are both biphasic scaffolds which are currently undergoing clinical investigation. Chondromimetic<sup>TM</sup> consists of collagen type I and chondroitin-6-sulfate in the cartilage phase and calcium phosphate in the subchondral bone phase, while TruFit<sup>TM</sup> consists of poly(D,L-lactide-co-glycolide) and poly(glycolic acid) fibres in the cartilage phase and calcium sulphate in the subchondral bone phase. The performance of these two scaffolds in repairing osteochondral defects of the knee joint was compared in a goat model, which showed significantly higher total histological score for Chondromimetic<sup>TM</sup> implants.<sup>414</sup> At 26 weeks post-implantation, Chondromimetic<sup>TM</sup> showed hyaline-like cartilage regeneration in 75% of defects compared to 50% for TruFit<sup>TM</sup>, with a lower incidence of subchondral bone cysts (17% compared to 67%). Although there is a lack of published studies on clinical results of the Chondromimetic<sup>TM</sup> implant, a series of studies have reported on the short- to long-term clinical outcomes of the TruFit<sup>TM</sup> implant. Earlier case reports showed failure of incorporation with foreign-body giant cell reaction when used as a bone graft substitute,<sup>415</sup> as well as delayed incorporation when used to treat cartilage defects with eventual symptom alleviation after 24 months.<sup>416</sup> More recent reports of short-term outcomes showed that TruFit<sup>TM</sup> implantation did not damage the opposing native cartilage and allowed the formation of cartilage-like tissue inside the implant,<sup>417</sup> although MRI outcomes were modest with 20% of patients displaying persistent or increased clinical symptoms.<sup>418</sup> Unfavourable outcomes by CT assessment were reported in a study with follow-up periods of 2 to 63 months, where the implant showed no evidence of bone ingrowth, osteoconductivity or integration with native tissue, with decline in density over time to that of fibrous tissue.<sup>419</sup> Osteochondral regeneration using MaioRegen<sup>®</sup>, a biomimetic multiphasic scaffold currently undergoing an extensive clinical trial in Europe

involving 150 patients, has demonstrated more optimistic results.<sup>420</sup> This scaffold consists of three layers to mimic the different regions of osteochondral anatomy, namely a cartilage layer composed of collagen type I overlying intermediate and subchondral bone layers composed of collagen type I and magnesium-hydroxyapatite in different ratios (60:40 and 30:70 respectively) (**Fig. 19**). Preliminary investigations showed that the scaffold layers were well integrated with the ability to differentially support cartilage and bone formation in an ectopic mouse model.<sup>421</sup> Preclinical studies involved implantation into deep osteochondral defects of load-bearing joints in the sheep<sup>422</sup> and horse<sup>423</sup> for 6 months. While the horse model showed fibrocartilaginous resurfacing of the defect, hyaline-like cartilage formation was observed in the sheep model. The scaffold promoted bone regeneration in both models which integrated well with surrounding bone, and a tidemark line was visible at the interface with regenerated cartilage in the horse model. Since its introduction into clinical practice, several studies have reported encouraging short-term results of using this scaffold for the treatment of osteochondral defects in the knee joint. An earlier case report showed good restoration of the articular surface with a hyaline-like signal by MRI evaluation, and functional restoration after 12 months.<sup>424</sup> Pilot clinical trials with treated defect sizes of 1.5–6cm<sup>2</sup> and follow-up periods of 1–6 months<sup>425</sup> and 6–24 months<sup>426</sup> showed complete defect filling in the cartilage region and complete integration of the scaffold in the majority of implanted defects. Clinical studies involving patients with large defect sizes of 4–8cm<sup>2</sup><sup>427</sup> and osteochondritis dissecans with average defect size of 3.4cm<sup>2</sup><sup>428</sup> showed similar results, with significant improvement in all clinical scores at follow-up times of 1 and 2 years. Nevertheless, these studies also noted subchondral bone changes such as oedema and sclerosis in the majority of patients.<sup>425–428</sup> The long-term clinical viability of this scaffold design remains to be confirmed.

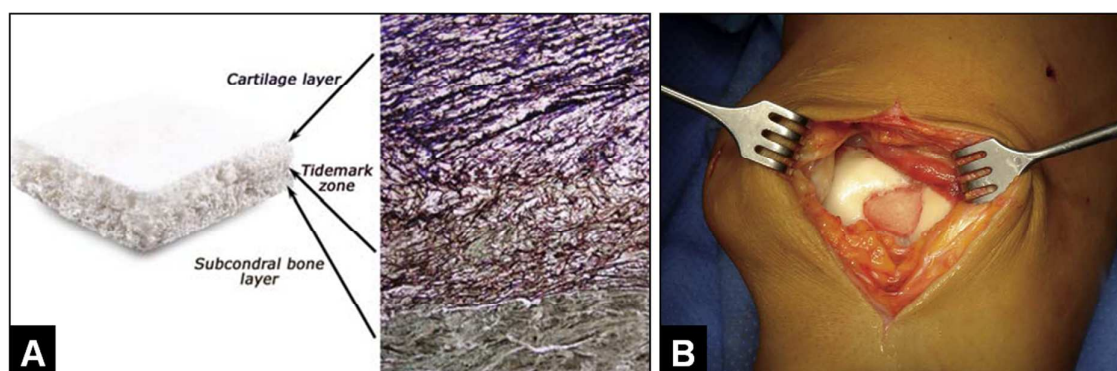


**Fig. 19** (A) Macroscopic and histological view of the MaioRegen<sup>®</sup> scaffold, which consists of three integrated layers.<sup>424</sup> This scaffold is undergoing extensive clinical testing for osteochondral regeneration and (B) is implanted using a press-fit technique.<sup>425</sup> (A) Adapted

with permission from Springer, Copyright © 2009; (B) adapted with permission from Elsevier, Copyright © 2009.

## 6.2 Looking into the future: potential contribution of novel scaffold designs

Comparison of preclinical and clinical outcomes amongst the commercially available osteochondral scaffolds suggests that natural composites are more effective at supporting the restoration of osteochondral tissue. The two scaffold designs which utilise natural polymeric materials, namely Chondromimetic<sup>TM</sup> and MaioRegen<sup>®</sup>, both consist of collagen type I as a prominent component of the cartilage phase. Compared to collagen, silk fibroin possesses many favourable characteristics for this application including lower inflammatory potential,<sup>230</sup> higher mechanical integrity of porous scaffolds,<sup>42,43</sup> more versatile processing<sup>217</sup> and sterilisation<sup>232</sup> options, and better ability to support chondrogenic differentiation of hMSCs.<sup>290,291</sup> The demonstrated efficacy of silk fibroin in bone regeneration is an additional advantage. These properties of silk fibroin raise possibilities of developing novel osteochondral scaffold designs via its incorporation into the cartilage and subchondral bone phases. Human bone marrow stromal cells have been shown to undergo selective chondrogenic or osteogenic differentiation depending on medium composition when cultured on silk scaffolds in a rotating bioreactor for 5 weeks,<sup>429</sup> which underlines the ability of silk-based matrices to facilitate differentiation of relevant stem cell populations towards the formation of osteochondral tissue when exposed to the correct environmental cues. Since then, a number of studies have reported on the use of silk-based scaffold systems for osteochondral regeneration with optimistic results (summarised in **Table 4**). Nevertheless, these studies involved mostly *in vitro* characterisations<sup>430-435</sup> and the only *in vivo* study was performed in an orthotopic rat model,<sup>436</sup> which provide insufficient evidence to establish the clinical relevance of such scaffold systems. A primary concern of using silk-based scaffold systems for regenerating the entire osteochondral unit is that the subchondral bone phase, even when reinforced with various modifications, may not have adequate mechanical properties to withstand *in vivo* forces in a high load-bearing environment. This issue is actually common to most, if not all, osteochondral scaffold designs. The difficulty of achieving satisfactory subchondral bone restoration in scaffold-based osteochondral reconstruction is highlighted by the clinical results obtained using MaioRegen<sup>®</sup>.<sup>425-428</sup> Recently, increasing focus has been directed to the critical role of the subchondral bone in the pathophysiology of osteochondral defects,<sup>437</sup> as well as its importance as the key foundation for successful cartilage repair.<sup>193</sup> Emerging evidence suggests that structural changes of the

subchondral bone resulting from inferior repair of this tissue may translate into altered biomechanical properties of the entire osteochondral unit and ultimately impact the long-term performance of cartilaginous repair tissue.<sup>438</sup> Experimental evidence has also indicated that the chondrogenesis of MSCs in an osteochondral environment is mediated by the subchondral bone.<sup>439</sup> In the context of osteochondral defect reconstruction, therefore, better and more durable cartilage restoration may be anticipated for scaffold systems which facilitate adequate regeneration of the subchondral bone and its integration with native tissues. In light of this, silk-coated ceramic scaffolds may find a unique niche in functioning as the subchondral bone phase of novel osteochondral scaffold systems, while silk-based scaffolds may be integrated into such systems as the cartilage phase to complete the design. The efficacy of this approach may be further enhanced by the concurrent development of innovative bioactive ceramic scaffolds as discussed in Section 3.3. The continuous development of novel osteochondral scaffold designs exploiting different material combinations, methods of fabrication and repair strategies will ultimately result in the realisation of simple, effective and durable solutions for the clinical treatment of osteochondral defects to prevent or retard degenerative processes.

## 7. Conclusions

Scaffold-based tissue engineering strategies for the repair and regeneration of skeletal tissues need to meet the physical, mechanical and biological requirements of the target tissue and, in the case of osteochondral tissue, the requirements of each segment need to be incorporated into the scaffold design. The difficulty of reaching a clinically viable scaffold design is accentuated when the practical requirements of clinical translation are taken into consideration, including the ease of manufacture and sterilisation, reproducibility of material properties, low demand for storage conditions, cost effectiveness, and preference for cell-free approaches. From a translational standpoint, scaffold designs incorporating natural and/or bioactive materials which have already obtained regulatory approval for human use possess a distinct advantage. In light of this, novel scaffold systems involving silk matrices, silk-coated ceramic scaffolds or potential combination of these show promise in satisfying the diverse sets of requirements for the regeneration of bone, cartilage and osteochondral tissues. Continuous research advances in scaffold-based tissue engineering and their efficient translation is fundamental to the achievement of tangible and clinically relevant outcomes in the treatment of skeletal tissue defects.

**Table 1.** Critical sizes of bone and cartilage/osteocondral defects in a range of *in vivo* models and in humans.

| <i>In Vivo</i> Model Compared to Human | Bone Defects                              |                              | Cartilage/Osteochondral Defects   |  |
|--|---|------------------------------|---|--|
|  | Type of Defect                            | Critical Defect Size         | Average Cartilage Thickness (Medial Femoral Condyle) <sup>440,441</sup> | Typical Diameter of Critical-Sized Defect <sup>440</sup>   |
| Mouse                                  | Calvarial                                 | 4mm diameter <sup>268</sup>  | 0.1mm   | 1.5mm  |
| Rat                                    | Calvarial                                 | 8mm diameter <sup>442</sup>  |   |  |
|  |   | Long bone segmental          | 8mm length <sup>102</sup>   |  |
| Rabbit                                 | Calvarial                                 | 15mm diameter <sup>442</sup> | 0.3mm   | 3mm  |
|  |   | Long bone segmental          |   |  |
| Dog                                    | Long bone segmental                       | 21mm length <sup>102</sup>   | 0.6–1.3mm   | 4mm  |
| Pig                                    | Calvarial                                 | 10mm diameter <sup>443</sup> | 1.5–2.0mm   | 6mm  |
|  |   | Long bone segmental          |   |  |
| Horse                                  | 4 <sup>th</sup> metatarsal bone segmental | 4mm length <sup>442</sup>    | 1.5–2.0mm   | 9mm  |
| Goat                                   | Long bone segmental                       | 26mm length <sup>81</sup>    | 0.7–1.5mm   | 6mm  |
| Sheep                                  | Long bone segmental                       | 30mm length <sup>445</sup>   | 0.4–0.5mm   | 7mm  |
| Human                                  | Long bone segmental                       | 4–7cm length <sup>61</sup>   | 2.2–2.5mm   | < 2.0cm small, 2.0–2.9cm intermediate, ≥ 3.0cm large <sup>446</sup><br>(1.5–16.0cm <sup>2</sup> defect volume <sup>426,446</sup> ) |
|  |   | Segmental                    |   |  |

**Table 2.** Fabrication techniques for the processing of ceramic and polymeric biomaterials into porous scaffolds for the regeneration of skeletal tissues.<sup>17,447-451</sup> Example studies were selected from references cited elsewhere in this review.

| Scaffold Type   | Fabrication Technique                    | Brief Description   | Main Advantages  | Main Disadvantages   | Example Studies    |
|---|--|---|--|--|--------------------|
| Ceramic scaffolds                                       | Polymer foam replication                 | Ceramic slurry is used to infiltrate and coat a sacrificial polymer foam template with desired pore structure, which is removed during sintering leaving a ceramic scaffold that replicates the foam structure  | Can produce highly porous and interconnected structures resembling cancellous bone<br>Offers control over pore structure   | Large samples may require long burnout times to completely remove the polymer  | 38,48,380          |
|   | Impregnate sintering                     | Particles of an organic phase are mixed with ceramic powders to act as porogens during scaffold shaping, and are later removed during sintering   | Simple and efficient process of generating highly porous structures for bone regeneration  | Less control over pore structure and interconnectivity   | 39,107,172         |
|   | Gel-cast foaming                         | Organic monomers mixed within ceramic powders form a gel during polymerisation which binds the ceramic together and is later removed during sintering, foaming is induced prior to gelation via vigorous agitation with the aid of a surfactant   | Can produce highly porous and interconnected structures resembling cancellous bone<br>Improved mechanical properties over other sacrificial polymer techniques   | Less control over pore structure and interconnectivity<br>Optimisation of process may be difficult due to numerous variables                               | 40                 |
| Polymer scaffolds and polymer-based composite scaffolds | Solvent casting and particulate leaching | Polymer solution is cast into a mould containing soluble porogens (e.g. NaCl), the polymer scaffold forms after solvent evaporation and leaching away the porogen with water to create pores  | Simple process of generating highly porous structures that allows control over pore size and porosity  | Less control over pore shape and interconnectivity<br>Limited scaffold thickness (porogen leaching requires contact with water)<br>Low mechanical strength | 42,196,245,389,396 |
|   | Phase separation                         | Thermal treatment (e.g. low temperature) causes a homogeneous polymer solution to become thermodynamically unstable and separate into polymer-rich and polymer-lean phases, the former solidifies to form the polymer scaffold while the latter becomes pores after solvent removal   | Can generate highly porous and interconnected structures, and potentially anisotropic and tubular pores  | Pores are often small and pore size ranges may be limited<br>Long time required to sublime non-aqueous solvent   | 43,296,299         |
|   | Microsphere sintering                    | Polymer microspheres are stacked and joined together via sintering (by being exposed to heat or solvent) to form microsphere scaffold (or template)   | Can form gradient structures by encapsulating bioactive molecules or cells within the microspheres<br>Can make scaffolds with graded pore sizes from templates comprising different sized microspheres | Low interconnectivity of pores<br>Microsphere scaffolds have low mechanical strength<br>Microsphere templates require removal with organic solvents        | 44,394,395         |
|   | Electrospinning                          | The polymer solution is loaded in a capillary tube and a jet is ejected from the tip as the surface tension is overcome by applied voltage, the jet dries during flight and elongates due to external and internal electric forces, eventually depositing on a conductive substrate in the form of uniform nanometre-sized fibres | Can generate nanofibrous structures resembling natural ECM, with high porosity and surface area to volume ratio  | Potential issues with beading and small pore sizes<br>May be difficult or time-consuming to generate thick scaffolds                                       | 45,195,241,243,407 |

| Scaffold Type  | Fabrication Technique             | Brief Description   | Main Advantages   | Main Disadvantages  | Example Studies |
|--|-----------------------------------|---|---|---|-----------------|
| Ceramic scaffolds, polymer scaffolds and polymer-based composite scaffolds | Solid Free-form Fabrication (SFF) | A range of computer-controlled scaffold fabrication techniques for the realisation of 3D computer-aided design (CAD) models; the CAD model is expressed as a series of cross-sections and manufactured layer by layer using a SFF machine from material stock (solid sheet, liquid or powder) | Can generate scaffolds with complex and customised geometries to precisely match the tissue defect<br>Allows precise control over material composition, and offers the potential of generating composite structures with multiple materials or material gradients<br>Offers complete control over internal structure without processing or size limitations experienced by traditional techniques<br>Can produce scaffolds with higher strength to porosity ratio compared to traditional techniques<br>Reproducible and reliable fabrication | Higher cost compared to traditional techniques<br>Relatively limited material selection<br>Limited accuracy and resolution particularly for small-scale systems<br>Various technical difficulties, e.g. poor binding of material in 3D printing, thermal degradation of material in FDM, nozzle clogging in robocasting<br>The gain in biological performance due to geometrical improvements has not been quantified |                 |
|  | 3D printing                       | The inkjet head prints binder fluid on a powder bed to bind the material powder layer by layer until the 3D scaffold is complete, after which the loose powder is removed   |   |   | 384             |
|  | Fused Deposition Modelling (FDM)  | Thermoplastic fibres are heated and selectively extruded through a nozzle layer by layer, scaffolds with honeycomb-like internal structures are formed by changing the direction of material deposition for consecutively deposited layers  |   |   | 195,197         |
|  | Robocasting                       | Strands of material slurry are extruded from a robot-controlled nozzle in a defined trajectory to form each layer of the scaffold, the slurry in each layer must solidify before the next layer is added  |   |   | 41,114,174      |

**Table 3.** Overview of current scaffold strategies for osteochondral tissue regeneration.

| Osteochondral Scaffold Strategy   | Schematic   | Description   | Advantages  | Disadvantages  | Representative Studies   |
|---|---|---|---|--|--|
| Monophasic scaffold   |    | Homogeneous material composition with no spatial variations in structure, cell type or distribution of bioactive molecules  | Fabrication simplicity and reproducibility; ability to regenerate both cartilage and bone reported in some <i>in vivo</i> models, particularly in combination with cells and/or bioactive molecules   | Homogeneous properties typically do not address the different requirements of two tissues; cartilage and/or bone regeneration is often incomplete particularly in large animal models  | 194,204-207,390,399,405,406,408,411  |
| Cells for cartilage phase and scaffold for bone phase                       |    | Cartilage phase is scaffold-free and consists of cells (chondrocytes or MSCs) grown on top of the bone phase scaffold   | Relative ease of production; evidence for seeded cells to form neocartilage on top of bone phase <i>in vitro</i> and <i>in vivo</i>   | Cell layer prone to delamination due to low interfacial shear strength; necessity for pre-culture of cells prior implantation may hinder translation   | 202,213,373,377,385,386  |
| Assembled scaffold with individual scaffolds for cartilage and bone         |    | Cartilage and bone phases (often seeded or pre-cultured separately) sutured, glued or pressed together before or during implantation  | Straightforward method of producing two phases with different properties; evidence for variable degrees of osteochondral regeneration in a range of <i>in vivo</i> models   | Good integration between phases may be difficult to achieve; distinct interface does not allow gradual transition of properties; heavy reliance on pre-culture of cells; several <i>in vivo</i> studies reported substantial fibrocartilage regeneration | 195,197,208-210,215,379,381,382,391,400,403,404,410                            |
| Homogeneous scaffold with different cell populations for cartilage and bone |    | Scaffold has homogeneous composition and structure, but its two ends contain different cell populations respectively intended for cartilage and bone regeneration   | Potential of producing stratified layers of cartilage and bone tissue with well integrated interface, and maintenance of cell phenotype without ongoing bioactive molecule supplementation  | Necessitates pre-culture of cells; hydrogel systems often employed as scaffold which may have insufficient mechanical integrity; lack of evidence for performance in orthotopic <i>in vivo</i> models  | 376,383,387,388  |
| Homogeneous scaffold with continuous gradient of bioactive molecules        |  | Scaffold has homogeneous composition and structure, but contains one or more bioactive molecules bound to the scaffold or encapsulated in microspheres to form a continuous concentration gradient  | Evidence for selective differentiation of cells to form cartilage and bone tissue according to spatial presentation of bioactive molecules <i>in vitro</i> and <i>in vivo</i> , without necessitating different cell populations or even inclusion of cells   | Processing complexity may hinder translation; difficult to determine optimal dosage, distribution and release rate of bioactive molecules; scaffold often consists of hydrogels or microspheres which may have insufficient mechanical integrity         | 374,394,395,402,452  |
| Single scaffold with integrated phases                                      |  | Cartilage and bone phases integrated during fabrication, with interface featuring continuous transition or an intermediate layer; alternatively a homogeneous scaffold is differentially modified along its length to form two or more phases | Integrated phases have heterogeneous properties to suit each osteochondral segment, with continuous transition at interface(s) and reduced risk of delamination; extensive <i>in vitro</i> and <i>in vivo</i> evidence of adequate osteochondral regeneration | Potential processing complexity and lack of reproducibility for multi-component designs; variable level of integration between phases depending on fabrication method; effective regeneration often relies on inclusion of cells or bioactive molecules  | 44,196,203,216,375,378,380,384,389,392,393,396-398,401,407,409,412,414,421-423 |

**Table 4.** Summary of silk-based scaffold systems for osteochondral tissue regeneration.

| Scaffold Strategy   | Study                     | Cartilage Phase   | Subchondral Bone Phase                              | Integration   | Experimental Model   | Findings   |
|---|---------------------------|---|---|---|--|--|
| Assembled scaffold with individual scaffolds for cartilage and bone | Augst 2008 <sup>430</sup> | Silk scaffold with cells grown in chondrogenic medium     | Silk scaffold with cells grown in osteogenic medium | Scaffolds for cartilage and bone phases were pre-cultured separately, then joined with silk suture before co-culture                                | Bone marrow-derived hMSCs were pre-cultured in separate silk scaffolds in chondrogenic or osteogenic medium for 3 weeks in a rotating bioreactor, then combined and co-cultured <i>in vitro</i> for another 3 weeks in chondrogenic, osteogenic or growth medium | During co-culture, formation of bone-like tissue progressed to a much greater extent than cartilage-like tissue in all three types of media, while chondrogenic medium produced the best integration between phases<br>For all constructs, GAG content was significantly higher in the cartilage phase while calcium deposition was only present in the bone phase<br>Constructs had very low compressive modulus of 20-30kPa at the end of the culture period |
|   | Chen 2013 <sup>432</sup>  | Silk scaffold with cells grown in chondrogenic medium     | Silk scaffold with cells grown in osteogenic medium | Scaffolds for cartilage and bone phases were pre-cultured separately, then combined using RADA self-assembling peptide before co-culture            | Rabbit bone marrow-derived stromal cells were pre-cultured in separate silk scaffolds in chondrogenic or osteogenic medium for 2 weeks, then combined and co-cultured <i>in vitro</i> for another 2 weeks in cocktail medium                                     | Cartilage phase showed higher expression of aggrecan and higher GAG deposition, while bone phase showed higher expression of collagen I and osteonectin and exclusive calcium deposition<br>Intermediate region expressed the hypertrophic markers collagen X and MMP-13, with interface-like structures shown by GAG and calcium staining   |
|   | Saha 2013 <sup>436</sup>  | Mulberry or non-mulberry silk scaffold +/- TGF- $\beta$ 3 | Mulberry or non-mulberry silk scaffold +/- BMP-2    | Silk discs were stacked together to form the two phases, which were joined using fibrin glue before implantation                                    | <i>In vivo</i> implantation of the assembled scaffold (cell-free) in osteochondral defects of the rat patellar groove (1.8mm diameter $\times$ 1mm deep) for 8 weeks   | All implants were positive for collagen type I and GAG, while collagen type II was only significantly positive in non-mulberry implants; more intense staining was observed in implants containing growth factors<br>All implanted defects showed neovascularisation at the base   |
| Single scaffold with integrated phases                              | Yan 2014 <sup>435</sup>   | Silk scaffold   | Silk / calcium phosphate scaffold                   | Bone phase scaffold was formed and silk solution containing porogen (NaCl) was added on top, followed by drying, porogen removal and lyophilisation | Preliminary characterisations  | Scaffold showed porous and interconnected structure with good integration between phases<br>Compressive modulus reached 16MPa<br>Only the bone phase showed mineralisation ability in simulated body fluid   |

| Scaffold Strategy   | Study                    | Scaffold   | Cell Populations / Bioactive Molecule Gradient  | Experimental Model   | Findings  |
|---|--------------------------|--|---|--|---|
| Homogeneous scaffold with different cell populations for cartilage and bone | Chen 2012 <sup>433</sup> | Silk scaffold  | Scaffold was first cultured with bone marrow stromal cells in chondrogenic medium and later co-cultured with osteoblast layer   | Separate culture of rabbit bone marrow stromal cells in the scaffold in chondrogenic medium and rabbit osteoblasts on a cell culture plate in growth medium for 1 week, then the scaffold was placed in contact with the osteoblast layer and co-cultured <i>in vitro</i> for another 3 weeks in chondrogenic medium | An osteochondral interface layer formed with lower GAG content and lower expression of the chondrogenic markers collagen type II and aggrecan, but higher expression of the hypertrophic markers collagen X and MMP-13 compared to scaffolds not co-cultured with osteoblasts   |
|   | Chen 2013 <sup>431</sup> | Silk-RADA peptide hybrid scaffold  | Scaffold was seeded with bone marrow stromal cells and the two ends were exposed respectively to chondrogenic and osteogenic medium   | Rabbit bone marrow stromal cells were seeded in the scaffold and cultured <i>in vitro</i> for 2 weeks in a static two-chambered co-culture well, which held chondrogenic and osteogenic medium in two separate chambers  | Cartilage-like tissue formed in the chondrogenic region (positive for GAG with higher expression of collagen II, aggrecan and Sox9), while bone-like tissue formed in the osteogenic region (mineralisation with higher expression of Runx2 and osteopontin) Hypertrophic chondrocytes were found in the intermediate region with calcified ECM containing GAG and collagen I, II and X   |
| Homogeneous scaffold with continuous gradient of bioactive molecules        | Wang 2009 <sup>434</sup> | 1. Alginate hydrogel containing PLGA or silk microspheres<br>2. Silk scaffold containing silk microspheres | rhIGF-1 was used for chondrogenesis and rhBMP-2 was used for osteogenesis<br>Microspheres encapsulating growth factors were used to create a single or reverse gradient in the alginate hydrogel or silk scaffold via a modified gradient maker | <i>In vitro</i> culture of bone marrow-derived hMSCs encapsulated in alginate hydrogel for 3 weeks, or seeded in silk scaffold for 5 weeks, all in cocktail medium   | In the alginate hydrogel, silk microspheres were more efficient in delivering BMP-2 but less efficient in delivering IGF-1 compared to PLGA microspheres; single and reverse gradients of IGF-1 and BMP-2 induced both chondrogenesis and osteogenesis in hMSCs, but levels of differentiation did not follow the gradient and were randomly distributed in the hydrogel The silk scaffold showed formation of a deeper and more linear growth factor gradient; hMSCs showed chondrogenic and osteogenic differentiation (confirmed by gene expression and staining for proteoglycan and mineralisation) along the BMP-2 gradient which was enhanced in the BMP-2/IGF-1 reverse gradient, although the IGF-1 gradient alone had no effect |

## References

1. M. Doblaré, J. M. García, and M. J. Gómez, *Eng. Fract. Mech.*, 2004, **71**, 1809-1840.
2. J. I. Dawson, and R. O. C. Oreffo, *Arch. Biochem. Biophys.*, 2008, **473**, 124-131.
3. J. P. Schmitz, and J. O. Hollinger, *Clin. Orthop. Relat. Res.*, 1986, **205**, 299-308.
4. M. J. Yaszemski, R. G. Payne, W. C. Hayes, R. Langer, and A. G. Mikos, *Biomaterials*, 1996, **17**, 175-185.
5. J. Aronson, *J. Bone Jt. Surg.*, 1997, **79**, 1243-58.
6. S. A. Green, J. M. Jackson, D. M. Wall, H. Marinow, and J. Ishkanian, *Clin. Orthop. Relat. Res.*, 1992, **280**, 136-142.
7. P. V. Giannoudis, H. Dinopoulos, and E. Tsiridis, *Injury*, 2005, **36**, S20-S27.
8. C. J. Damien, and J. R. Parsons, *J. Appl. Biomater.*, 1991, **2**, 187-208.
9. E. D. Arrington, W. J. Smith, H. G. Chambers, A. L. Bucknell, and N. A. Davino, *Clin. Orthop. Relat. Res.*, 1996, **329**, 300-309.
10. J. C. Banwart, M. A. Asher, and R. S. Hassanein, *Spine*, 1995, **20**, 1055-1060.
11. D. M. Strong, G. E. Friedlaender, W. W. Tomford, D. S. Springfield, T. C. Shives, H. Burchardt, W. F. Enneking, and H. J. Mankin, *Clin. Orthop. Relat. Res.*, 1996, **326**, 107-114.
12. W. W. Tomford, *J. Bone Jt. Surg., Am. Vol.*, 1995, **77A**, 1742-1754.
13. J. Y. Rho, L. Kuhn-Spearing, and P. Zioupos, *Medical Engineering & Physics*, 1998, **20**, 92-102.
14. S. Bose, M. Roy, and A. Bandyopadhyay, *Trends Biotechnol.*, 2012, **30**, 546-554.
15. A. J. Salgado, O. P. Coutinho, and R. L. Reis, *Macromol. Biosci.*, 2004, **4**, 743-765.
16. T. Albrektsson, and C. Johansson, *Eur. Spine J.*, 2001, **10**, S96-S101.
17. K. Rezwan, Q. Z. Chen, J. J. Blaker, and A. R. Boccaccini, *Biomaterials*, 2006, **27**, 3413-3431.
18. D. W. Hutmacher, J. T. Schantz, C. X. F. Lam, K. C. Tan, and T. C. Lim, *J. Tissue Eng. Regener. Med.*, 2007, **1**, 245-260.
19. V. Karageorgiou, and D. Kaplan, *Biomaterials*, 2005, **26**, 5474-5491.
20. Y. Ikada, *J. R. Soc., Interface*, 2006, **3**, 589-601.
21. T. M. Simon, and D. W. Jackson, *Sports Med. Arthrosc.*, 2006, **14**, 146-154.
22. L. u. Danišovič, I. Varga, R. Zamborský, and D. Böhmer, *Exp. Biol. Med.*, 2012, **237**, 10-17.
23. A. R. Poole, T. Kojima, T. Yasuda, F. Mwale, M. Kobayashi, and S. Lavery, *Clin. Orthop. Relat. Res.*, 2001, **391**, S26-S33.
24. T. A. E. Ahmed, and M. T. Hincke, *Tissue Eng., Part B*, 2009, **16**, 305-329.
25. S. P. Nukavarapu, and D. L. Dorcenus, *Biotechnol. Adv.*, 2013, **31**, 706-721.
26. J. W. Alford, and B. J. Cole, *Am. J. Sports Med.*, 2005, **33**, 295-306.
27. E. Kon, A. Gobbi, G. Filardo, M. Delcogliano, S. Zaffagnini, and M. Marcacci, *Am. J. Sports Med.*, 2009, **37**, 33-41.
28. K. Mithoefer, T. McAdams, R. J. Williams, P. C. Kreuz, and B. R. Mandelbaum, *Am. J. Sports Med.*, 2009, **37**, 2053-2063.
29. M. Brittberg, *Injury*, 2008, **39**, 40-49.

30. L. Peterson, H. S. Vasiliadis, M. Brittberg, and A. Lindahl, *Am. J. Sports Med.*, 2010, **38**, 1117-1124.
31. J. D. Harris, R. A. Siston, R. H. Brophy, C. Lattermann, J. L. Carey, and D. C. Flanigan, *Osteoarthritis Cartilage*, 2011, **19**, 779-791.
32. M. Brittberg, *Am. J. Sports Med.*, 2010, **38**, 1259-1271.
33. M.-H. Zheng, C. Willers, L. Kirilak, P. Yates, J. Xu, D. Wood, and A. Shimmin, *Tissue Eng.*, 2007, **13**, 737-746.
34. C. M. Hettrich, D. Crawford, and S. A. Rodeo, *Sports Med. Arthrosc.*, 2008, **16**, 230-235.
35. J. T. Kerker, A. J. Leo, and N. A. Sgaglione, *Sports Med. Arthrosc.*, 2008, **16**, 208-216.
36. K. E. M. Benders, P. R. van Weeren, S. F. Badylak, D. B. F. Saris, W. J. A. Dhert, and J. Malda, *Trends Biotechnol.*, 2013, **31**, 169-176.
37. J. Raghunath, J. Rollo, K. M. Sales, P. E. Butler, and A. M. Seifalian, *Biotechnol. Appl. Biochem.*, 2007, **46**, 73-84.
38. S. I. Roohani-Esfahani, C. R. Dunstan, J. J. Li, Z. Lu, B. Davies, S. Pearce, J. Field, R. Williams, and H. Zreiqat, *Acta Biomater.*, 2013, **9**, 7014-7024.
39. P. Habibovic, H. Yuan, M. van den Doel, T. M. Sees, C. A. van Blitterswijk, and K. de Groot, *J. Orthop. Res.*, 2006, **24**, 867-876.
40. Z. Y. Wu, R. G. Hill, S. Yue, D. Nightingale, P. D. Lee, and J. R. Jones, *Acta Biomater.*, 2011, **7**, 1807-1816.
41. C. Wu, Y. Luo, G. Cuniberti, Y. Xiao, and M. Gelinsky, *Acta Biomater.*, 2011, **7**, 2644-2650.
42. U. J. Kim, J. Park, H. J. Kim, M. Wada, and D. L. Kaplan, *Biomaterials*, 2005, **26**, 2775-2785.
43. R. Nazarov, H. J. Jin, and D. L. Kaplan, *Biomacromolecules*, 2004, **5**, 718-726.
44. A. Galperin, R. A. Oldinski, S. J. Florczyk, J. D. Bryers, M. Zhang, and B. D. Ratner, *Adv. Healthcare Mater.*, 2013, **2**, 872-883.
45. C. Li, C. Vepari, H. J. Jin, H. J. Kim, and D. L. Kaplan, *Biomaterials*, 2006, **27**, 3115-3124.
46. S. M. Best, A. E. Porter, E. S. Thian, and J. Huang, *J. Eur. Ceram. Soc.*, 2008, **28**, 1319-1327.
47. P. Ducheyne, and Q. Qiu, *Biomaterials*, 1999, **20**, 2287-2303.
48. Q. Z. Chen, I. D. Thompson, and A. R. Boccaccini, *Biomaterials*, 2006, **27**, 2414-2425.
49. H. R. Ramay, and M. Zhang, *Biomaterials*, 2003, **24**, 3293-3302.
50. M. Schieker, H. Seitz, I. Drosse, S. Seitz, and W. Mutschler, *European Journal of Trauma*, 2006, **32**, 114-124.
51. G. Daculsi, R. Z. LeGeros, M. Heughebaert, and I. Barbieux, *Calcif. Tissue Int.*, 1990, **46**, 20-27.
52. F. Barrère, C. A. van Blitterswijk, and K. de Groot, *Int. J. Nanomed.*, 2006, **1**, 317-332.
53. R. Z. LeGeros, *Chem. Rev.*, 2008, **108**, 4742-4753.
54. M. M. Dvorak, and D. Riccardi, *Cell Calcium*, 2004, **35**, 249-255.
55. S. L. Godwin, and S. P. Soltoff, *J. Biol. Chem.*, 1997, **272**, 11307-11312.

56. A. M. C. Barradas, H. A. M. Fernandes, N. Groen, Y. C. Chai, J. Schrooten, J. van de Peppel, J. P. T. M. van Leeuwen, C. A. van Blitterswijk, and J. de Boer, *Biomaterials*, 2012, **33**, 3205-3215.
57. G. R. Beck, B. Zerler, and E. Moran, *Proc. Natl. Acad. Sci. U. S. A.*, 2000, **97**, 8352-8357.
58. M. Murshed, D. Harmey, J. L. Millán, M. D. McKee, and G. Karsenty, *Genes Dev.*, 2005, **19**, 1093-1104.
59. R. Z. LeGeros, *Clin. Orthop. Relat. Res.*, 2002, **395**, 81-98.
60. U. Heise, J. F. Osborn, and F. Duwe, *Int. Orthop.*, 1990, **14**, 329-338.
61. R. Quarto, M. Mastrogiacomo, R. Cancedda, S. M. Kutepov, V. Mukhachev, A. Lavroukov, E. Kon, and M. Marcacci, *N. Engl. J. Med.*, 2001, **344**, 385-386.
62. M. Marcacci, E. Kon, V. Moukhachev, A. Lavroukov, S. Kutepov, R. Quarto, M. Mastrogiacomo, and R. Cancedda, *Tissue Eng.*, 2007, **13**, 947-955.
63. C. A. Vacanti, L. J. Bonassar, M. P. Vacanti, and J. Shufflebarger, *N. Engl. J. Med.*, 2001, **344**, 1511-1514.
64. T. Morishita, K. Honoki, H. Ohgushi, N. Kotobuki, A. Matsushima, and Y. Takakura, *Artif. Organs*, 2006, **30**, 115-118.
65. C. Wang, Y. Duan, B. Markovic, J. Barbara, C. R. Howlett, X. Zhang, and H. Zreiqat, *Biomaterials*, 2004, **25**, 2949-2956.
66. J. Xie, M. J. Baumann, and L. R. McCabe, *J. Biomed. Mater. Res., Part A*, 2004, **71A**, 108-117.
67. M. Mastrogiacomo, A. Muraglia, V. Komlev, F. Peyrin, F. Rustichelli, A. Crovace, and R. Cancedda, *Orthod. Craniofac. Res.*, 2005, **8**, 277-284.
68. P. Proussaefs, J. Lozada, G. Valencia, and M. D. Rohrer, *J. Prosthet. Dent.*, 2002, **87**, 481-484.
69. C. Benaqqa, J. Chevalier, M. Saâdaoui, and G. Fantozzi, *Biomaterials*, 2005, **26**, 6106-6112.
70. J. Shepherd, D. Shepherd, and S. Best, *J. Mater. Sci.: Mater. Med.*, 2012, **23**, 2335-2347.
71. F. Yang, W.-j. Dong, F.-m. He, X.-x. Wang, S.-f. Zhao, and G.-l. Yang, *Oral Surg. Oral Med. Oral Pathol. Oral Radiol.*, 2012, **113**, 313-318.
72. V. Stanić, S. Dimitrijević, J. Antić-Stanković, M. Mitrić, B. Jokić, I. B. Plećaš, and S. Raičević, *Appl. Surf. Sci.*, 2010, **256**, 6083-6089.
73. C. Capuccini, P. Torricelli, E. Boanini, M. Gazzano, R. Giardino, and A. Bigi, *J. Biomed. Mater. Res., Part A*, 2009, **89A**, 594-600.
74. G.-X. Ni, Z.-P. Yao, G.-T. Huang, W.-G. Liu, and W. Lu, *J. Mater. Sci.: Mater. Med.*, 2011, **22**, 961-967.
75. E. Landi, G. Logroscino, L. Proietti, A. Tampieri, M. Sandri, and S. Sprio, *J. Mater. Sci.: Mater. Med.*, 2008, **19**, 239-247.
76. C. M. Botelho, R. A. Brooks, S. M. Best, M. A. Lopes, J. D. Santos, N. Rushton, and W. Bonfield, *J. Biomed. Mater. Res., Part A*, 2006, **79A**, 723-730.
77. A. E. Porter, N. Patel, J. N. Skepper, S. M. Best, and W. Bonfield, *Biomaterials*, 2004, **25**, 3303-3314.
78. T. V. Safronova, V. I. Putlyaev, O. A. Avramenko, M. A. Shekhirev, and A. G. Veresov, *Glass Ceram.*, 2011, **68**, 28-32.

79. S. Samavedi, A. R. Whittington, and A. S. Goldstein, *Acta Biomater.*, 2013, **9**, 8037-8045.
80. N. Kondo, A. Ogose, K. Tokunaga, T. Ito, K. Arai, N. Kudo, H. Inoue, H. Irie, and N. Endo, *Biomaterials*, 2005, **26**, 5600-5608.
81. G. Liu, L. Zhao, W. Zhang, L. Cui, W. Liu, and Y. Cao, *J. Mater. Sci.: Mater. Med.*, 2008, **19**, 2367-2376.
82. N. Kondo, A. Ogose, K. Tokunaga, H. Umezumi, K. Arai, N. Kudo, M. Hoshino, H. Inoue, H. Irie, K. Kuroda, H. Mera, and N. Endo, *Biomaterials*, 2006, **27**, 4419-4427.
83. R. D. A. Gaasbeek, H. G. Toonen, R. J. van Heerwaarden, and P. Buma, *Biomaterials*, 2005, **26**, 6713-6719.
84. L. Galois, D. Mainard, and J. P. Delagoutte, *Int. Orthop.*, 2002, **26**, 109-115.
85. A. Ogose, N. Kondo, H. Umezumi, T. Hotta, H. Kawashima, K. Tokunaga, T. Ito, N. Kudo, M. Hoshino, W. Gu, and N. Endo, *Biomaterials*, 2006, **27**, 1542-1549.
86. C. J. Anker, S. P. Holdridge, B. Baird, H. Cohen, and T. A. Damron, *Clin. Orthop. Relat. Res.*, 2005, **434**, 251-257.
87. A. Ogose, T. Hotta, H. Kawashima, N. Kondo, W. Gu, T. Kamura, and N. Endo, *J. Biomed. Mater. Res., Part B*, 2005, **72B**, 94-101.
88. M. Hirata, H. Murata, H. Takeshita, T. Sakabe, Y. Tsuji, and T. Kubo, *Int. Orthop.*, 2006, **30**, 510-513.
89. I. R. Zerbo, A. L. J. J. Bronckers, G. d. Lange, and E. H. Burger, *Biomaterials*, 2005, **26**, 1445-1451.
90. M. C. von Doernberg, B. von Rechenberg, M. Bohner, S. Grünenfelder, G. H. van Lenthe, R. Müller, B. Gasser, R. Mathys, G. Baroud, and J. Auer, *Biomaterials*, 2006, **27**, 5186-5198.
91. K. A. Hing, L. F. Wilson, and T. Buckland, *Spine J.*, 2007, **7**, 475-490.
92. T. Okuda, K. Ioku, I. Yonezawa, H. Minagi, G. Kawachi, Y. Gonda, H. Murayama, Y. Shibata, S. Minami, S. Kamihira, H. Kurosawa, and T. Ikeda, *Biomaterials*, 2007, **28**, 2612-2621.
93. R. Z. LeGeros, S. Lin, R. Rohanizadeh, D. Mijares, and J. P. LeGeros, *J. Mater. Sci.: Mater. Med.*, 2003, **14**, 201-209.
94. S. V. Dorozhkin, *Biomaterials*, 2010, **31**, 1465-1485.
95. T. L. Arinzeh, T. Tran, J. McAlary, and G. Daculsi, *Biomaterials*, 2005, **26**, 3631-3638.
96. B. H. Fella, O. Gauthier, P. Weiss, D. Chappard, and P. Layrolle, *Biomaterials*, 2008, **29**, 1177-1188.
97. S. S. Jensen, A. Yeo, M. Dard, E. Hunziker, R. Schenk, and D. Buser, *Clin. Oral Implants Res.*, 2007, **18**, 752-760.
98. G. Daculsi, N. Passuti, S. Martin, C. Deudon, R. Z. Legeros, and S. Raheer, *J. Biomed. Mater. Res.*, 1990, **24**, 379-396.
99. O. Gauthier, J. M. Bouler, E. Aguado, P. Pilet, and G. Daculsi, *Biomaterials*, 1998, **19**, 133-139.
100. L. Guehenec, E. Goyenvale, E. Aguado, P. Pilet, M. D'Arc, M. Bilban, R. Spaethe, and G. Daculsi, *J. Mater. Sci.: Mater. Med.*, 2005, **16**, 29-35.
101. S. Lobo, F. Wykrota, A. Oliveira, I. Kerkis, G. Mahecha, and H. Alves, *J. Mater. Sci.: Mater. Med.*, 2009, **20**, 1137-1147.

102. T. L. Livingston, S. Gordon, M. Archambault, S. Kadiyala, K. McIntosh, A. Smith, and S. J. Peter, *J. Mater. Sci.: Mater. Med.*, 2003, **14**, 211-218.
103. H. Yuan, C. A. van Blitterswijk, K. de Groot, and J. D. de Bruijn, *J. Biomed. Mater. Res., Part A*, 2006, **78A**, 139-147.
104. P. Habibovic, M. C. Kruyt, M. V. Juhl, S. Clyens, R. Martinetti, L. Dolcini, N. Theilgaard, and C. A. van Blitterswijk, *J. Orthop. Res.*, 2008, **26**, 1363-1370.
105. K. Kurashina, H. Kurita, Q. Wu, A. Ohtsuka, and H. Kobayashi, *Biomaterials*, 2002, **23**, 407-412.
106. H. Yuan, C. A. van Blitterswijk, K. de Groot, and J. D. de Bruijn, *Tissue Eng.*, 2006, **12**, 1607-1615.
107. H. Yuan, M. van den Doel, S. Li, C. A. van Blitterswijk, K. de Groot, and J. D. de Bruijn, *J. Mater. Sci.: Mater. Med.*, 2002, **13**, 1271-1275.
108. J. O. Eniwumide, H. Yuan, S. H. Cartmell, G. J. Meijer, and J. D. de Bruijn, *Eur. Cells Mater.*, 2007, **14**, 30-8; discussion 39.
109. D. Le Nihouannen, G. Daculsi, A. Saffarzadeh, O. Gauthier, S. Delplace, P. Pilet, and P. Layrolle, *Bone*, 2005, **36**, 1086-1093.
110. F. Ye, X. Lu, B. Lu, J. Wang, Y. Shi, L. Zhang, J. Chen, Y. Li, and H. Bu, *J. Mater. Sci.: Mater. Med.*, 2007, **18**, 2173-2178.
111. P. Müller, U. Bulnheim, A. Diener, F. Lüthen, M. Teller, E.-D. Klinkenberg, H.-G. Neumann, B. Nebe, A. Liebold, G. Steinhoff, and J. Rychly, *J. Cell. Mol. Med.*, 2008, **12**, 281-291.
112. H. Sun, F. Ye, J. Wang, Y. Shi, Z. Tu, J. Bao, M. Qin, H. Bu, and Y. Li, *Transplant. Proc.*, 2008, **40**, 2645-2648.
113. G. Song, P. Habibovic, C. Bao, J. Hu, C. A. van Blitterswijk, H. Yuan, W. Chen, and H. H. K. Xu, *Biomaterials*, 2013, **34**, 2167-2176.
114. S. K. Lan Levengood, S. J. Polak, M. B. Wheeler, A. J. Maki, S. G. Clark, R. D. Jamison, and A. J. Wagoner Johnson, *Biomaterials*, 2010, **31**, 3552-3563.
115. L. Cordaro, D. D. Bosshardt, P. Palattella, W. Rao, G. Serino, and M. Chiapasco, *Clin. Oral Implants Res.*, 2008, **19**, 796-803.
116. A. Friedmann, M. Dard, B.-M. Kleber, J.-P. Bernimoulin, and D. D. Bosshardt, *Clin. Oral Implants Res.*, 2009, **20**, 708-714.
117. J. H. Lee, U. W. Jung, C. S. Kim, S. H. Choi, and K. S. Cho, *Clin. Oral Implants Res.*, 2008, **19**, 767-771.
118. M. Ozalay, O. Sahin, S. Akpınar, G. Ozkoc, M. Cinar, and N. Cesur, *Arch. Orthop. Trauma Surg.*, 2009, **129**, 747-752.
119. J. L. Rouvillain, F. Lavallé, H. Pascal-Mousselard, Y. Catonné, and G. Daculsi, *The Knee*, 2009, **16**, 392-397.
120. C. Schwartz, P. Liss, B. Jacquemaire, P. Lecestre, and P. Frayssinet, *J. Mater. Sci.: Mater. Med.*, 1999, **10**, 821-825.
121. C. A. Garrido, S. E. Lobo, F. M. Turibio, and R. Z. LeGeros, *Int. J. Biomater.*, 2011, **2011**,
122. Y. C. Chai, A. Carlier, J. Bolander, S. J. Roberts, L. Geris, J. Schrooten, H. Van Oosterwyck, and F. P. Luyten, *Acta Biomater.*, 2012, **8**, 3876-3887.
123. J. R. Jones, *Acta Biomater.*, 2013, **9**, 4457-4486.
124. L. L. Hench, *J. Am. Ceram. Soc.*, 1998, **81**, 1705-1728.

125. L. L. Hench, *J. Mater. Sci.: Mater. Med.*, 2006, **17**, 967-978.
126. L.-C. Gerhardt, and A. R. Boccaccini, *Materials*, 2010, **3**, 3867-3910.
127. M. Bosetti, and M. Cannas, *Biomaterials*, 2005, **26**, 3873-3879.
128. E. A. B. Effah Kaufmann, P. Ducheyne, and I. M. Shapiro, *Tissue Eng.*, 2000, **6**, 19-28.
129. J. E. Gough, J. R. Jones, and L. L. Hench, *Biomaterials*, 2004, **25**, 2039-2046.
130. I. D. Xynos, M. V. J. Hukkanen, J. J. Batten, L. D. Buttery, L. L. Hench, and J. M. Polak, *Calcif. Tissue Int.*, 2000, **67**, 321-329.
131. G. Jell, I. Notingher, O. Tsigkou, P. Notingher, J. M. Polak, L. L. Hench, and M. M. Stevens, *J. Biomed. Mater. Res., Part A*, 2008, **86A**, 31-40.
132. O. Tsigkou, J. R. Jones, J. M. Polak, and M. M. Stevens, *Biomaterials*, 2009, **30**, 3542-3550.
133. A. Hoppe, N. S. Güldal, and A. R. Boccaccini, *Biomaterials*, 2011, **32**, 2757-2774.
134. L. L. Hench, *J. Eur. Ceram. Soc.*, 2009, **29**, 1257-1265.
135. I. D. Xynos, A. J. Edgar, L. D. K. Buttery, L. L. Hench, and J. M. Polak, *Biochem. Biophys. Res. Commun.*, 2000, **276**, 461-465.
136. I. D. Xynos, A. J. Edgar, L. D. K. Buttery, L. L. Hench, and J. M. Polak, *J. Biomed. Mater. Res.*, 2001, **55**, 151-157.
137. G. Jell, and M. M. Stevens, *J. Mater. Sci.: Mater. Med.*, 2006, **17**, 997-1002.
138. R. M. Day, *Tissue Eng.*, 2005, **11**, 768-777.
139. R. M. Day, A. R. Boccaccini, S. Shurey, J. A. Roether, A. Forbes, L. L. Hench, and S. M. Gabe, *Biomaterials*, 2004, **25**, 5857-5866.
140. D. L. Wheeler, K. E. Stokes, R. G. Hoellrich, D. L. Chamberland, and S. W. McLoughlin, *J. Biomed. Mater. Res.*, 1998, **41**, 527-533.
141. D. L. Wheeler, E. J. Eschbach, R. G. Hoellrich, M. J. Montfort, and D. L. Chamberland, *J. Orthop. Res.*, 2000, **18**, 140-148.
142. M. Vogel, C. Voigt, U. M. Gross, and C. M. Müller-Mai, *Biomaterials*, 2001, **22**, 357-362.
143. H. Oonishi, S. Kushitani, E. Yasukawa, H. Iwaki, L. L. Hench, J. Wilson, E. Tsuji, and T. Sugihara, *Clin. Orthop. Relat. Res.*, 1997, **334**, 316-325.
144. H. Oonishi, L. L. Hench, J. Wilson, F. Sugihara, E. Tsuji, S. Kushitani, and H. Iwaki, *J. Biomed. Mater. Res.*, 1999, **44**, 31-43.
145. H. Oonishi, L. L. Hench, J. Wilson, F. Sugihara, E. Tsuji, M. Matsuura, S. Kin, T. Yamamoto, and S. Mizokawa, *J. Biomed. Mater. Res.*, 2000, **51**, 37-46.
146. E. J. G. Schepers, and P. Ducheyne, *J. Oral Rehabil.*, 1997, **24**, 171-181.
147. J. Wilson, and S. B. Low, *J. Appl. Biomater.*, 1992, **3**, 123-129.
148. H. Yuan, J. D. de Bruijn, X. Zhang, C. A. van Blitterswijk, and K. de Groot, *J. Biomed. Mater. Res.*, 2001, **58**, 270-276.
149. S. J. Froum, M. A. Weinberg, and D. Tarnow, *J. Periodontol.*, 1998, **69**, 698-709.
150. T. B. Lovelace, J. T. Mellonig, R. M. Meffert, A. A. Jones, P. V. Nummikoski, and D. L. Cochran, *J. Periodontol.*, 1998, **69**, 1027-1035.
151. S. B. Low, C. J. King, and J. Krieger, *International Journal of Periodontics & Restorative Dentistry*, 1997, **17**, 358-67.
152. R. Mengel, M. Soffner, and L. Flores-de-Jacoby, *J. Periodontol.*, 2003, **74**, 899-908.

153. J.-S. Park, J.-J. Suh, S.-H. Choi, I.-S. Moon, K.-S. Cho, C.-K. Kim, and J.-K. Chai, *J. Periodontol.*, 2001, **72**, 730-740.
154. J. S. Zamet, U. R. Darbar, G. S. Griffiths, J. S. Bulman, U. Brägger, W. Bürgin, and H. N. Newman, *J. Clin. Periodontol.*, 1997, **24**, 410-418.
155. J. T. Heikkilä, J. Kukkonen, A. J. Aho, S. Moisander, T. Kyyrönen, and K. Mattila, *J. Mater. Sci.: Mater. Med.*, 2011, **22**, 1073-1080.
156. T. Goff, N. K. Kanakaris, and P. V. Giannoudis, *Injury*, 2013, **44**, **S1**, S86-S94.
157. N. C. Lindfors, J. T. Heikkilä, I. Koski, K. Mattila, and A. J. Aho, *J. Biomed. Mater. Res., Part B*, 2009, **90B**, 131-136.
158. N. C. Lindfors, I. Koski, J. T. Heikkilä, K. Mattila, and A. J. Aho, *J. Biomed. Mater. Res., Part B*, 2010, **94B**, 157-164.
159. T. Turunen, J. Peltola, A. Yli-Urpo, and R.-P. Happonen, *Clin. Oral Implants Res.*, 2004, **15**, 135-141.
160. B. Ilharreborde, E. Morel, F. Fitoussi, A. Presedo, P. Souchet, G.-F. Penneçot, and K. Mazda, *J. Pediatr. Orthop.*, 2008, **28**, 347-351.
161. N. C. Lindfors, P. Hyvönen, M. Nyssönen, M. Kirjavainen, J. Kankare, E. Gullichsen, and J. Salo, *Bone*, 2010, **47**, 212-218.
162. Q. Fu, E. Saiz, M. N. Rahaman, and A. P. Tomsia, *Mater. Sci. Eng., C*, 2011, **31**, 1245-1256.
163. O. Peitl Filho, G. P. La Torre, and L. L. Hench, *J. Biomed. Mater. Res.*, 1996, **30**, 509-514.
164. D. Bellucci, V. Cannillo, and A. Sola, *Ceram. Int.*, 2011, **37**, 145-157.
165. L. Moimas, M. Biasotto, R. D. Lenarda, A. Olivo, and C. Schmid, *Acta Biomater.*, 2006, **2**, 191-199.
166. H. Oudadesse, E. Dietrich, Y. L. Gal, P. Pellen, B. Bureau, A. A. Mostafa, and G. Cathelineau, *Biomed. Mater.*, 2011, **6**, 035006.
167. Q. Z. Chen, Y. Li, L. Y. Jin, J. M. W. Quinn, and P. A. Komesaroff, *Acta Biomater.*, 2010, **6**, 4143-4153.
168. J. R. Jones, L. M. Ehrenfried, and L. L. Hench, *Biomaterials*, 2006, **27**, 964-973.
169. N. Li, Q. Jie, S. Zhu, and R. Wang, *Ceram. Int.*, 2005, **31**, 641-646.
170. A. C. Marques, R. M. Almeida, A. Thiema, S. Wang, M. Falk, and H. Jain, *J. Mater. Res.*, 2009, **24**, 3495-3502.
171. Y. Zhu, C. Wu, Y. Ramaswamy, E. Kockrick, P. Simon, S. Kaskel, and H. Zreiqat, *Microporous Mesoporous Mater.*, 2008, **112**, 494-503.
172. D. Bellucci, V. Cannillo, A. Sola, F. Chiellini, M. Gazzarri, and C. Migone, *Ceram. Int.*, 2011, **37**, 1575-1585.
173. Q. Chen, D. Mohn, and W. J. Stark, *J. Am. Ceram. Soc.*, 2011, **94**, 4184-4190.
174. N. Doiphode, T. Huang, M. Leu, M. Rahaman, and D. Day, *J. Mater. Sci.: Mater. Med.*, 2011, **22**, 515-523.
175. W. Cao, and L. L. Hench, *Ceram. Int.*, 1996, **22**, 493-507.
176. W. Suchanek, and M. Yoshimura, *J. Mater. Res.*, 1998, **13**, 94-117.
177. A. J. Wagoner Johnson, and B. A. Herschler, *Acta Biomater.*, 2011, **7**, 16-30.
178. K. A. Hing, *Int. J. Appl. Ceram. Technol.*, 2005, **2**, 184-199.
179. Y. Liu, J. Lim, and S.-H. Teoh, *Biotechnol. Adv.*, 2013, **31**, 688-705.

180. S. Ni, J. Chang, L. Chou, and W. Zhai, *J. Biomed. Mater. Res., Part B*, 2007, **80B**, 174-183.
181. N. Zhang, J. A. Molenda, J. H. Fournelle, W. L. Murphy, and N. Sahai, *Biomaterials*, 2010, **31**, 7653-7665.
182. C. Wu, W. Fan, Y. Zhou, Y. Luo, M. Gelinsky, J. Chang, and Y. Xiao, *J. Mater. Chem.*, 2012, **22**, 12288-12295.
183. S. Ni, J. Chang, and L. Chou, *J. Biomed. Mater. Res., Part A*, 2006, **76A**, 196-205.
184. Y. Iimori, Y. Kameshima, K. Okada, and S. Hayashi, *J. Mater. Sci.: Mater. Med.*, 2005, **16**, 73-79.
185. Y. Ramaswamy, C. Wu, A. Van Hummel, V. Combes, G. Grau, and H. Zreiqat, *Biomaterials*, 2008, **29**, 4392-4402.
186. Y. Ramaswamy, C. T. Wu, H. Zhou, and H. Zreiqat, *Acta Biomater.*, 2008, **4**, 1487-1497.
187. C. T. Wu, Y. Ramaswamy, D. Kwik, and H. Zreiqat, *Biomaterials*, 2007, **28**, 3171-3181.
188. H. Zreiqat, Y. Ramaswamy, C. Wu, A. Paschalidis, Z. Lu, B. James, O. Birke, M. McDonald, D. Little, and C. R. Dunstan, *Biomaterials*, 2010, **31**, 3175-3184.
189. Y. Huang, X. Jin, X. Zhang, H. Sun, J. Tu, T. Tang, J. Chang, and K. Dai, *Biomaterials*, 2009, **30**, 5041-5048.
190. C. Wu, J. Chang, J. Wang, S. Ni, and W. Zhai, *Biomaterials*, 2005, **26**, 2925-2931.
191. C. Wu, Y. Ramaswamy, and H. Zreiqat, *Acta Biomater.*, 2010, **6**, 2237-2245.
192. S. I. Roohani-Esfahani, C. R. Dunstan, B. Davies, S. Pearce, R. Williams, and H. Zreiqat, *Acta Biomater.*, 2012, **8**, 4162-4172.
193. A. Gomoll, H. Madry, G. Knutsen, N. van Dijk, R. Seil, M. Brittberg, and E. Kon, *Knee Surg. Sports Traumatol. Arthrosc.*, 2010, **18**, 434-447.
194. D. Xue, Q. Zheng, C. Zong, Q. Li, H. Li, S. Qian, B. Zhang, L. Yu, and Z. Pan, *J. Biomed. Mater. Res., Part A*, 2010, **94A**, 259-270.
195. S. T. B. Ho, D. W. Hutmacher, A. K. Ekaputra, D. Hitendra, and J. H. Hui, *Tissue Eng., Part A*, 2010, **16**, 1123-1141.
196. C.-C. Jiang, H. Chiang, C.-J. Liao, Y.-J. Lin, T.-F. Kuo, C.-S. Shieh, Y.-Y. Huang, and R. S. Tuan, *J. Orthop. Res.*, 2007, **25**, 1277-1290.
197. X. Shao, J. C. H. Goh, D. W. Hutmacher, E. H. Lee, and G. Zigang, *Tissue Eng.*, 2006, **12**, 1539-1551.
198. X. Huang, D. Yang, W. Yan, Z. Shi, J. Feng, Y. Gao, W. Weng, and S. Yan, *Biomaterials*, 2007, **28**, 3091-3100.
199. G. G. Niederauer, M. A. Slivka, N. C. Leatherbury, D. L. Korvick, H. Hugh Harroff Jr, W. C. Ehler, C. J. Dunn, and K. Kieswetter, *Biomaterials*, 2000, **21**, 2561-2574.
200. N. Tamai, A. Myoui, M. Hirao, T. Kaito, T. Ochi, J. Tanaka, K. Takaoka, and H. Yoshikawa, *Osteoarthritis Cartilage*, 2005, **13**, 405-417.
201. S. Kitahara, K. Nakagawa, R. L. Sah, Y. Wada, T. Ogawa, H. Moriya, and K. Masuda, *Tissue Eng., Part A*, 2008, **14**, 1905-1913.
202. K. Shimomura, Y. Moriguchi, W. Ando, R. Nansai, H. Fujie, D. A. Hart, A. Gobbi, K. Kita, S. Horibe, K. Shino, H. Yoshikawa, and N. Nakamura, *Tissue Eng., Part A*, 2014,

203. R. M. Schek, J. M. Taboas, S. J. Segvich, S. J. Hollister, and P. H. Krebsbach, *Tissue Eng.*, 2004, **10**, 1376-1385.
204. A. Bernstein, P. Niemeyer, G. Salzmann, N. P. Südkamp, R. Hube, J. Klehm, M. Menzel, R. von Eisenhart-Rothe, M. Bohner, L. Görz, and H. O. Mayr, *Acta Biomater.*, 2013, **9**, 7490-7505.
205. H. O. Mayr, J. Klehm, S. Schwan, R. Hube, N. P. Südkamp, P. Niemeyer, G. Salzmann, R. von Eisenhart-Rothe, A. Heilmann, M. Bohner, and A. Bernstein, *Acta Biomater.*, 2013, **9**, 4845-4855.
206. X. Guo, C. Wang, C. Duan, M. Descamps, Q. Zhao, L. Dong, S. Lü, K. Anselme, J. Lu, and Y. Q. Song, *Tissue Eng.*, 2004, **10**, 1830-1840.
207. X. Guo, C. Wang, Y. Zhang, R. Xia, M. Hu, C. Duan, Q. Zhao, L. Dong, J. Lu, and Y. Q. Song, *Tissue Eng.*, 2004, **10**, 1818-1829.
208. W. Cui, Q. Wang, G. Chen, S. Zhou, Q. Chang, Q. Zuo, K. Ren, and W. Fan, *J. Biosci. Bioeng.*, 2011, **111**, 493-500.
209. B. Marquass, J. S. Somerson, P. Hepp, T. Aigner, S. Schwan, A. Bader, C. Josten, M. Zscharnack, and R. M. Schulz, *J. Orthop. Res.*, 2010, **28**, 1586-1599.
210. T. Tanaka, H. Komaki, M. Chazono, and K. Fujii, *Tissue Eng.*, 2005, **11**, 331-339.
211. T. Gotterbarm, W. Richter, M. Jung, S. Berardi Vilei, P. Mainil-Varlet, T. Yamashita, and S. J. Breusch, *Biomaterials*, 2006, **27**, 3387-3395.
212. G.-I. Im, J.-H. Ahn, S.-Y. Kim, B.-S. Choi, and S.-W. Lee, *Tissue Eng., Part A*, 2009, **16**, 1189-1200.
213. R. A. Kandel, M. Grynepas, R. Pilliar, J. Lee, J. Wang, S. Waldman, P. Zalzal, and M. Hurtig, *Biomaterials*, 2006, **27**, 4120-4131.
214. J. Gao, J. E. Dennis, L. A. Solchaga, A. S. Awadallah, V. M. Goldberg, and A. I. Caplan, *Tissue Eng.*, 2001, **7**, 363-371.
215. J. Gao, J. E. Dennis, L. A. Solchaga, V. M. Goldberg, and A. I. Caplan, *Tissue Eng.*, 2002, **8**, 827-837.
216. B. S. Bal, M. N. Rahaman, P. Jayabalan, K. Kuroki, M. K. Cockrell, J. Q. Yao, and J. L. Cook, *J. Biomed. Mater. Res., Part B*, 2010, **93B**, 164-174.
217. C. Vepari, and D. L. Kaplan, *Prog. Polym. Sci.*, 2007, **32**, 991-1007.
218. O. Hakimi, D. P. Knight, F. Vollrath, and P. Vadgama, *Composites, Part B*, 2007, **38**, 324-337.
219. N. Kasoju, and U. Bora, *Adv. Healthcare Mater.*, 2012, **1**, 393-412.
220. G. H. Altman, F. Diaz, C. Jakuba, T. Calabro, R. L. Horan, J. Chen, H. Lu, J. Richmond, and D. L. Kaplan, *Biomaterials*, 2003, **24**, 401-416.
221. D. N. Rockwood, R. C. Preda, T. Yucel, X. Wang, M. L. Lovett, and D. L. Kaplan, *Nat. Protoc.*, 2011, **6**, 1612-1631.
222. J. G. Hardy, L. M. Römer, and T. R. Scheibel, *Polymer*, 2008, **49**, 4309-4327.
223. E. M. Pritchard, and D. L. Kaplan, *Expert Opin. Drug Delivery*, 2011, **8**, 797-811.
224. B. Kundu, R. Rajkhowa, S. C. Kundu, and X. Wang, *Adv. Drug Delivery Rev.*, 2013, **65**, 457-470.
225. R. L. Horan, K. Antle, A. L. Collette, Y. Wang, J. Huang, J. E. Moreau, V. Volloch, D. L. Kaplan, and G. H. Altman, *Biomaterials*, 2005, **26**, 3385-3393.
226. Y. Wang, D. D. Rudym, A. Walsh, L. Abrahamsen, H. J. Kim, H. S. Kim, C. Kirker-Head, and D. L. Kaplan, *Biomaterials*, 2008, **29**, 3415-3428.

227. Q. Lu, B. Zhang, M. Li, B. Zuo, D. L. Kaplan, Y. Huang, and H. Zhu, *Biomacromolecules*, 2011, **12**, 1080-1086.
228. M. Santin, A. Motta, G. Freddi, and M. Cannas, *J. Biomed. Mater. Res.*, 1999, **46**, 382-389.
229. B. Panilaitis, G. H. Altman, J. Chen, H. J. Jin, V. Karageorgiou, and D. L. Kaplan, *Biomaterials*, 2003, **24**, 3079-3085.
230. L. Meinel, S. Hofmann, V. Karageorgiou, C. Kirker-Head, J. McCool, G. Gronowicz, L. Zichner, R. Langer, G. Vunjak-Novakovic, and D. L. Kaplan, *Biomaterials*, 2005, **26**, 147-155.
231. Y. Wang, H. J. Kim, G. Vunjak-Novakovic, and D. L. Kaplan, *Biomaterials*, 2006, **27**, 6064-6082.
232. S. Hofmann, K. S. Stok, T. Kohler, A. J. Meinel, and R. Müller, *Acta Biomater.*, 2014, **10**, 308-317.
233. V. Karageorgiou, L. Meinel, S. Hofmann, A. Malhotra, V. Volloch, and D. Kaplan, *J. Biomed. Mater. Res., Part A*, 2004, **71A**, 528-537.
234. S. Sofia, M. B. McCarthy, G. Gronowicz, and D. L. Kaplan, *J. Biomed. Mater. Res.*, 2001, **54**, 139-148.
235. T. Tanaka, M. Hirose, N. Kotobuki, H. Ohgushi, T. Furuzono, and J. Sato, *Mater. Sci. Eng., C*, 2007, **27**, 817-823.
236. A. J. Mieszawska, N. Fourligas, I. Georgakoudi, N. M. Ouhib, D. J. Belton, C. C. Perry, and D. L. Kaplan, *Biomaterials*, 2010, **31**, 8902-8910.
237. L. W. Tien, E. S. Gil, S.-H. Park, B. B. Mandal, and D. L. Kaplan, *Macromol. Biosci.*, 2012, **12**, 1671-1679.
238. U. J. Kim, J. Park, C. Li, H. J. Jin, R. Valluzzi, and D. L. Kaplan, *Biomacromolecules*, 2004, **5**, 786-792.
239. A. Motta, C. Migliaresi, F. Faccioni, P. Torricelli, M. Fini, and R. Giardino, *J. Biomater. Sci., Polym. Ed.*, 2004, **15**, 851-864.
240. M. Fini, A. Motta, P. Torricelli, G. Giavaresi, N. Nicoli Aldini, M. Tschon, R. Giardino, and C. Migliaresi, *Biomaterials*, 2005, **26**, 3527-3536.
241. H. J. Jin, J. Chen, V. Karageorgiou, G. H. Altman, and D. L. Kaplan, *Biomaterials*, 2004, **25**, 1039-1047.
242. C. Ki, S. Park, H. Kim, H.-M. Jung, K. Woo, J. Lee, and Y. Park, *Biotechnol. Lett.*, 2008, **30**, 405-410.
243. S. Y. Park, C. S. Ki, Y. H. Park, H. M. Jung, K. M. Woo, and H. J. Kim, *Tissue Eng., Part A*, 2009, **16**, 1271-1279.
244. K. Wei, Y. Li, K.-O. Kim, Y. Nakagawa, B.-S. Kim, K. Abe, G.-Q. Chen, and I.-S. Kim, *J. Biomed. Mater. Res., Part A*, 2011, **97A**, 272-280.
245. H. J. Kim, H. S. Kim, A. Matsumoto, I. Chin, H. Jin, and D. L. Kaplan, *Aust. J. Chem.*, 2005, **58**, 716-720.
246. C. Correia, S. Bhumiratana, L.-P. Yan, A. L. Oliveira, J. M. Gimble, D. Rockwood, D. L. Kaplan, R. A. Sousa, R. L. Reis, and G. Vunjak-Novakovic, *Acta Biomater.*, 2012, **8**, 2483-2492.
247. S. H. Park, E. S. Gil, H. Shi, H. J. Kim, K. Lee, and D. L. Kaplan, *Biomaterials*, 2010, **31**, 6162-6172.
248. H. J. Kim, U. J. Kim, G. G. Leisk, C. Bayan, I. Georgakoudi, and D. L. Kaplan, *Macromol. Biosci.*, 2007, **7**, 643-655.

249. S. Hofmann, H. Hagenmüller, A. M. Koch, R. Müller, G. Vunjak-Novakovic, D. L. Kaplan, H. P. Merkle, and L. Meinel, *Biomaterials*, 2007, **28**, 1152-1162.
250. L. Uebersax, H. Hagenmüller, S. Hofmann, E. Gruenblatt, R. Müller, G. Vunjak-Novakovic, D. L. Kaplan, H. P. Merkle, and L. Meinel, *Tissue Eng.*, 2006, **12**, 3417-3429.
251. L. Meinel, V. Karageorgiou, R. Fajardo, B. Snyder, V. Shinde-Patil, L. Zichner, D. Kaplan, R. Langer, and G. Vunjak-Novakovic, *Ann. Biomed. Eng.*, 2004, **32**, 112-122.
252. L. Meinel, V. Karageorgiou, S. Hofmann, R. Fajardo, B. Snyder, C. Li, L. Zichner, R. Langer, G. Vunjak-Novakovic, and D. L. Kaplan, *J. Biomed. Mater. Res., Part A*, 2004, **71A**, 25-34.
253. H. J. Kim, U. J. Kim, G. Vunjak-Novakovic, B. H. Min, and D. L. Kaplan, *Biomaterials*, 2005, **26**, 4442-4452.
254. V. Karageorgiou, M. Tomkins, R. Fajardo, L. Meinel, B. Snyder, K. Wade, J. Chen, G. Vunjak-Novakovic, and D. L. Kaplan, *J. Biomed. Mater. Res., Part A*, 2006, **78A**, 324-334.
255. Y. Zhang, C. Wu, T. Luo, S. Li, X. Cheng, and R. J. Miron, *Bone*, 2012, **51**, 704-713.
256. L. Meinel, S. Hofmann, O. Betz, R. Fajardo, H. P. Merkle, R. Langer, C. H. Evans, G. Vunjak-Novakovic, and D. L. Kaplan, *Biomaterials*, 2006, **27**, 4993-5002.
257. Y. Zhang, W. Fan, Z. Ma, C. Wu, W. Fang, G. Liu, and Y. Xiao, *Acta Biomater.*, 2010, **6**, 3021-3028.
258. J. Jiang, W. Hao, Y. Li, J. Yao, Z. Shao, H. Li, J. Yang, and S. Chen, *Biotechnol. Lett.*, 2013, **35**, 657-661.
259. H. J. Kim, U. J. Kim, H. S. Kim, C. Li, M. Wada, G. G. Leisk, and D. L. Kaplan, *Bone*, 2008, **42**, 1226-1234.
260. Y. Zhao, J. Chen, A. H. K. Chou, G. Li, and R. Z. LeGeros, *J. Biomed. Mater. Res., Part A*, 2009, **91A**, 1140-1149.
261. Y. Zhang, C. Wu, T. Friis, and Y. Xiao, *Biomaterials*, 2010, **31**, 2848-2856.
262. N. Cheng, J. Dai, X. Cheng, S. e. Li, R. Miron, T. Wu, W. Chen, Y. Zhang, and B. Shi, *J. Mater. Sci.: Mater. Med.*, 2013, **24**, 1963-1975.
263. S. Bhumiratana, W. L. Grayson, A. Castaneda, D. N. Rockwood, E. S. Gil, D. L. Kaplan, and G. Vunjak-Novakovic, *Biomaterials*, 2011, **32**, 2812-2820.
264. L.-P. Yan, A. J. Salgado, J. M. Oliveira, A. L. Oliveira, and R. L. Reis, *J. Bioact. Compat. Polym.*, 2013, **28**, 439-452.
265. T. Diab, E. M. Pritchard, B. A. Uhrig, J. D. Boerckel, D. L. Kaplan, and R. E. Guldberg, *J. Mech. Behav. Biomed. Mater.*, 2012, **11**, 123-131.
266. K.-H. Kim, L. Jeong, H.-N. Park, S.-Y. Shin, W.-H. Park, S.-C. Lee, T.-I. Kim, Y.-J. Park, Y.-J. Seol, Y.-M. Lee, Y. Ku, I.-C. Rhyu, S.-B. Han, and C.-P. Chung, *J. Biotechnol.*, 2005, **120**, 327-339.
267. N. Kuboyama, H. Kiba, K. Arai, R. Uchida, Y. Tanimoto, U. K. Bhawal, Y. Abiko, S. Miyamoto, D. Knight, T. Asakura, and N. Nishiyama, *J. Biomed. Mater. Res., Part B*, 2013, **101B**, 295-302.
268. L. Meinel, R. Fajardo, S. Hofmann, R. Langer, J. Chen, B. Snyder, G. Vunjak-Novakovic, and D. Kaplan, *Bone*, 2005, **37**, 688-698.
269. L. Meinel, O. Betz, R. Fajardo, S. Hofmann, A. Nazarian, E. Cory, M. Hilbe, J. McCool, R. Langer, G. Vunjak-Novakovic, H. P. Merkle, B. Rechenberg, D. L. Kaplan, and C. Kirker-Head, *Bone*, 2006, **39**, 922-931.

270. C. Kirker-Head, V. Karageorgiou, S. Hofmann, R. Fajardo, O. Betz, H. P. Merkle, M. Hilbe, B. von Rechenberg, J. McCool, L. Abrahamsen, A. Nazarian, E. Cory, M. Curtis, D. Kaplan, and L. Meinel, *Bone*, 2007, **41**, 247-255.
271. G. Wang, H. Yang, M. Li, S. Lu, X. Chen, and X. Cai, *J. Bone Jt. Surg., Br. Vol.*, 2010, **92B**, 320-325.
272. H. Kweon, K.-G. Lee, C.-H. Chae, C. Balázsi, S.-K. Min, J.-Y. Kim, J.-Y. Choi, and S.-G. Kim, *J. Oral Maxillofac. Surg.*, 2011, **69**, 1578-1586.
273. J. Zhao, Z. Zhang, S. Wang, X. Sun, X. Zhang, J. Chen, D. L. Kaplan, and X. Jiang, *Bone*, 2009, **45**, 517-527.
274. X. Jiang, J. Zhao, S. Wang, X. Sun, X. Zhang, J. Chen, D. L. Kaplan, and Z. Zhang, *Biomaterials*, 2009, **30**, 4522-4532.
275. R. E. Unger, A. Sartoris, K. Peters, A. Motta, C. Migliaresi, M. Kunkel, U. Bulnheim, J. Rychly, and C. J. Kirkpatrick, *Biomaterials*, 2007, **28**, 3965-3976.
276. R. E. Unger, S. Ghanaati, C. Orth, A. Sartoris, M. Barbeck, S. Halstenberg, A. Motta, C. Migliaresi, and C. J. Kirkpatrick, *Biomaterials*, 2010, **31**, 6959-6967.
277. S. Ghanaati, R. E. Unger, M. J. Webber, M. Barbeck, C. Orth, J. A. Kirkpatrick, P. Booms, A. Motta, C. Migliaresi, R. A. Sader, and C. J. Kirkpatrick, *Biomaterials*, 2011, **32**, 8150-8160.
278. S. Fuchs, X. Jiang, H. Schmidt, E. Dohle, S. Ghanaati, C. Orth, A. Hofmann, A. Motta, C. Migliaresi, and C. J. Kirkpatrick, *Biomaterials*, 2009, **30**, 1329-1338.
279. A. M. Collins, N. J. V. Skaer, T. Gheysens, D. Knight, C. Bertram, H. I. Roach, R. O. C. Oreffo, S. Von-Aulock, T. Baris, J. Skinner, and S. Mann, *Adv. Mater.*, 2009, **21**, 75-78.
280. R. Rajkhowa, E. S. Gil, J. Kluge, K. Numata, L. Wang, X. Wang, and D. L. Kaplan, *Macromol. Biosci.*, 2010, **10**, 599-611.
281. D. N. Rockwood, E. S. Gil, S. H. Park, J. A. Kluge, W. Grayson, S. Bhumiratana, R. Rajkhowa, X. Wang, S. J. Kim, G. Vunjak-Novakovic, and D. L. Kaplan, *Acta Biomater.*, 2011, **7**, 144-151.
282. B. B. Mandal, A. Grinberg, E. S. Gil, B. Panilaitis, and D. L. Kaplan, *Proc. Natl. Acad. Sci. U. S. A.*, 2012, **109**, 7699-7704.
283. K. Gellynck, P. M. Verdonk, E. Nimmen, K. Almqvist, T. Gheysens, G. Schoukens, L. Langenhove, P. Kiekens, J. Mertens, and G. Verbruggen, *J. Mater. Sci.: Mater. Med.*, 2008, **19**, 3399-3409.
284. P.-H. G. Chao, S. Yodmuang, X. Wang, L. Sun, D. L. Kaplan, and G. Vunjak-Novakovic, *J. Biomed. Mater. Res., Part B*, 2010, **95B**, 84-90.
285. H. S. Baek, Y. H. Park, C. S. Ki, J.-C. Park, and D. K. Rah, *Surf. Coat. Technol.*, 2008, **202**, 5794-5797.
286. S. Jin, H. Baek, Y. Woo, M. Lee, J.-S. Kim, J.-C. Park, Y. Park, D. Rah, K.-H. Chung, S. Lee, and I. Han, *Macromol. Res.*, 2009, **17**, 703-708.
287. S. Ghosh, M. Laha, S. Mondal, S. Sengupta, and D. L. Kaplan, *Biomaterials*, 2009, **30**, 6530-6540.
288. L.-P. Yan, J. M. Oliveira, A. L. Oliveira, S. G. Caridade, J. F. Mano, and R. L. Reis, *Acta Biomater.*, 2012, **8**, 289-301.
289. Y. Wang, U. J. Kim, D. J. Blasioli, H. J. Kim, and D. L. Kaplan, *Biomaterials*, 2005, **26**, 7082-7094.

290. S. Hofmann, S. Knecht, R. Langer, D. L. Kaplan, G. Vunjak-Novakovic, H. P. Merkle, and L. Meinel, *Tissue Eng.*, 2006, **12**, 2729-2738.
291. L. Meinel, S. Hofmann, V. Karageorgiou, L. Zichner, R. Langer, D. Kaplan, and G. Vunjak-Novakovic, *Biotechnol. Bioeng.*, 2004, **88**, 379-391.
292. L. Uebersax, H. P. Merkle, and L. Meinel, *J. Controlled Release*, 2008, **127**, 12-21.
293. Y. Wang, D. J. Blasioli, H. J. Kim, H. S. Kim, and D. L. Kaplan, *Biomaterials*, 2006, **27**, 4434-4442.
294. K. Makaya, S. Terada, K. Ohgo, and T. Asakura, *J. Biosci. Bioeng.*, 2009, **108**, 68-75.
295. H. Aoki, N. Tomita, Y. Morita, K. Hattori, Y. Harada, M. Sonobe, S. Wakitani, and Y. Tamada, *Bio-Med. Mater. Eng.*, 2003, **13**, 309-317.
296. M. Kawakami, N. Tomita, Y. Shimada, K. Yamamoto, Y. Tamada, N. Kachi, and T. Suguro, *Bio-Med. Mater. Eng.*, 2011, **21**, 53-61.
297. Y. Morita, N. Tomita, H. Aoki, S. Wakitani, Y. Tamada, T. Suguro, and K. Ikeuchi, *Bio-Med. Mater. Eng.*, 2002, **12**, 291-299.
298. Y. Morita, N. Tomita, H. Aoki, S. Wakitani, Y. Tamada, T. Suguro, and K. Ikeuchi, *Bio-Med. Mater. Eng.*, 2003, **13**, 345-353.
299. Y. Morita, N. Tomita, H. Aoki, M. Sonobe, S. Wakitani, Y. Tamada, T. Suguro, and K. Ikeuchi, *J. Biomech.*, 2006, **39**, 103-109.
300. Y. Kambe, K. Yamamoto, K. Kojima, Y. Tamada, and N. Tomita, *Biomaterials*, 2010, **31**, 7503-7511.
301. K. Yamamoto, N. Tomita, Y. Fukuda, S. Suzuki, N. Igarashi, T. Suguro, and Y. Tamada, *Biomaterials*, 2007, **28**, 1838-1846.
302. S. D. Waldman, C. G. Spiteri, M. D. Grynepas, R. M. Pilliar, J. Hong, and R. A. Kandel, *J. Bone Jt. Surg., Am. Vol.*, 2003, **85A**, 101-105.
303. C. V. Gemmiti, and R. E. Guldborg, *Tissue Eng.*, 2006, **12**, 469-479.
304. P. Angele, D. Schumann, M. Angele, B. Kinner, C. Englert, R. Hente, B. Füchtmeier, M. Nerlich, C. Neumann, and R. Kujat, *Biorheology*, 2004, **41**, 335-346.
305. K. Miyanishi, M. C. D. Trindade, D. P. Lindsey, G. S. Beaupré, D. R. Carter, S. B. Goodman, D. J. Schurman, and R. L. Smith, *Tissue Eng.*, 2006, **12**, 2253-2262.
306. R. Seda Tıǧlı, C. Cannizaro, M. Gümüşderelioǧlu, and D. L. Kaplan, *J. Biomed. Mater. Res., Part A*, 2011, **96A**, 21-28.
307. Y. Wang, E. Bella, C. S. D. Lee, C. Migliaresi, L. Pelcastre, Z. Schwartz, B. D. Boyan, and A. Motta, *Biomaterials*, 2010, **31**, 4672-4681.
308. C. Shangkai, T. Naohide, Y. Koji, H. Yasuji, N. Masaaki, T. Tomohiro, and T. Yasushi, *Tissue Eng.*, 2007, **13**, 483-492.
309. F. Li, Y.-Z. Chen, Z.-N. Miao, S.-y. Zheng, and J. Jin, *Cell. Reprogramming*, 2012, **14**, 334-341.
310. N. Bhardwaj, Q. T. Nguyen, A. C. Chen, D. L. Kaplan, R. L. Sah, and S. C. Kundu, *Biomaterials*, 2011, **32**, 5773-5781.
311. N. Bhardwaj, and S. C. Kundu, *Biomaterials*, 2012, **33**, 2848-2857.
312. J. Deng, R. She, W. Huang, Z. Dong, G. Mo, and B. Liu, *J. Mater. Sci.: Mater. Med.*, 2013, **24**, 2037-2046.
313. M. Garcia-Fuentes, A. J. Meinel, M. Hilbe, L. Meinel, and H. P. Merkle, *Biomaterials*, 2009, **30**, 5068-5076.

314. M. Garcia-Fuentes, E. Giger, L. Meinel, and H. P. Merkle, *Biomaterials*, 2008, **29**, 633-642.
315. S. S. Silva, A. Motta, M. r. T. Rodrigues, A. F. M. Pinheiro, M. E. Gomes, J. o. F. Mano, R. L. Reis, and C. Migliaresi, *Biomacromolecules*, 2008, **9**, 2764-2774.
316. C. Foss, E. Merzari, C. Migliaresi, and A. Motta, *Biomacromolecules*, 2012, **14**, 38-47.
317. W. Xiao, W. Liu, J. Sun, X. Dan, D. Wei, and H. Fan, *J. Bioact. Compat. Polym.*, 2012, **27**, 327-341.
318. Y. W. Cheon, W. J. Lee, H. S. Baek, Y. D. Lee, J.-C. Park, Y. H. Park, C. S. Ki, K.-H. Chung, and D. K. Rah, *Artif. Organs*, 2010, **34**, 384-392.
319. D. Mohamad Yunos, O. Bretcanu, and A. R. Boccaccini, *J. Mater. Sci.*, 2008, **43**, 4433-4442.
320. G. Pezzotti, and S. M. F. Asmus, *Mater. Sci. Eng., A*, 2001, **316**, 231-237.
321. X. Wang, R. A. Bank, J. M. Tekoppele, and C. M. Agrawal, *J. Orthop. Res.*, 2001, **19**, 1021-1026.
322. M. Dressler, F. Dombrowski, U. Simon, J. Börnstein, V. D. Hodoroaba, M. Feigl, S. Grunow, R. Gildenhaar, and M. Neumann, *J. Eur. Ceram. Soc.*, 2011, **31**, 523-529.
323. M. Foroughi, S. Karbasi, and R. Ebrahimi-Kahrizangi, *J. Porous Mater.*, 2012, **19**, 667-675.
324. X. Huang, and X. Miao, *J. Biomater. Appl.*, 2007, **21**, 351-374.
325. S. Sharifi, Y. Shafieyan, H. Mirzadeh, S. Bagheri-Khoulenjani, S. M. Rabiee, M. Imani, M. Atai, M. A. Shokrgozar, and A. Hatampoor, *J. Biomed. Mater. Res., Part A*, 2011, **98A**, 257-267.
326. S. Teixeira, H. Fernandes, A. Leusink, C. van Blitterswijk, M. P. Ferraz, F. J. Monteiro, and J. de Boer, *J. Biomed. Mater. Res., Part A*, 2010, **93A**, 567-575.
327. T. Tian, D. Jiang, J. Zhang, and Q. Lin, *Mater. Sci. Eng., C*, 2008, **28**, 51-56.
328. J. Zhao, L. Y. Guo, X. B. Yang, and J. Weng, *Appl. Surf. Sci.*, 2008, **255**, 2942-2946.
329. J. Zhao, X. Lu, K. Duan, L. Y. Guo, S. B. Zhou, and J. Weng, *Colloids Surf., B*, 2009, **74**, 159-166.
330. Y. Kang, A. Scully, D. A. Young, S. Kim, H. Tsao, M. Sen, and Y. Yang, *Eur. Polym. J.*, 2011, **47**, 1569-1577.
331. F. J. Martínez-Vázquez, F. H. Perera, P. Miranda, A. Pajares, and F. Guiberteau, *Acta Biomater.*, 2010, **6**, 4361-4368.
332. F. J. Martínez-Vázquez, P. Miranda, F. Guiberteau, and A. Pajares, *J. Biomed. Mater. Res., Part A*, 2013, **101**, 3551-3559.
333. F. J. Martínez-Vázquez, F. H. Perera, I. v. d. Meulen, A. Heise, A. Pajares, and P. Miranda, *J. Biomed. Mater. Res., Part A*, 2013, **101**, 3086-3096.
334. B. Liu, P. Lin, Y. Shen, and Y. Dong, *J. Mater. Sci.: Mater. Med.*, 2008, **19**, 1203-1207.
335. X. Miao, D. M. Tan, J. Li, Y. Xiao, and R. Crawford, *Acta Biomater.*, 2008, **4**, 638-645.
336. X. Miao, L. P. Tan, L. S. Tan, and X. Huang, *Mater. Sci. Eng., C*, 2007, **27**, 274-279.
337. L. Nie, D. Chen, Q. Yang, P. Zou, S. Feng, H. Hu, and J. Suo, *Mater. Lett.*, 2013, **92**, 25-28.
338. L. Nie, J. Suo, P. Zou, and S. Feng, *J. Nanomater.*, 2012, **2012**, 2-2.

339. M. Peroglio, L. Gremillard, C. Gauthier, L. Chazeau, S. Verrier, M. Alini, and J. Chevalier, *Acta Biomater.*, 2010, **6**, 4369-4379.
340. S. I. Roohani-Esfahani, S. Nouri-Khorasani, Z. Lu, R. Appleyard, and H. Zreiqat, *Biomaterials*, 2010, **31**, 5498-5509.
341. S. I. Roohani-Esfahani, S. Nouri-Khorasani, Z. F. Lu, R. C. Appleyard, and H. Zreiqat, *Acta Biomater.*, 2011, **7**, 1307-1318.
342. Y.-J. Seol, D. Y. Park, J. Y. Park, S. W. Kim, S. J. Park, and D.-W. Cho, *Biotechnol. Bioeng.*, 2013, **110**, 1444-1455.
343. A. L. Torres, V. M. Gaspar, I. R. Serra, G. S. Diogo, R. Fradique, A. P. Silva, and I. J. Correia, *Mater. Sci. Eng., C*, 2013, **33**, 4460-4469.
344. D. Bellucci, A. Sola, P. Gentile, G. Ciardelli, and V. Cannillo, *J. Biomed. Mater. Res., Part A*, 2012, **100A**, 3259-3266.
345. O. Bretcanu, S. Misra, I. Roy, C. Renghini, F. Fiori, A. R. Boccaccini, and V. Salih, *J. Tissue Eng. Regener. Med.*, 2009, **3**, 139-148.
346. Q. Z. Chen, and A. R. Boccaccini, *J. Biomed. Mater. Res., Part A*, 2006, **77A**, 445-457.
347. D. Desimone, W. Li, J. A. Roether, D. W. Schubert, M. C. Crovace, A. C. M. Rodrigues, E. D. Zanotto, and A. R. Boccaccini, *Sci. Technol. Adv. Mater.*, 2013, **14**, 045008.
348. M. M. Erol, V. Mouriño, P. Newby, X. Chatzistavrou, J. A. Roether, L. Hupa, and A. R. Boccaccini, *Acta Biomater.*, 2012, **8**, 792-801.
349. J. Hum, K. W. Luczynski, P. Nooeaid, P. Newby, O. Lahayne, C. Hellmich, and A. R. Boccaccini, *Strain*, 2013, **49**, 431-439.
350. T. Mantsos, X. Chatzistavrou, J. A. Roether, L. Hupa, H. Arstila, and A. R. Boccaccini, *Biomed. Mater.*, 2009, **4**, 055002.
351. V. Mouriño, P. Newby, and A. R. Boccaccini, *Adv. Eng. Mater.*, 2010, **12**, B283-B291.
352. W. Xue, A. Bandyopadhyay, and S. Bose, *J. Biomed. Mater. Res., Part B*, 2009, **91B**, 831-838.
353. H. W. Kim, J. C. Knowles, and H. E. Kim, *Biomaterials*, 2004, **25**, 1279-1287.
354. H.-W. Kim, J. C. Knowles, and H.-E. Kim, *J. Biomed. Mater. Res., Part B*, 2004, **70B**, 240-249.
355. H.-W. Kim, J. Knowles, and H.-E. Kim, *J. Mater. Sci.: Mater. Med.*, 2005, **16**, 189-195.
356. Q. Yao, P. Nooeaid, J. A. Roether, Y. Dong, Q. Zhang, and A. R. Boccaccini, *Ceram. Int.*, 2013, **39**, 7517-7522.
357. W. Li, P. Nooeaid, J. A. Roether, D. W. Schubert, and A. R. Boccaccini, *J. Eur. Ceram. Soc.*, 2014, **34**, 505-514.
358. L. Medvecký, R. Štulajterová, and J. Briančin, *Chem. Pap.*, 2007, **61**, 477-484.
359. I. dal Prà, P. Petrini, A. Charini, S. Bozzini, S. Farè, and U. Armato, *Tissue Eng.*, 2003, **9**, 1113-1121.
360. K. Cai, K. Yao, Y. Cui, Z. Yang, X. Li, H. Xie, T. Qing, and L. Gao, *Biomaterials*, 2002, **23**, 1603-1611.
361. K. Cai, K. Yao, S. Lin, Z. Yang, X. Li, H. Xie, T. Qing, and L. Gao, *Biomaterials*, 2002, **23**, 1153-1160.

362. C. Wu, Y. Zhang, Y. Zhu, T. Friis, and Y. Xiao, *Biomaterials*, 2010, **31**, 3429-3438.
363. S. I. Roohani-Esfahani, Z. F. Lu, J. J. Li, R. Ellis-Behnke, D. L. Kaplan, and H. Zreiqat, *Acta Biomater.*, 2012, **8**, 302-312.
364. J. J. Li, E. S. Gil, R. S. Hayden, C. Li, S.-I. Roohani-Esfahani, D. L. Kaplan, and H. Zreiqat, *Biomacromolecules*, 2013, **14**, 2179-2188.
365. E. Wenk, H. P. Merkle, and L. Meinel, *J. Controlled Release*, 2011, **150**, 128-141.
366. R. Shirazi, and A. Shirazi-Adl, *J. Biomech.*, 2009, **42**, 2458-2465.
367. S. Sundelacruz, and D. L. Kaplan, *Seminars in Cell & Developmental Biology*, 2009, **20**, 646-655.
368. M. Keeney, and A. Pandit, *Tissue Eng., Part B*, 2009, **15**, 55-73.
369. J. F. Mano, and R. L. Reis, *J. Tissue Eng. Regener. Med.*, 2007, **1**, 261-273.
370. I. Martin, S. Miot, A. Barbero, M. Jakob, and D. Wendt, *J. Biomech.*, 2007, **40**, 750-765.
371. P. Nooeaid, V. Salih, J. P. Beier, and A. R. Boccaccini, *J. Cell. Mol. Med.*, 2012, **16**, 2247-2270.
372. T. M. O'Shea, and X. Miao, *Tissue Eng., Part B*, 2008, **14**, 447-464.
373. K. S. Allan, R. M. Pilliar, J. Wang, M. D. Grynepas, and R. A. Kandel, *Tissue Eng.*, 2007, **13**, 167-177.
374. C. Erisken, D. M. Kalyon, H. Wang, C. Örnek-Ballanco, and J. Xu, *Tissue Eng., Part A*, 2010, **17**, 1239-1252.
375. J. Jiang, A. Tang, G. A. Ateshian, X. E. Guo, C. T. Hung, and H. H. Lu, *Ann. Biomed. Eng.*, 2010, **38**, 2183-2196.
376. J. Lam, S. Lu, V. V. Meretoja, Y. Tabata, A. G. Mikos, and F. K. Kasper, *Acta Biomater.*, 2014, **10**, 1112-1123.
377. X. Li, L. Jin, G. Balian, C. T. Laurencin, and D. Greg Anderson, *Biomaterials*, 2006, **27**, 2426-2433.
378. S.-M. Lien, C.-H. Chien, and T.-J. Huang, *Mater. Sci. Eng., C*, 2009, **29**, 315-321.
379. N. Mahmoudifar, and P. M. Doran, *Biotechnol. Prog.*, 2013, **29**, 176-185.
380. J. M. Oliveira, M. T. Rodrigues, S. S. Silva, P. B. Malafaya, M. E. Gomes, C. A. Viegas, I. R. Dias, J. T. Azevedo, J. F. Mano, and R. L. Reis, *Biomaterials*, 2006, **27**, 6123-6137.
381. D. Schaefer, I. Martin, P. Shastri, R. F. Padera, R. Langer, L. E. Freed, and G. Vunjak-Novakovic, *Biomaterials*, 2000, **21**, 2599-2606.
382. C. Scotti, D. Wirz, F. Wolf, D. J. Schaefer, V. Bürgin, A. U. Daniels, V. Valderrabano, C. Candrian, M. Jakob, I. Martin, and A. Barbero, *Biomaterials*, 2010, **31**, 2252-2259.
383. E. J. Sheehy, T. Vinardell, C. T. Buckley, and D. J. Kelly, *Acta Biomater.*, 2013, **9**, 5484-5492.
384. J. K. Sherwood, S. L. Riley, R. Palazzolo, S. C. Brown, D. C. Monkhouse, M. Coates, L. G. Griffith, L. K. Landeen, and A. Ratcliffe, *Biomaterials*, 2002, **23**, 4739-4751.
385. R. Tuli, S. Nandi, W. J. Li, S. Tuli, X. Huang, P. A. Manner, P. Laquerriere, U. Nöth, D. J. Hall, and R. S. Tuan, *Tissue Eng.*, 2004, **10**, 1169-1179.
386. X. Wang, S. P. Grogan, F. Rieser, V. Winkelmann, V. Maquet, M. La Berge, and P. Mainil-Varlet, *Biomaterials*, 2004, **25**, 3681-3688.
387. A. Alhadlaq, J. Elisseeff, L. Hong, C. Williams, A. Caplan, B. Sharma, R. Kopher, S. Tomkoria, D. Lennon, A. Lopez, and J. Mao, *Ann. Biomed. Eng.*, 2004, **32**, 911-923.

388. A. Alhadlaq, and J. J. Mao, *J. Bone Jt. Surg., Am. Vol.*, 2005, **87A**, 936-944.
389. P. Giannoni, E. Lazzarini, L. Ceseracciu, A. C. Barone, R. Quarto, and S. Scaglione, *J. Tissue Eng. Regener. Med.*, 2012,
390. J. M. Coburn, M. Gibson, S. Monagle, Z. Patterson, and J. H. Elisseeff, *Proc. Natl. Acad. Sci. U. S. A.*, 2012, **109**, 10012-10017.
391. J. Chen, H. Chen, P. Li, H. Diao, S. Zhu, L. Dong, R. Wang, T. Guo, J. Zhao, and J. Zhang, *Biomaterials*, 2011, **32**, 4793-4805.
392. H. Da, S. J. Jia, G. L. Meng, J. H. Cheng, W. Zhou, Z. Xiong, Y. J. Mu, and J. Liu, *PLoS One*, 2013, **8**, e54838.
393. T. Deng, J. Lv, J. Pang, B. Liu, and J. Ke, *J. Tissue Eng. Regener. Med.*, 2012,
394. N. H. Dormer, M. Singh, L. Zhao, N. Mohan, C. J. Berkland, and M. S. Detamore, *J. Biomed. Mater. Res., Part A*, 2012, **100A**, 162-170.
395. N. Mohan, N. H. Dormer, K. L. Caldwell, V. H. Key, C. J. Berkland, and M. S. Detamore, *Tissue Eng., Part A*, 2011, **17**, 2845-2855.
396. P. Duan, Z. Pan, L. Cao, Y. He, H. Wang, Z. Qu, J. Dong, and J. Ding, *J. Biomed. Mater. Res., Part A*, 2014, **102**, 180-192.
397. T. A. Holland, E. W. H. Bodde, L. S. Baggett, Y. Tabata, A. G. Mikos, and J. A. Jansen, *J. Biomed. Mater. Res., Part A*, 2005, **75A**, 156-167.
398. T. A. Holland, E. W. H. Bodde, V. M. J. I. Cuijpers, L. S. Baggett, Y. Tabata, A. G. Mikos, and J. A. Jansen, *Osteoarthritis Cartilage*, 2007, **15**, 187-197.
399. M. R. Jung, I. K. Shim, H. J. Chung, H. R. Lee, Y. J. Park, M. C. Lee, Y. I. Yang, S. H. Do, and S. J. Lee, *J. Controlled Release*, 2012, **162**, 485-491.
400. M. Pei, F. He, B. M. Boyce, and V. L. Kish, *Osteoarthritis Cartilage*, 2009, **17**, 714-722.
401. Y. Qi, Y. Du, W. Li, X. Dai, T. Zhao, and W. Yan, *Knee Surg. Sports Traumatol. Arthrosc.*, 2012, 1-10.
402. T. Re'em, F. Witte, E. Willbold, E. Ruvinov, and S. Cohen, *Acta Biomater.*, 2012, **8**, 3283-3293.
403. D. Schaefer, I. Martin, G. Jundt, J. Seidel, M. Heberer, A. Grodzinsky, I. Bergin, G. Vunjak-Novakovic, and L. E. Freed, *Arthritis Rheum.*, 2002, **46**, 2524-2534.
404. X. X. Shao, D. W. Hutmacher, S. T. Ho, J. C. H. Goh, and E. H. Lee, *Biomaterials*, 2006, **27**, 1071-1080.
405. L. A. Solchaga, J. S. Temenoff, J. Gao, A. G. Mikos, A. I. Caplan, and V. M. Goldberg, *Osteoarthritis Cartilage*, 2005, **13**, 297-309.
406. W. Wang, B. Li, J. Yang, L. Xin, Y. Li, H. Yin, Y. Qi, Y. Jiang, H. Ouyang, and C. Gao, *Biomaterials*, 2010, **31**, 8964-8973.
407. S. Zhang, L. Chen, Y. Jiang, Y. Cai, G. Xu, T. Tong, W. Zhang, L. Wang, J. Ji, P. Shi, and H. W. Ouyang, *Acta Biomater.*, 2013, **9**, 7236-7247.
408. C.-H. Chang, T.-F. Kuo, C.-C. Lin, C.-H. Chou, K.-H. Chen, F.-H. Lin, and H.-C. Liu, *Biomaterials*, 2006, **27**, 1876-1888.
409. E. Kon, G. Filardo, D. Robinson, J. A. Eisman, A. Levy, K. Zaslav, J. Shani, and N. Altschuler, *Knee Surg. Sports Traumatol. Arthrosc.*, 2013, 1-13.
410. S. Miot, W. Brehm, S. Dickinson, T. Sims, A. Wixmerten, C. Longinotti, A. P. Hollander, P. Mainil-Varlet, and I. Martin, *Eur. Cells Mater.*, 2012, **23**, 222-236.

411. M. Zscharnack, P. Hepp, R. Richter, T. Aigner, R. Schulz, J. Somerson, C. Josten, A. Bader, and B. Marquass, *Am. J. Sports Med.*, 2010, **38**, 1857-1869.
412. G. Chen, T. Sato, J. Tanaka, and T. Tateishi, *Mater. Sci. Eng., C*, 2006, **26**, 118-123.
413. S. Lopa, and H. Madry, *Tissue Eng., Part A*, 2014,
414. A. M. J. Getgood, S. J. Kew, R. Brooks, H. Aberman, T. Simon, A. K. Lynn, and N. Rushton, *The Knee*, 2012, **19**, 422-430.
415. N. A. Sgaglione, and A. S. Florence, *Arthroscopy*, 2009, **25**, 815-819.
416. M. R. Carmont, R. Carey-Smith, A. Saithna, M. Dhillon, P. Thompson, and T. Spalding, *Arthroscopy*, 2009, **25**, 810-814.
417. J. E. J. Bekkers, L. W. Bartels, K. L. Vincken, W. J. A. Dhert, L. B. Creemers, and D. B. F. Saris, *Am. J. Sports Med.*, 2013, **41**, 1290-1295.
418. A. A. M. Dhollander, K. Liekens, K. F. Almqvist, R. Verdonk, S. Lambrecht, D. Elewaut, G. Verbruggen, and P. C. M. Verdonk, *Arthroscopy*, 2012, **28**, 225-233.
419. F. A. Barber, and W. D. Dockery, *Arthroscopy*, 2011, **27**, 60-64.
420. S. Panseri, A. Russo, C. Cunha, A. Bondi, A. Di Martino, S. Patella, and E. Kon, *Knee Surg. Sports Traumatol. Arthrosc.*, 2012, **20**, 1182-1191.
421. A. Tampieri, M. Sandri, E. Landi, D. Pressato, S. Francioli, R. Quarto, and I. Martin, *Biomaterials*, 2008, **29**, 3539-3546.
422. E. Kon, M. Delcogliano, G. Filardo, M. Fini, G. Giavaresi, S. Francioli, I. Martin, D. Pressato, E. Arcangeli, R. Quarto, M. Sandri, and M. Marcacci, *J. Orthop. Res.*, 2010, **28**, 116-124.
423. E. Kon, A. Mutini, E. Arcangeli, M. Delcogliano, G. Filardo, N. Nicoli Aldini, D. Pressato, R. Quarto, S. Zaffagnini, and M. Marcacci, *J. Tissue Eng. Regener. Med.*, 2010, **4**, 300-308.
424. E. Kon, M. Delcogliano, G. Filardo, G. Altadonna, and M. Marcacci, *Knee Surg. Sports Traumatol. Arthrosc.*, 2009, **17**, 1312-1315.
425. E. Kon, M. Delcogliano, G. Filardo, D. Pressato, M. Busacca, B. Grigolo, G. Desando, and M. Marcacci, *Injury*, 2010, **41**, 693-701.
426. E. Kon, M. Delcogliano, G. Filardo, M. Busacca, A. Di Martino, and M. Marcacci, *Am. J. Sports Med.*, 2011, **39**, 1180-1190.
427. M. Delcogliano, F. Caro, E. Scaravella, G. Ziveri, C. Biase, D. Marotta, P. Marengi, and A. Delcogliano, *Knee Surg. Sports Traumatol. Arthrosc.*, 2013, 1-10.
428. G. Filardo, E. Kon, A. Di Martino, M. Busacca, G. Altadonna, and M. Marcacci, *Am. J. Sports Med.*, 2013, **41**, 1786-1793.
429. D. Marolt, A. Augst, L. E. Freed, C. Vepari, R. Fajardo, N. Patel, M. Gray, M. Farley, D. Kaplan, and G. Vunjak-Novakovic, *Biomaterials*, 2006, **27**, 6138-6149.
430. A. Augst, D. Marolt, L. E. Freed, C. Vepari, L. Meinel, M. Farley, R. Fajardo, N. Patel, M. Gray, D. L. Kaplan, and G. Vunjak-Novakovic, *J. R. Soc., Interface*, 2008, **5**, 929-939.
431. K. Chen, K. S. Ng, S. Ravi, J. C. H. Goh, and S. L. Toh, *J. Tissue Eng. Regener. Med.*, 2013,
432. K. Chen, P. Shi, T. K. H. Teh, S. L. Toh, and J. C. H. Goh, *J. Tissue Eng. Regener. Med.*, 2013,
433. K. Chen, T. K. H. Teh, S. Ravi, S. L. Toh, and J. C. H. Goh, *Tissue Eng., Part A*, 2012, **18**, 1902-1911.

434. X. Wang, E. Wenk, X. Zhang, L. Meinel, G. Vunjak-Novakovic, and D. L. Kaplan, *J. Controlled Release*, 2009, **134**, 81-90.
435. L.-P. Yan, J. M. Oliveira, A. L. Oliveira, and R. L. Reis, *Key Eng. Mater.*, 2014, **587**, 245-248.
436. S. Saha, B. Kundu, J. Kirkham, D. Wood, S. C. Kundu, and X. B. Yang, *PLoS One*, 2013, **8**, e80004.
437. H. Madry, C. N. Dijk, and M. Mueller-Gerbl, *Knee Surg. Sports Traumatol. Arthrosc.*, 2010, **18**, 419-433.
438. P. Orth, M. Cucchiarini, D. Kohn, and H. Madry, *Eur. Cells Mater.*, 2013, **25**, 299-316.
439. M. L. de Vries-van Melle, R. Narcisi, N. Kops, W. J. L. M. Koevoet, P. K. Bos, J. M. Murphy, J. A. N. Verhaar, P. M. van der Kraan, and G. J. V. M. van Osch, *Tissue Eng., Part A*, 2013, **20**, 23-33.
440. B. J. Ahern, J. Parvizi, R. Boston, and T. P. Schaer, *Osteoarthritis Cartilage*, 2009, **17**, 705-713.
441. D. D. Frisbie, M. W. Cross, and C. W. McIlwraith, *Vet. Comp. Orthop. Traumatol.*, 2006, **19**, 142-146.
442. J. O. Hollinger, and J. C. Kleinschmidt, *J. Craniofac. Surg.*, 1990, **1**, 60-68.
443. M. Thorwarth, S. Schultze-Mosgau, P. Kessler, J. Wiltfang, and K. A. Schlegel, *J. Oral Maxillofac. Surg.*, 2005, **63**, 1626-1633.
444. R. P. Meinig, C. M. Buesing, J. Helm, and S. Gogolewski, *J. Orthop. Trauma*, 1997, **11**, 551-558.
445. P. Niemeyer, K. Fechner, S. Milz, W. Richter, N. P. Suedkamp, A. T. Mehlhorn, S. Pearce, and P. Kasten, *Biomaterials*, 2010, **31**, 3572-3579.
446. R. P. Jakob, T. Franz, E. Gautier, and P. Mainil-Varlet, *Clin. Orthop. Relat. Res.*, 2002, **401**, 170-184.
447. P. X. Ma, *Mater. Today*, 2004, **7**, 30-40.
448. B. Stevens, Y. Yang, A. Mohandas, B. Stucker, and K. T. Nguyen, *J. Biomed. Mater. Res., Part B*, 2008, **85B**, 573-582.
449. H. Zhou, J. G. Lawrence, and S. B. Bhaduri, *Acta Biomater.*, 2012, **8**, 1999-2016.
450. A. Butscher, M. Bohner, S. Hofmann, L. Gauckler, and R. Müller, *Acta Biomater.*, 2011, **7**, 907-920.
451. K. F. Leong, C. M. Cheah, and C. K. Chua, *Biomaterials*, 2003, **24**, 2363-2378.
452. N. Dormer, M. Singh, L. Wang, C. Berkland, and M. Detamore, *Ann. Biomed. Eng.*, 2010, **38**, 2167-2182.

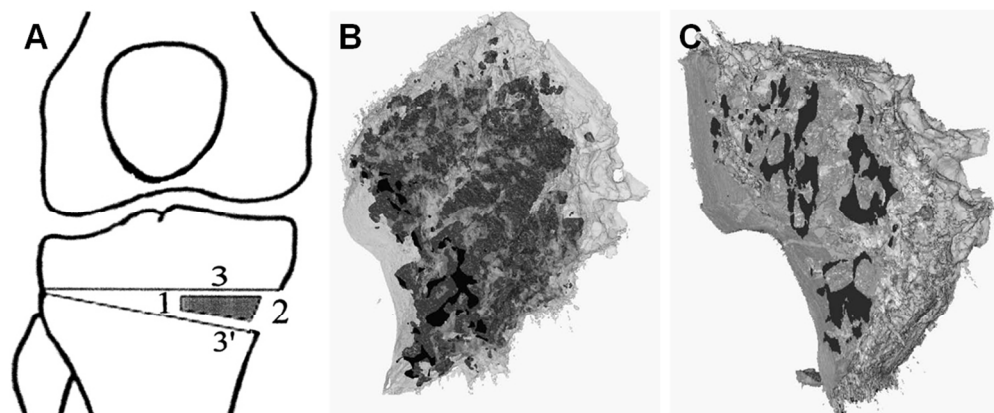


Fig. 6